65950

COMPUTER AIDED DESIGN

OF

MACHINE TOOL BED STRUCTURES

A Ph. D. THESIS

in

Mechanical Engineering

University of Gaziantep

By

Abdullah AKPOLAT

April 1997

Approval of the Graduate School of Natural and Applied Sciences

Assoc. Prof. Dr. Ali Rıza TEKİN

Director

I certify that I have read this thesis and that in my opinion it is fully adequate, in scope and quality, as a dissertation for the degree of Doctor of Philosophy.

Assoc. Prof. Dr. Sedat BAYSEÇ
Chairman of the Department

I certify that I have read this thesis and that in my opinion it is fully adequate, in scope and quality, as a thesis for the degree of Doctor of Philosophy.

Prof. Dr. İ. Hüseyin FİLİZ

Major Supervisor

Examining Committee in Charge

Prof. Dr. Erdem KOÇ (Chairman)

Prof. Dr. İ. Hüseyin FİLİZ

Assoc. Prof. Dr. A. İhsan SÖNMEZ

Assoc. Prof. Dr. Mustafa ÖZAKÇA

Assist. Prof. Dr. İbrahim H. GÜZELBEY

ABSTRACT

COMPUTER AIDED DESIGN
OF
MACHINE TOOL BED STRUCTURES

AKPOLAT, Abdullah
Ph.D. in Mechanical Engineering
Supervisor: Prof. Dr. İ. Hüseyin FİLİZ
April 1997, 147 pages

In this thesis, a study on the design of machine tool bed structures by using the finite element method is presented. Bolted and welded joints are analysed. Emphasis is given to the analysis and design of slideways. Deformations and pressure distribution on the slideway surfaces are mainly considered.

A thorough review on the stiffness of the members of bolted joints is presented. The effects of bolt diameter, grip length and thickness ratio on the stiffness of the members are investigated. A practical formula is suggested for the calculation of member stiffness. Fillet welded joints are analysed and stress distribution on welded regions in different directions are represented in graphical form.

Analysis of machine tool slideways has been carried out by using two and three dimensional slideway models. Models are considered to consist of contact elements at the interface of sliding surfaces. Flat, combined (flat and vee) and dovetail type of slideways are modelled. Pressure distributions and deformations are determined with the use of ANSYS Rev. 5.0A non-linear contact elements.

Key Words: Machine Tool Slideways, Contact Deformations, Stiffness, Pressure Distribution

ÖZET

TAKIM TEZGAHI GÖVDELERİNİN BİLGİSAYAR DESTEKLİ TASARIMI

AKPOLAT, Abdullah
Doktora Tezi, Makina Mühendisliği Bölümü
Tez Yöneticisi: Prof. Dr. İ. Hüseyin FİLİZ
Nisan 1997, 147 sayfa

Bu tezde, takım tezgahı gövdelerinin sonlu elemanlar metodu kullanılarak tasarımıyla ilgili bir çalışma sunulmaktadır. Civatalı ve kaynaklı bağlantılar analiz edildi. Daha çok kızakların analiz ve tasarımınına önem verilerek, kızak yüzeylerindeki basınç dağılımı ve deformasyonlar incelendi.

Civatalı bağlantılarda bağlantı elemanlarının rijiditelerinin bulunması üzerine ayrıntılı bir inceleme yapıldı. Civata çapı, bağlantı kalınlığı ve elemanların kalınlıklarının oranının; bağlantı elemanlarının rijiditesi üzerinde etkileri incelendi. Elemanların rijiditelerinin pratik olarak hesaplanması için bir formül önerildi. Köşe kaynaklı bağlantılar incelendi ve kaynak metalinde çeşitli doğrultularda gerilme bilişenlerinin değişimleri grafik olarak gösterildi.

Takım tezgahı kızakları iki ve üç boyutlu modeller hazırlanarak incelendi. Modeller kızakların temas eden yüzeylerinde kontak elemanları tanımlanarak hazırlandı. Düz, ikili (düz ve V tipi), ve kırlangıç kuyruğu şeklinde kızak çeşitleri modellendi. Temas eden kızak yüzeylerindeki basınç dağılımları ve deformasyonlar ANSYS Rev. 5.0A'nın lineer olmayan kontak elemenları kullanılarak bulundu.

Anahtar Kelimeler: Takım Tezgahı Kızakları, Kontak Deformasyonları, Rijidite, Basınç Dağılımı

ACKNOWLEDGEMENT

I would like to express my sincere gratitude to my supervisor, Prof. Dr. İ. Hüseyin Filiz for his encouragement, guidance, suggestions, patience and help in making this thesis understandable.

I also wish to thank Assist. Prof. Dr. İbrahim H. Güzelbey, Assist. Prof. Dr. Cengiz Doğan and Assist. Prof. Dr. Nihat Yıldırım for their valuable criticism during the study.

I am very grateful to Mr. Türkay Dereli for his supports throughout the work and continuous helps in preparing the manuscript.

Special thanks are due to my dearest wife, my son and daughters for their patience.

TABLE OF CONTENTS

	PAGE
ABSTRACT	iii
ÖZET	iv
ACKNOWLEDGEMENTS	v
LIST OF TABLES	x
LIST OF FIGURES	xi
NOMENCLATURE	xvi
1. INTRODUCTION	1
2. LITERATURE SURVEY	6
2.1 Introduction	6
2.2 Computer Aided Design	6
2.3 Deformation of the Machined Surfaces	8
2.3.1 Theory of Contact Deformation	9
2.3.2 Experimental Studies on Contact Deformation	11
2.4 Factors Affecting the Normal Stiffness of the Surfaces	17
2.4.1 Pair of Materials	19
2.4.2 Surface Asperities and Machine Lay Orientation	20
2.4.3 Effect of Hardness	21
2.4.4 Effect of Flatness Deviation and Surface Size	22
2.5 The Stiffness of Machine Tool Joints	24
2.5.1 Bolted Joints	25
2.5.2 Sliding Joints	29

3. FINITE ELEMENT METHOD AND CONTACT ELEMENTS 32

3.1 Introduction 32
3.2 Finite Element Method 32

3.2.1 How the Finite Element Method Works 34
3.2.2 Steps of FEM 37
3.2.3 Range of Application 40
3.2.4 Background Needed for Effective Use of Finite Element Computer Programs 41
3.2.5 Available Finite Element Computer Programs 42

3.3 ANSYS as a Finite Element Analysis Package 43

3.3.1 General Information 43
3.3.2 Program Capability 43
3.3.3 User Interface and Modelling Capability 44

3.4 Contact Phenomenon 47

3.4.1 Contact Nonlinearities 47
3.4.2 Contact Elements 48
3.4.3 Contact Stiffness 49

4. DESIGN OF MACHINE TOOL JOINTS 53

4.1 Introduction 53
4.2 Machine Tool Joints 53
4.3 Bolted Joints 55

4.3.1 Member Stiffness with Finite Element Method 56
4.3.2 Examples 60

4.3.2.1 Effects of Aspect Ratio(d/L) 61
4.3.2.2 Effects of Member Thickness(L) 63

4.3.3 Results 63
4.3.4 Discussions 65

4.4 Welded Joints 68

4.4.1 Example 1: Lapped Welded Joint 69

4.4.1.1 Results 71

4.4.2 Example 2: Cantilever Beam Welded Joint 76

4.4.2.1 Results 78

4.4.3 Discussions 83

5. DESIGN PRINCIPLES OF MACHINE TOOL SLIDEWAYS 84

5.1 Introduction 84
5.2 Functions of Slideways 85

5.2.1 Forces on Slideways 86
5.2.2 Slideway Configurations 89

5.3 Design Principles of Slideways 91
5.4 Finite Element Analysis 92

5.4.1 Contact Deformations 93

6. TWO DIMENSIONAL ANALYSIS OF SLIDEWAYS 95

6.1 Introduction 95
6.2 Two Dimensional Models of Slideways 95
6.3 Examples 96

6.3.1 Example 1: 2-D Open Type Flat Slideway 96
6.3.2 Example 2: 2-D Closed Type Flat Slideway 100
6.3.3 Example 3: 2-D Dovetail Slideway 103

7. THREE DIMENSIONAL MODELS OF SLIDEWAYS 106

7.1 Introduction 106
7.2 General Considerations of Three Dimensional Slideways 106
7.3 Three Dimensional Slideway Models 107

7.3.1 Example 1: 3-D Open Type Flat Slideway 108
7.3.2 Example 2: 3-D Closed Type Flat Slideway 114
7.3.3 Example 3: 3-D Dovetail Slideway 120
7.3.4 Example 4: 3-D Vee-Flat Combined Slideway 126
7.3.5 Example 5: 3-D Model of Closed Type Lathe 132

8. DISCUSSIONS AND CONCLUSIONS 138

8.1 Discussions and Conclusions 134
8.2 Recommendations for Future Works 141

LIST OF REFERENCES 143

LIST OF TABLES

Table		Page
2.1	Coefficients c and m for Different Surface Finishes of Cast Iron.	18
2.2	Stiffness Formulae of Previous Studies	28
4.1	Properties of Materials Used in the Bolted Joints	61

LIST OF FIGURES

Figure		Page
2.1	Relation Between Interface Pressure and Deformations[10]	13
2.2	Relation Between Interface Pressure and Deformations for Cast Iron Hand Scraped Surfaces[2]	14
2.3	Relation Between Interface Pressure and Deformations for Cast Iron[5]	15
2.4	Loading and Unloading Deformations of Mild Steel Interfaces Subjected to High Loading Pressures[14,17]	16
3.1	A Beam Represented by Finite Elements	35
3.2	Some Element Shapes Used in Finite Element Analysis	38
3.3	A Relational Diagram of the ANSYS Centralized Database	46
3.4	Two and Three Dimensional Point to Point Contact Elements[45]	50
3.5	Two and Three Dimensional Point to Surface Contact Elements[45]	51
4.1	A Typical Bolted Joint	57
4.2	Symmetries in a Bolted Joint	59
4.3	The Finite Element Model of Members	60
4.4	Stiffness Variations with d/L for Different Materials	62
4.5	Stiffness of Joints which Consists of Members Having Different Materials	64
4.6	Stiffness Variations with respect to Thickness Ratio	64
4.7	Comparisons of Results of FEM, Wileman's Formula and Equation 4.3	66

4.8 Comparisons of Results of FEM, Equation 4.3 and Previous Studies for Different Member Materials 67

4.9 Comparisons of Results of FEM, Equation 4.3 and Previous Studies for Different Thickness Ratios 67

4.10 Schematic View of the Lapped Welded Joint 70

4.11 Finite Element Model of the Lapped Welded Joint 71

4.12 Deformed Shape of the Lapped Welded Joint 72

4.13 Von Mises Stress Contours (for Example 1) 72

4.14 Stress Distributions Along Line BA (for Example 1) 74

4.15 Stress Distributions Along Line BC (for Example 1) 75

4.16 Stress Distributions Along Line BD (for Example 1) 75

4.17 Cantilever Beam Welded Joint 76

4.18 Finite Element Model of Cantilever Beam Welded Joint 77

4.19 The Deformed Shape of Cantilever Beam Welded Joint 79

4.20 Von Mises Stress Contours (for Example 1) 80

4.21 Stress Distributions Along Line BA (for Example 2) 81

4.22 Stress Distributions Along Line BC (for Example 2) 82

4.23 Stress Distributions Along Line BD (for Example 2) 82

5.1 Forces on a Lathe Slideway System[55] 87

5.2 Forces on the Table Slideways of a Horizontal Boring Machine[56] 88

5.3 Basic Types of Slideway Guiding Elements[55] 90

6.1 Finite Element Division of the Open Type Flat Slideway Model and Load Application Points. F is the Total External Load 97

6.2 Deformed Shape of the Open Type Flat Slideway Model for 1.6 MPa Mean Interface Pressure 97

6.3 Pressure Distribution at the Contacting Surfaces of the Open Type Flat Slideway Model for Several Mean Interface Pressures 98

6.4 Relationship Between the Applied Interface Pressure and the Deflection at the Center of the Open Type Flat Slideway Model 99

6.5 Finite Element Division of the Closed Type Flat Slideway Model and Load Application Points. F is the Total External Load 101

6.6 Deformed Shape of the Closed Type Flat Slideway Model for 1.6 MPa Mean Interface Pressure 101

6.7 Pressure Distribution at the Contacting Surfaces of the Closed Type Flat Slideway Model for Several Mean Interface Pressures 102

6.8 Finite Element Division of the Dovetail Slideway Model and Load Application Points. F is the Total External Load 104

6.9 Deformed Shape of the Dovetail Slideway Model for 1.6 MPa Mean Interface Pressure 104

6.10 Pressure Distribution at the Contacting Surfaces of the Dovetail Slideway Model for Several Mean Interface Pressures 105

7.1 Finite Element Division of the Open Type Flat Slideway and Load Application Points 109

7.2 Deformed Shape of the Open Type Flat Slideway for 1.6 MPa Mean Interface Pressure 110

7.3 Pressure Distribution at the Contacting Surfaces and Stress Distribution in x-axis for 1.6 MPa Mean Interface Pressure (for Example 1) 111

7.4 Pressure Distribution at the Contacting Surfaces and Stress Distribution in y-axis for 1.6 MPa Mean Interface Pressure (for Example 1) 112

7.5 Pressure Distribution at the Contacting Surfaces and Stress Distribution z-axis for 1.6 MPa Mean Interface Pressure (for Example 1) 113

7.6 Finite Element Division of the Closed Type Flat Slideway and Load Application Points 115

7.7 Deformed Shape of the Closed Type Flat Slideway for 1.6 MPa Mean Interface Pressure 116

7.8 Pressure Distribution at the Contacting Surfaces and Stress Distribution in x-axis for 1.6 MPa Mean Interface Pressure (for Example 2) 117

7.9 Pressure Distribution at the Contacting Surfaces and Stress Distribution in y-axis for 1.6 MPa Mean Interface Pressure (for Example 2) 118

7.10 Pressure Distribution at the Contacting Surfaces and Stress Distribution in z-axis for 1.6 MPa Mean Interface Pressure (for Example 2) 119

7.11 Finite Element Division of the Dovetail Slideway and Load Application Points 121

7.12 Deformed Shape of the Dovetail Slideway for 1.6 MPa Mean Interface Pressure 122

7.13 Pressure Distribution at the Contacting Surfaces and Stress Distribution in x-axis for 1.6 MPa Mean Interface Pressure (for Example 3) 123

7.14 Pressure Distribution at the Contacting Surfaces and Stress Distribution in y-axis for 1.6 MPa Mean Interface Pressure (for Example 3) 124

7.15 Pressure Distribution at the Contacting Surfaces and Stress Distribution in z-axis for 1.6 MPa Mean Interface Pressure (for Example 3) 125

7.16 Finite Element Division of the Combined Slideway Model and Load Application Points 127

7.17 Deformed Shape of the Combined Slideway Model for 1.6 MPa Mean Interface Pressure 128

7.18 Pressure Distribution at the Contacting Surfaces and Stress Distribution in x-axis for 1.6 MPa Mean Interface Pressure (for Example 4) 129

7.19 Pressure Distribution at the Contacting Surfaces and Stress Distribution in y-axis for 1.6 MPa Mean Interface Pressure (for Example 4) 130

7.20 Pressure Distribution at the Contacting Surfaces and Stress Distribution in z-axis for 1.6 MPa Mean Interface Pressure (for Example 4) 131

7.21 Finite Element Division of Small Student Lathe and Load Application Points 133
7.22 Deformed Shape of the Small Student Lathe 134

7.23 Pressure Distribution at the Contacting Surfaces and Stress Distribution in x-axis (for Example 5) 135

7.24 Pressure Distribution at the Contacting Surfaces and Stress Distribution in y-axis (for Example 5) 136

7.25 Pressure Distribution at the Contacting Surfaces and Stress Distribution in z-axis (for Example 5) 137

NOMENCLATURE

Item	Description
a	Constant relating normal contact deformation and pressure
b	Exponential law coefficient relating normal deflection and pressure
c	Constant relating normal contact deformation and pressure
d	Bolt diameter
d_h	Bolt hole diameter
d_w	Washer diameter
h	Asperity height peak to valley
h_l	Characteristic contact length.
h_n	Nut height
h_w	Length of weld leg
k	Constant relating normal contact deformation and pressure
k_1, k_2	Stiffness of each member
k_b	Bolt stiffness
k_m	Equivalent stiffness of members
k_n	Contact stiffness
l	Length of a contact element
m	Power law coefficient relating normal contact deformation and pressure

n Number of asperities per unit area

p Mean interface pressure

r Radial coordinate

t_d Depth of the model

x Coordinate

y Coordinate

z Axial coordinate

z Coordinate

z Number of contacting spots per square inch of hand scrapped surfaces

A Cross-sectional area

A_a Apparent area of contact

A_b Cross sectional area of bolt

A_i Area of contact of the asperities

A_m Equivalent cross sectional area of the members

A_r Real area of contact of the asperities

C_L Asperity height in C.L.A.

E Modulus of elasticity

E_1, E_2 Modulus of elasticity of individual member

E_b Modulus of elasticity of bolt material

E_{eq} Equivalent modulus of elasticity of the material of the members

F Applied force

F_x x component of applied force

F_y y component of applied force

F_z z component of applied force

K	Constant
L	Grip length of the bolted joint
L_1, L_2	Individual thickness of each member in bolted joints
L_1, L_2	Length of base metals in welded joints
M	Moment
MN	Minimum stress value
MX	Maximum stress value
M_x	applied moment about x axis
M_y	applied moment about y axis
M_z	applied moment about z axis
NFOR	Normal force
W	Energy
W	Weight of slide
X	Coordinate
Y	Coordinate
Z	Coordinate
α	Cone Angle
β	Correction factor
λ	Normal contact deformation
μ	Coefficient of friction
ν	Poisson's ratio of the material
σ	Stresses
τ	Shear stresses
$\varnothing$	Contact probability

CHAPTER I

INTRODUCTION

In design and manufacturing, the main objective is to design and produce components with high quality in shortest possible time and at a minimum cost. On a machine tool, precision and productivity are the two important, and often conflicting requirements. A well designed machine tool should enable maximum metal removal without sacrificing the specified accuracy requirements. This is mainly dependent upon the static and dynamic stiffness of the machine tool structures. Based on this fact, in the last decades, studies on the determination of static and dynamic response of machine tool structures by using computers have been increasing very rapidly.

Machine tool structures generally consist of welded, bolted and sliding joints. Forces are transmitted across the joint interfaces and, the overall static and dynamic characteristics of machine tool are influenced by the compliance at these individual connections. The main sliding joints, however, the friction and wear properties must also be considered by the designer, since these can influence both the short- and long-term accuracy of the machine tools. In this study, only static rigidity will be considered for both fixed and sliding joints.

Welded and bolted joints have received considerable attention from researchers. In addition to analytical and experimental methods, there are many works using finite element method(FEM). Sliding joints, that is, slideways, however, have not received similar attention. Studies on contact deformations could be seen in early 1960s. There are some studies on slideways in 1970s. With the advent of high speed and high storage capacity computers, the analysis and the design studies are eased with FEM after 1980s. But, there are only few number of studies which used finite element technique.

In general, qualitative influences of all factors on the behaviour of the joints are known from experiments and simple theoretical models. A method of solution taking into account all the factors in quantitative terms and permitting the calculation of the pressure distribution and deflections is still not available. For this reason, in the present study, ANSYS Finite Element package which can handle models with non-linear contact elements, is used for fast and efficient analysis of both simple and relatively complex slideway geometry for the determination of deformations and pressure distribution of slideways.

This thesis is organised in such a way that, in the second chapter, an analysis of published results on the stiffness of machined surfaces are summarised. In all these studies the joint deformations have been determined by assuming that the components are rigid and only the surfaces are flexible. In the majority of designs, there are very large differences between the theoretical and experimental results. The main source of the error is the assumption that the components are rigid in calculating the joint deformations.

The use of classical theoretical methods in determination of deformations and pressure distribution in machine tools is very difficult because of the complexity of the components forming the joints. In chapter 3, the FEM which is used as a tool in this study is outlined with a short description of its theory and applications. General information and program capabilities of ANSYS; as a finite element analysis package is outlined with the description of contact phenomenon, contact non-linearities, contact elements and contact stiffness.

In chapter 4, bolted and welded joints are analysed by using the FEM. A computer program is prepared to determine member stiffness directly from the given joint geometry. In order to evaluate the effect of joint geometry upon member stiffness, a number of models having different geometry are created.

A practical formula is suggested for the determination of the member stiffness of bolted joints which may consist of members made from different materials and with different thicknesses. The method could easily be used for design purposes by changing the design parameters (i.e. grip length, individual member thicknesses, member material, bolt diameter, etc.).

Two types of joints are modelled to analyse welded joints. The first one is an axially loaded lapped joint with fillet welds and, the second one is a cantilever beam welded to a support with fillet welds and loaded at the tip to obtain a bending stress at the support. The stress distribution along weld legs and throat area are given in graphical form. Maximum stress values and maximum stress concentration points are given. The results are compared with the results given in literature, and it is concluded that the design stress values must be increased for these types of welded joints.

The design principle and analysis of machine tool slideways are explained in chapter 5. Functions of the slideways are given to achieve the required precision and productivity. The basic combination of slideway elements are explained to provide the necessary guidance and constraints to the moving member of a machine tool. The main design principles of slideways are explained and finite element analysis and implementation of contact stiffness to calculate contact deformation are given.

In chapter 6, different types of slideways have been analysed by using two dimensional models in which ANSYS Rev. 5.0A's non-linear contact elements are used. Contact elements are defined between the contacting components of these models. Flat and dovetail types of slideways are modelled and under static loading conditions, deformations and pressure distribution on the slideway elements are illustrated. In the determination of the deformations and pressure distribution at the joints of machine tools; compliance of the surfaces and surrounding components are taken into account.

In chapter 7, three dimensional models of the same examples of chapter 6 are analysed. In three dimensional modelling, it is possible to analyse the effects of forces and tilting moments in any axis. In addition to the flat and dovetail types of slideways a flat and vee combination model is analysed. A practical example which consists of flat and vee combination of slideway is given to illustrate the use of the method to a practical machine.

CHAPTER II

LITERATURE SURVEY

2.1 INTRODUCTION

This chapter presents a brief survey of the most relevant literature related to the study reported in this thesis. Section 2.2 is devoted to the reviews on the developments of computer aided design. Deformation of machined surfaces are dealt with in Section 2.3 and factors effecting the normal stiffness of the surfaces are reviewed in Section 2.4. Previous works on the design of machine tool joints are reviewed in Section 2.5.

2.2 COMPUTER AIDED DESIGN

Computers have an important role in the development of machine tool industry as in the case of other fields of industry. Computer aided design techniques have considerable benefit on design improvements and on reduction of design time, cost and development time. Computing is increasing in importance, because the cost of computing continues to fall and is likely to continue decreasing whereas traditional design procedures are progressively becoming more expensive.

The designer now has access to substantial computing power and the computer resources can be exploited to speed up and improve the accuracy of the design process.

Computer aided design has many roles to play in the world of engineering, such as: the application of computer systems to the production of engineering drawings, the use of finite element techniques to solve stress and contact problems on complex components, the analysis of mechanisms and linkages plus a host of additional engineering applications.

The design of machine tool structures is a typical and important example of a computer aided design procedure. A computer technique for analysing a wide variety of machine tool structures is described by Taylor[1].

Finite element methods are now being used extensively as an aid to engineering analysis and design with the wide spread use of high speed and high storage capacity computers. The finite element method analyses complex components by breaking them down into small elements of simple shape and can be used for solving structural, thermal, non-linear, contact and many other engineering problems.

2.3 DEFORMATION OF THE MACHINED SURFACES

On a machine tool, in order to make a component, generally, two metal surfaces are mounted together through flat machined surfaces. If a normal load applied, the deformation of the surfaces is proportional to the interface pressure which is the load per unit area of the contacting surfaces. This approach of the surfaces is due to deformation of the asperities which are always present on all of the very fine machined surfaces.

Several model have been proposed to define relation between the deformation and pressure distribution of the machined surfaces. The equations resulting from these models are satisfied in a certain range of interface pressure and surface finish.

Many studies were carried out to relate theoretically the normal approach of the surfaces with the interface pressure[2-9]. Basically, there are two models to relate these quantities:

1. Theories based on asperities model, and
2. Profilometric theories.

In the asperity models the rough surface is formed by assuming the idealised asperities of hemispheres; truncated pyramids, rods and cylindrical shape obtained from a single tool point machined surface. When this model is used, it was assumed that the rough surface is formed from asperities with the same cross-sectional dimensions, but different heights. By using Hertz Theory, the radius of hemispheres, the number of spots per unit area and distribution of the asperities height can be calculated to obtain a relation between the deformation and interface pressure. The distribution of asperities height can be normal, exponential, power law, linear and uniform depending upon the machined surface. For smooth surfaces the distribution can be assumed to be normal or exponential, but rough surfaces can be represented with a linear or uniform distribution.

For profilometric theories the bearing area is the main parameter that must be known. Ideal plastic flow of the asperities is assumed to relate the interface pressure with the deflection. Bearing area can be defined from any of the distribution mentioned in asperities model.

It is obvious that in order to relate the deflection with the interface pressure, it is always necessary to know several surface parameters and material properties, and the resulting equations are very complicated [4-9].

2.3.1 Theory of Contact Deformation

For all models it can be assumed that the real area of contact between the surfaces is proportional to the applied load, or given by the following relationship

$$W = KA_r \tag{2.1}$$

The real area of contact is assumed to be the product of the number of contacting points N and the area of the individual contacts A_i

$$A_r = NA_i \tag{2.2}$$

The assumption of constant areas A_i, as the deflection increased is not true in practice.

If A_a is taken as the area of contact, n is the number of contacting points per unit area, $\varnothing(z)$ is the probability that a contact is made at the height or deformation λ, then the number of contacts is given by:

$$N = A_a \int_0^{\lambda} \varnothing(z)dz \tag{2.3}$$

Equation 2.1 can be reduced with the relations 2.2 and 2.3

$$p = \frac{W}{A_a} = a\int_0^{\lambda} \varnothing(z)dz \tag{2.4}$$

where $a = KA_i n$ and p is the interface pressure.

If the distribution of the contact points is assumed to be the relation given by Dolbey[10]

$$\varnothing(z) = bz^{(1-m)/m} \tag{2.5}$$

then equation (2.4) can reduced to the following:

$$p = abm\lambda^{1/m} \tag{2.6}$$

or

$$\lambda = cp^{m} \tag{2.7}$$

Equation (2.7) is the most used relation between the surface deformation; λ, and the interface pressure; p. Levina[2,3,11], Ostrovskii[5], Tenner[12] and Dolbey[10] carried out research and have shown that the above equation gives the best correlation with experimental results for a range of interface pressures and surface finish used in the machine tool joints. In this equation p is in kg/cm^2 and λ is in μm. The coefficients c and m are constants for a particular pair of material and surface finish.

2.3.2 Experimental Studies on Contact Deformation

Connolly and Thornley[13] used a similar formula, in exponential form, and it is valid only after a certain initial pressure. The test specimens were made from mild steel with different surface finish and interface pressure is between 8 to 500 kg/cm^2. The following equation was found

$$p = ae^{b\lambda} \tag{2.8}$$

where again the coefficients a and b depend upon the surface finish and properties of pair of materials.

Dolbey[10] made experiments to find rigidity of several combinations of surface finish and materials with the specimens of dimensions 76x76 mm. The interface pressures are below 5 kg/cm^2 and results are shown in Figure 2.1.

As it can be seen from Figure 2.1 for the same pair of material, when the quality of surface finish is decreased, the contact stiffness is also decreased. The same phenomena occurs when the compliance of the pair of materials is increased.

Levina[2] and Ostrovskii[5] have found similar experimental patterns as shown in Figures 2.2 and 2.3 respectively. In Figure 2.2 different qualities of hand scraped cast iron surfaces are compared, in Figure 2.3 planned and ground surfaces are also shown. In these figures results for a range of interface pressure used in non-fixed machine tool joints are presented.

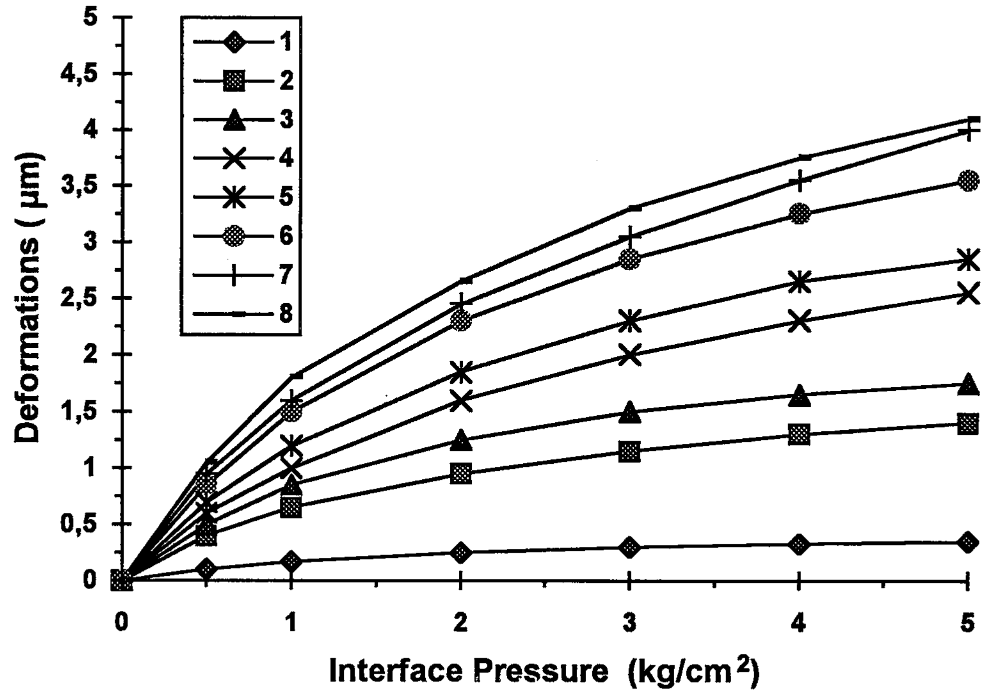

Figure 2.1 Relation Between the Interface Pressure and Deformations[10].

1. C.I. Lapped / C.I. Lapped,
2. C.I. Ground / C.I. Ground,
3. C.I. Ground / C.I. Scraped,
4. C.I. Ground / Ferrosbestos Ground,
5. C.I. Ground / Glacier DX-Plain Ground,
6. C.I. Ground / Glacier DX-Dimpled Ground,
7. C.I. Ground / Glacier DU-as Received,
8. C.I. Ground / Tufnol Ground.

In the case of fixed or bolted joints the total interface pressure reaches relatively high values. Connolly at al.[14], Schoffield and Thornley[8,15], and Thornley at al.[16,17] have tested the rigidity of different machined surfaces of mild steel by applying higher interface pressures.

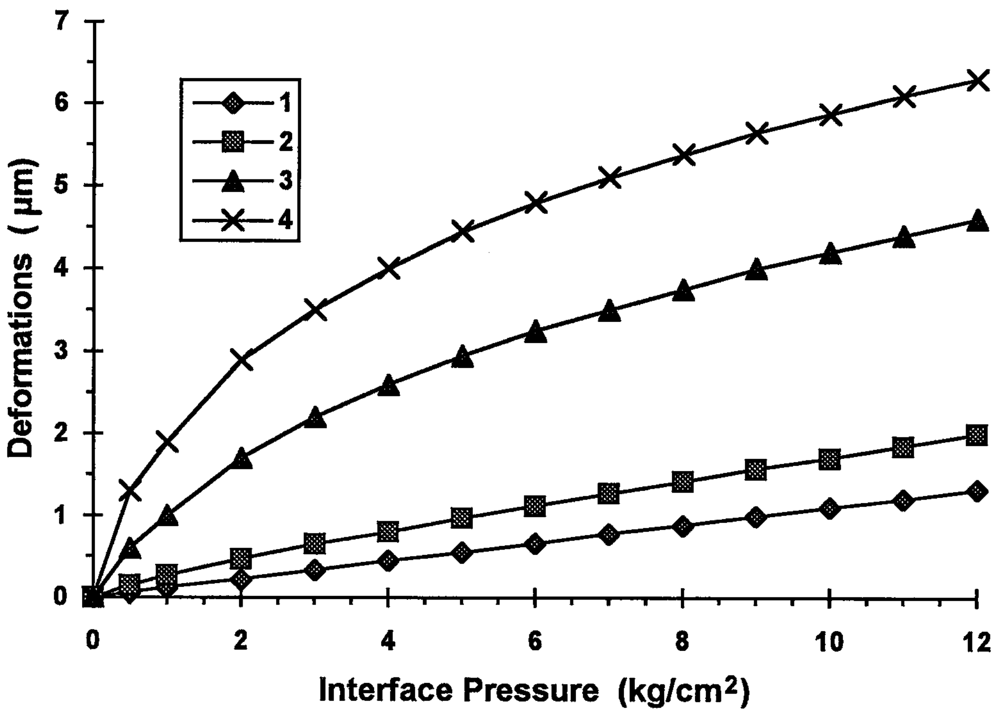

Figure 2.2 Relation Between the Interface Pressure and Deformations for Cast Iron Hand Scraped Surfaces[2].

1. h=3 to 4 μm, Z=20 to 25 spots / in^2,
2. h=7 to 8 μm, Z=20 to 25 spots / in^2,
3. h=7 to 8 μm, Z=12 to 15 spots / in^2,
4. h=15 to 20 μm, Z=12 to 20 spots / in^2.

The experimental relation between the deformation and interface pressure is shown in Figure 2.4.

It was observed that for the first loading the total deflection was the sum of the plastic and elastic deformations. When the joint unloaded without separation of the surfaces then repeatability of the deformations was found for subsequent loading.

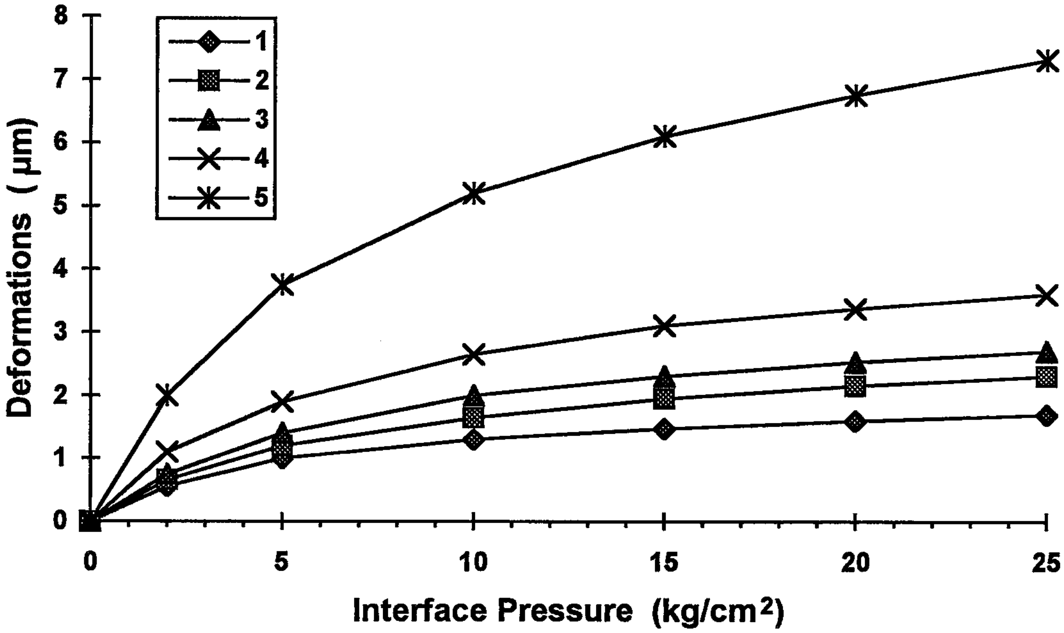

Figure 2.3 Relation Between the Interface Pressure and Deformations for Cast Iron[5].
1. Peripheral Grinding,
2. Fine Scraping, Z= 24 to 36 spots / in^2,
3. Finish Planning,
4. Conventional Scraping,
5. Coarse Scraping, Z= 5 to 10 spots / in^2.

The plastic deformation is important for the initial positioning of the components of machine tool when assembled, but not for a further purpose of defining the stiffness of the joints, because only elastic deflection takes place after the first loading.

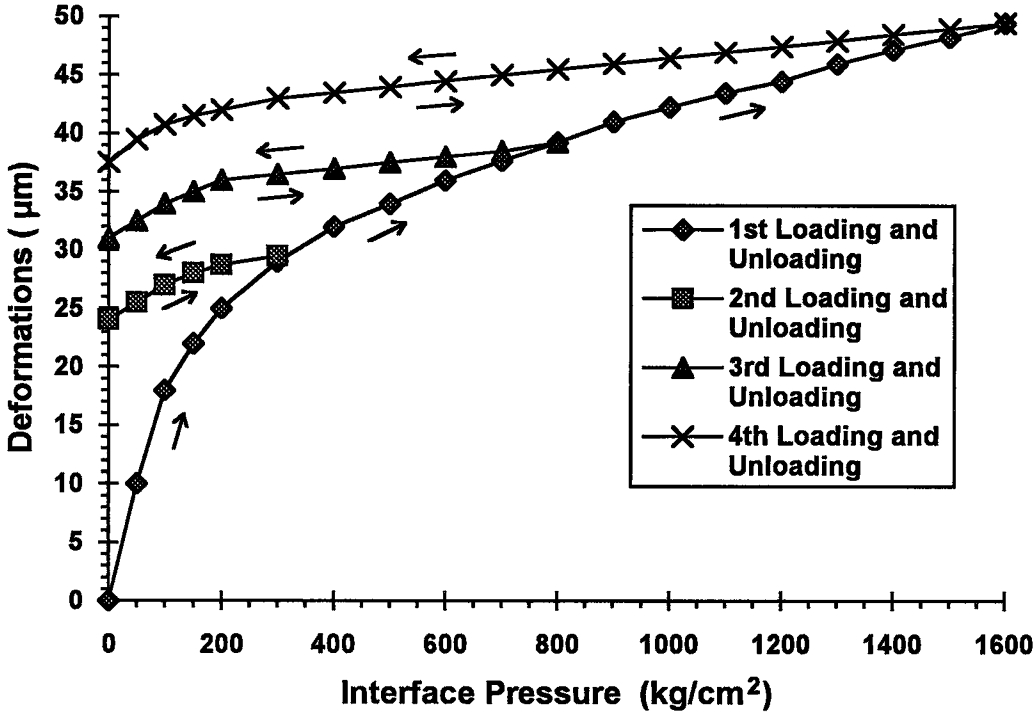

Figure 2.4 Loading and Unloading Deformations of Mild Steel Interfaces Subjected to High Loading Pressures[14,17].

Equation (2.7) can be used to calculate joint deflection for normal loading, but in practice, the loading can be complicated, i.e. a moment can be applied, then this equation is not recommended for a quick calculation. Levina[2] recommends a linearised equation of the form

$$\lambda = kp \tag{2.9}$$

When k is chosen carefully, it was shown that, this is a reasonable approximation.

2. 4 FACTORS AFFECTING THE NORMAL STIFFNESS OF THE SURFACES

As it is seen in Equation (2.7), it is obvious that the parameters which affect the normal stiffness of the machined surfaces are the coefficients c and m. These values depend upon the following factors:

- Pair of Materials;
- Machining Process;
- Orientation of Machining Lays;
- Asperities Height;
- Hardness;
- Flatness Deviation and Size of Contact Area.

To determine the coefficients c and m generally small test specimens are used to reduce the effect of waviness and to obtain uniform contact between the surfaces. Ostrovskii[5] and Dolbey[10] have used the test specimens with dimensions of 25x25 mm and 76x76 mm respectively. Dolbey[10] conducted the experiment for maximum interface pressure of 5 kg/cm^2 and calculated coefficients c and m based on the measured deflections at 2.15 kg/cm^2 and 4.30 kg/cm^2 using the following relations

$$m = \frac{\log \frac{\lambda_{4.30}}{\lambda_{2.15}}}{\log \frac{4.30}{2.15}} \qquad (2.10)$$

$$c = \frac{\lambda_{4.30}}{(4.30)^m} \tag{2.11}$$

Ostrovskii[5] have made experiments for higher interface pressures up to 30 kg/cm^2 and the coefficients *c* and *m* were derived by analysing the contact deformation curves constructed in double logarithmic grid by the least square method.

In Table 2.1, the range of coefficients *c* and *m* is shown for different surface finishes of cast iron that are most frequently used in practice for pressures applicable to non-fixed machine tool joints.

Table 2.1 Coefficients *c* and *m* for Different Surface Finishes of Cast Iron.

PAIR OF SURFACES IN CONTACT	c	m
C.I. Hand Scraped/C.I. Hand Scraped, h=3 to 5μm, Z=20 to 25 spots/in^2 [2,11]	0.3	0.5
C.I. Hand Scraped/C.I. Hand Scraped, h=6 to 8μm, Z=20 to 25 spots/in^2 [2,11]	0.5	0.5
C.I. Hand Scraped/C.I. Hand Scraped, h=6 to 8μm, Z=15 to 18 spots/in^2 [5,11]	0.8-1.0	0.5
C.I. Hand Scraped/C.I. Hand Scraped, h=6 to 8μm, Z=10 to 12 spots/in^2 [2,11]	1.3-1.5	0.5
C.I. Hand Scraped/C.I. Hand Scraped, h=15 to 20μm, Z=5 to 12 spots/in^2 [2]	1.5-2.0	0.5
C.I. Hand Scraped, h=6 to 8μm, Z=15 to 18 spots/in^2/ C.I. Ground, h=1 μm CLA [2]	0.8-1.0	0.4
C.I. Ground/ C.I. Ground, h=1 μm CLA [10,5]	0.6-0.7	0.5
C.I. Finish Planing/ C.I. Finish Planing [5]	0.6	0.5
C.I. Ground/ Ferrosbestos Ground [10]	3.98	0.32
C.I. Ground/ Tufnol Ground [10]	2.36	0.4
C.I. = Cast Iron h = Asperity Height Peak to Valley		

Levina and Reshetov[11] recommend to use these coefficients for an interface pressure below 50 kg/cm^2 and report that for the first compression, the loading and unloading curves do not coincide due to partial plastic deformations. But for further loading and unloading the deflections are only elastic and Equation (2.7) with the coefficients of Table 2.1 is reliable.

2.4.1 Pair of Materials

It is obvious that the rigidity of the surface increases with the increase of modulus of elasticity of the material. It is not dependent on whether the normal deformation of the surfaces are elastic, plastic or the sum. In machine tool joints from stiffness point of view only elastic deformation is important, therefore for a given surface finish and different materials the resulting surface stiffness is dominated by elastic properties of the material pairs. When different materials are considered, while c varies in the order of the variation of the modulus of elasticity, the values of m remain approximately constant and equal to 0.5. Values of c for several surface finishes of cast iron are tabulated in Table 2.1. When different materials are used, however, the value of c can be calculated as being inversely proportional to the modulus of elasticity.

2.4.2 Surface Asperities and Machine Lay Orientation

Depending upon the machining process, speeds and feeds used, a roughness is always present in all machined surfaces. When the profile of the asperities are analysed it is found that peak heights are distributed within the value of h, that is the maximum peak-to-valley height for a certain sample length.

As reported by Kragelskii[4], Greenwood[6], and Buc and Nowicki[7] the distribution of the asperities can be: normal, exponential, linear, uniform and power law, depending upon the machining process. If the asperities are replaced by equivalent rods with an average cross section, and elastic deflections are assumed; then as the interface pressure increases the area of contact increases resulting in an increase of the stiffness. If the maximum peak-to-valley value h decreases, for a fixed deflection the probability of a higher area in contact increases. Therefore, it is easy to see that when the rod model is used, the surface stiffness increases when the asperity height decreases.

In addition to the rod model; there is spherical or ellipsoidal models where Hertz theory is used to evaluate the deformation of the surfaces. When the roughness of the surfaces decreases then the tip radii of the peaks increases, and hence this is another reason for the increase in the stiffness of smoother surfaces.

When the surfaces are turned or shaped with a single point tool and with larger feeds then it is reported that the lay orientation influence the surfaces stiffness. Schofield[9] tested these types of surfaces and found that when the angle between machine lays increases, the stiffness also increases slightly. The conclusion from these works is that any parameter which increases the real area of contact also improves the stiffness of the surface.

2.4.3 The Effect of Hardness

Effect of hardness on surface stiffness was investigated by Dolbey[10] using cast iron specimens at low contact pressures and the results showed that the hardness had no considerable effect.

Connolly et al.[14] tested both shaped and ground specimens of steel with different surface finishes. These surfaces were tested up to pressures of 1600 kg/cm^2 and for the first loading, the total deflection was the sum of elastic and plastic deformations. For the first loading it was observed that the total deflection decreased with the increase in hardness since the plastic component considerably decreased. Subsequently when the unloading was recorded then as the hardness increased the elastic recovery also increased. Eventually, this means that the surface stiffness decreases with the increase in hardness. Reason for this behaviour can be explained as follows: when the asperities of soft material are compressed at high interface pressure the plastic flow at the asperities increases the real contact area of the surfaces. While the modulus of elasticity remains constant, the initial plastic flow and the real area of contact decreases. Then, It can be concluded that the increase of hardness has a negative effect on the stiffness of the surfaces.

2.4.4 The Effect of Flatness Deviation and Surface Size

Flatness deviation and surface size depend on each other, when the size of the surface increases, the probability of flatness deviation also increases. Then, they can be analysed together as one factor.

Buc and Nowicki[7] made experiments by measuring the real area of contact and, found that for constant interface pressure, the relative value of the real contact surface decreases as the nominal surface increases. It is then, concluded that for larger apparent areas the surface stiffness per unit area decreases.

Connolly and Thornley[13] tested mild steel specimens of annulus form, which had a constant interface area but different outside diameters. As the outside diameter increases the flatness deviation also increases. The shaped surfaces were less sensitive to flatness deviation than ground surfaces. They also compared two large surfaces, one hand scraped and another planed. With scraping, the machining errors are partially eliminated and only the planned surface stiffness was affected.

From the tests carried out by Connolly and Thornley[13], as stated above, rougher surfaces are less sensitive to flatness deviations. From this Schofield and Thornley[8] proposed that the surface stiffness of larger surfaces could be improved by the use of rougher surfaces to eliminate the influence of the flatness deviations.

Tenner[12] measured the slideway stiffness of seven single column jig borers. When the torque is applied about the vertical axis, the slideway stiffness was within the range of 220 to 560 kg cm/μm/m. But, the theoretical stiffness obtained by using Equation (2.7) was 5 to 13 times greater than the experimentally obtained values. If the relationship between the calculated and experimental values were constant for all machines then the difference could be explained only in terms of elastic deformations of the components. However, since there was considerable scatter in the results, this was explained in terms of the errors in manufacturing the mating surfaces, or the flatness deviations.

To show the effect of flatness deviations on the surface stiffness Levina[11] and Tenner[12] have derived equations relating the stiffness and some regular flatness deviations. Simple convex to sinusoidal surfaces against flat surfaces were analysed, both theoretically and experimentally. In the case of convex and concave deviation, the flatness error over the slideway length was represented by a parabola. The mating elements were assumed to be rigid and that over all the surface in contact, Equation (2.7) was valid. They have predicted the influence of several ideal shapes of flatness deviations. They found that the stiffness of the surfaces is largely dependent upon the shape and frequency of the deviations and not only upon the maximum value. For the low interface pressure the error in calculation of the deflections could be large if the flatness deviation is neglected.

If the influence of the flatness deviation is taken into account for the calculation of the deflection of surfaces, it would be necessary to have a complete record of the shape, frequency, distribution and maximum error of the machined surfaces in contact. This is a difficult task, and therefore the simplest way is to analyse the results of the idealised errors and include a safety factor.

2.5 THE STIFFNESS OF MACHINE TOOL JOINTS

The starting point for the calculation of the stiffness and pressure distribution of joints, is the behaviour of two machined surfaces when pressed against each other. If the contacting surfaces and components around the contact are assumed to be rigid; then depending upon conditions of joint and loading case, the distribution of the pressure at the surface in contact could be estimated easily. However, it is obvious that in practice both the surface and the components are not rigid. So, this leads to a situation where the contact condition and deformations are more difficult to solve. This is an undetermined system, where the pressure distribution is dependent upon both the surface characteristics and the deformation and vice-versa. This type of problem is generally solved by iterative methods.

Up to date, except a few study[18-23], the stiffness and pressure distribution of the joints was calculated by assuming that the components at the surrounding of the surface in contact are rigid and only the approach of the surfaces is considered. In some applications the whole joint was assumed to be rigid. When either of assumptions are used, the calculated and experimental results can only be compared in qualitative form.

2.5.1 Bolted Joints

The factors that are taken into account in the design of a bolted joint are the load, preload, material and stiffness of the bolt and the members. The manner of load sharing is dependent on the stiffness of the bolt and the members. The bolt and member stiffness, k_b and k_m, must be determined accurately to have an agreement between the theoretical analysis and the actual behaviour of joint. As the bolt an element with high stress concentration, fatigue life of the joint must be considered. In order to increase the fatigue life of a joint, it is necessary to have a low value of bolt load. To reduce the value of bolt load, it is necessary to decrease the bolt stiffness or to increase the members stiffness.

In general, the calculation of bolt stiffness is easy, because it can be considered as a bar in simple tension. Determination of the member stiffness, however, is complex because the compression spreads out between the bolt head and the nut and the compressed area is not uniform

There have been many attempts to determine the member stiffness, k_m. As Fritsche[24] reported, Rötscher is the first who proposed a conical stress distribution on the connected parts about the mid plane of the joint. He assumed a cone angle of 45° but in his formulation he replaced conical frustrum with a cylinder having the same cross sectional area.

Fritsche[24] himself after experimentation suggested an expression which takes only equal thicknesses into consideration. As reported by Stuck[25], Ten Bosch, Bach and Findeisen used the assumption of conical stress distribution. They assumed 45° cone angle and obtained the expression by using the method of integration of infinitesimal deflections through the thickness of single frustrum. Birger, however, suggested to use a cone angle of 21.8° instead of 45°. Weiss and Walner and Danilow have suggested formulas for the stiffness of the connected parts after experiments as also reported by Stuck[25].

Osgood's experiments in photo elasticity as reported by Dann[26], showed that the cone angle is in the range of 25° to 33° for most alloys.

He used nominal value of 30° in his calculations and suggested to use a cylinder instead of a cone for the formulation of stiffness of each part.

Ito[27] had used ultrasonic techniques to determine stress distribution at the part interface and proposed that proper value of cone angle is dependent on the material. Shigley and Mischke[28] pointed out that cone angle may be left as a variable during integration process but in their calculations, they have recommended to use 30°.

Motosh[29] provided a realistic technique, and compressive stress in the connected parts is described by a fourth order polynomial as the function of radius r, the co-ordinate z and the cone angle α. But due to complex and tedious calculations, this method seems to be not practical.

Osman et al.[30] suggested to use a hollow cylinder of height equal to the grip length, and annular area equal to 1.25A where A is the nominal area of the bolt.

Akkurt[31] suggested to use a formula, by using annular area expressed in terms of bolt diameter and the grip length which is equal to total thickness of the members plus half of the nut height.

Yıldırım[32], and Filiz and Yıldırım[33], from their experimental work, suggested a stiffness formula which includes thickness ratio of the members as a variable too. Wileman et al.[34] had made considerable contribution for the evaluation of part stiffness by using Finite Element Method and suggested a formula.

The formulas suggested in all these studies are given in Table 2.2 with the resulting k_m values for a specific bolted joint where d= 8 mm, d_w= 12 mm, L= 36 mm, L_1= L_2=18 mm, E= 206.8 GPa. As shown in this table,

Table 2.2 Stiffness Formulae of Previous Studies

	STIFFNESS FORMULAE	k_mx10^9 (N/m)	NOTES
MISCHKE	$k_m = \dfrac{0.577\pi E d}{2\ln(\dfrac{(0.577L+0.5d)}{(0.577L+2.5d)})}$	1.350	
TEN BOSCH et al.& BIRGER*	$k_i = \dfrac{C\pi E_i d_h}{\ln(\dfrac{(Bl_i+d_w-d_h)(d_w+d_h)}{(Bl_i+d_w+d_h)(d_w-d_h)})}$	2.041 1.056*	C=1, B=2 C^*=0.4, B^*=0.8
FRITSCHE	$k_m = C\dfrac{\pi}{4}d_h E_m(\dfrac{L}{d_h}(E_m*10^{-3})^2)^{-0.16}$	0.895	C=9810x1.82 E_m is in kg/mm^2
WEISS and WALLNER	$k_m = \dfrac{\pi E_m}{4L}((d_w+\dfrac{L}{10})^2-d_h^2)$	0.809	
DANILOW	$k_m = \dfrac{d_h^2 E_m}{L(0.5-0.1\dfrac{L}{d_h}+0.007(\dfrac{L}{d_h})^2)}$	1.917	
OSGOOD	$k_i = \dfrac{\pi E_i}{4l_i}((d_w+\dfrac{l_i}{2})^2-d_h^2)$	1.700	$\dfrac{1}{k_m}=\dfrac{1}{k_1}+\dfrac{1}{k_2}$
RÖTSCHER	$k_m = \dfrac{\pi E_m}{4L}((d_w+\dfrac{L}{2})^2-d_h^2)$	3.771	
OSMAN	$k_m = 1.25A_b E_m / L$	0.361	
AKKURT	$k_m = \dfrac{A_m E_m}{L}\qquad A_m = \dfrac{\pi}{4}(D_0^2-D_i^2)$	0.664	D_0=1.2D_i+0.1L D_i = 1.14d L= L_1+L_2+h_n/2
FİLİZ and YILDIRIM	$k_m = Cd_h E_m(\dfrac{L_1}{L_2})^{0.045\frac{L_1}{L_2}}(\dfrac{L}{d_h})^{-0.008L}$	1.399	$L_1 \geq L_2$ C=1.66(π/4)
WILEMAN et.al.	$k_m = E_m dCe^{B(\frac{d}{L})}$	1.502	C=0.78952 B=0.62914

some expressions could be used only when the materials of the members are the same and their thicknesses are equal. As it is also shown, there are large differences between the calculated values of the stiffness.

2.5.2 Sliding Joints

Surface compliance for a range of mean interface pressures and surface finish used in the machine tool slideways have been analysed by Levina[2,3], Ostrovskii[5] and Tenner[12]. They obtained the Equation (2.7) that is based on experimental data to describe the relationship between the normal pressure and the approach of the surfaces.

The factors affecting the relationship between the normal or interface pressure and the approaches of the surfaces are evaluated in detail by Back[21]. He recommended that it is adequate to have an approximate knowledge of the surface compliance parameters obtained from a test, and concentration must be given more to the compliance of the components of machine tool joints. Because, the static stiffness of joints is more dependent upon the elasticity of the components surrounding the surfaces in contact rather than the compliance of the contacting surfaces. This does not mean that all of the work on the surface contact compliance is unnecessary, instead, such surface characteristics are necessary to formulate the solution of the complete joints.

Masuko and Ito[35] analysed contact pressure distribution on the slideways under mixed lubricated condition with the use of ultrasonic wave method. The slideway design methods which have been used commonly among the machine tool designers, were re-examined through the experimental results of contact pressure distribution and it was confirmed that the design method is correct for most cases except for a heavy cutting machine tool.

Hinduja[20] and Back[21] have investigated the deformation and pressure distribution in the joints by FEM. They have developed hydrostatic, plate and spring methods for modelling the contact between fixed and sliding joints. On comparison with the experimental results, it was shown that the finite element technique is a powerful engineering tool that can be applied to joints with fixed and sliding components.

Furukawa and Moronuki[36] analysed contact deformation of a machine tool slideway and its effect on machining accuracy. They proposed a design policy to minimise the machining error by obtaining three dimensional displacements of the slider caused by contact deformation.

Hashimoto et al.[37] developed a method for contact stiffness estimation. They estimated contact stiffness by a beam model vibrating on an elastic foundation, and constructed an experimental equation as a function of the clamping load and surface topography.

Finally, it can be concluded that the total deflection at the contacting joints is more dependent upon the elasticity of the components surrounding the surface in contact than the compliance of the surface itself. In some cases, it would be wise to neglect the surface approach instead of the deformations of the components. If this assumption is used then due to the deformations of the components only points or lines of contact between the surfaces would occur. This is also not a reasonable assumption since further difficulties would appear for the general formulation of the problem.

Thus, it can be said that, in order to model contacting surfaces, and to determine the pressure distribution at the contact and deformation of components, it is necessary to have some information about the compliance of the machined surfaces, in addition to the elastic properties of the surrounding components.

CHAPTER III

FINITE ELEMENT METHOD
AND
CONTACT ELEMENTS

3.1 INTRODUCTION

The purpose of this chapter is to present a brief review about theory of finite element method(FEM) which is the tool to be used throughout this study. Section 3.2 is devoted to the reviews on the finite element analysis and application of FEM. ANSYS as a finite element software package is discussed in section 3.3. Contact phenomenon, contact non-linearities, ANSYS's contact elements and contact stiffness are explained in Section 3.4.

3.2 FINITE ELEMENT METHOD

The FEM is a numerical analysis technique for obtaining approximate solution to a wide variety of engineering problems and has become a useful tool for the stress analysis. Although originally developed to study the stresses in complex airframe structures, it has since been extended and applied to the broad field of continuum mechanics. Because of its diversity and flexibility as an analysis tool, it is receiving much attention in every field of engineering and industry. The FEM would not be practical without the availibility of fast computers with a large amount of memory. The development of method and computers have progressed simultaneously.

Today, it is clear that it is necessary to obtain numerical approximate solution to more and more engineering problems rather than exact closed form solutions. For example, it is required to find the load capacity of a plate which has several stiffeners and odd-shaped hole, the concentration of pollutants during non-uniform atmospheric conditions, or the rate of fluid flow through a passage of arbitrary shape. Without too much effort, the governing equations and boundary conditions can be written down, for these problems, it is seen immediately that no simple analytical solution can be found. The difficulty in the above three examples lies in the fact that either the geometry or some other feature of the problem is irregular or arbitrary. Analytical solutions to problems of this type seldom exist; yet engineers and scientist are called upon to solve these kinds of problems.

A finite element model of a problem gives a piece wise approximation to the governing equations. The basic premise of the FEM is that a solution region can analytically be modelled or approximated by replacing it with an assemblage of discrete elements. Since these elements can be put together in a variety of ways, they can be used to represent exceedingly complex shapes.

The analysis of joints which is presented in the thesis is based entirely upon the FEM. This technique is used as a tool for the determination of the deformation and pressure distribution at the contact of the components of the joints. Because of the importance of the FEM in this work, the technique with a short description of the contact elements is outlined below.

Finite element method basically consists of pointwise discretisation for the satisfaction of boundary conditions in terms of nodal values and interpolation of shape function and piece wise discretisation to simplify the assumed trial solution. There are a few different formulations for finite elements. The finite element can be formulated based on the assumed displacement field and the principle of minimisation of potential energy. It is called as the displacement element method whose detailed review can be found in many publications, for example, Zienkiewicz[38], Kardeştuncer[39], Iron and Ahmed[40], Reddy[41], and Güzelbey[42].

3.2.1 How the Finite Element Method Works

In a continuum problem of any dimension, the field variable (whether it is pressure, temperature, displacement, stress or some other quantity) possesses infinite number of values because it is a function of each generic point in the body or solution region. Consequently, the problem is one with an infinite number of unknowns. The finite element discretisation procedure reduces the problem to one of the finite number of unknowns by dividing the solution region into elements and by expressing the unknown field variable in terms of assumed approximating functions with each element. For example, a beam might be represented by a number of rectangles, as in Figure 3.1. The approximating functions are defined in terms of the values of the field variables at specified points called nodes or nodal points. Nodes usually lie on the element boundaries where adjacent elements are considered to be connected.

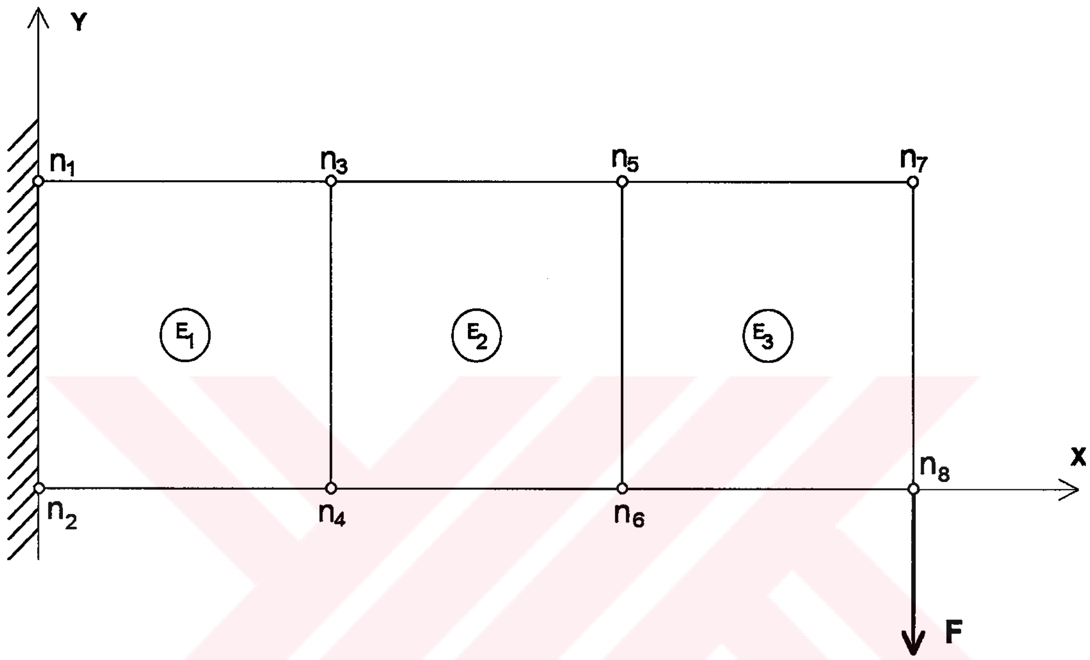

$n_{1,2,3...}$= Nodes
$E_{1,2,3...}$= Elements
F = Applied Force

Figure 3.1 A Beam Represented by Finite Elements.

In addition to boundary nodes, an element may also have a few interior nodes. The nodal values of the field variable and the interpolation functions for the elements completely define the behaviour of the field variables within the elements. For the finite element representation of a problem, the nodal values of the field variable become the new unknowns. Once these unknowns are found, the interpolation functions define the field variable throughout the assemblage of elements. Clearly, the nature of the solution and the degree of approximation depend not only on the size and number of elements used, but also on the interpolation function selected.

FEM has an important feature which sets it apart from other approximate numerical methods. That feature is the ability to formulate solutions for individual elements before putting them together to represent the entire problem. This means, for example, that if a problem in stress analysis will be treated, first the force-displacement or stiffness characteristics of each individual element is found and then assembled according to the element topology to find the stiffness of the whole structure. In essence, a complex problem reduces to a series of greatly simplified problems.

In the FEM one can formulate the properties of individual elements in some variety of ways. There are basically four different approaches. The first approach to obtain element properties is called the direct approach, because its origin is traceable to the direct stiffness method of structural analysis. The direct approach is generally used only for relatively simple problems, because it is the easiest to understand when meeting the FEM for the first time. This approach also suggests the need for matrix algebra in dealing with the finite element equations.

Element properties obtained by the direct approach can also be determined by the more versatile and more advanced variational approach. The variational approach relies on the calculus of variations and involves maximising a function. Knowledge of variational approach is necessary to work beyond the introductory level and to extend the FEM to a wide variety of engineering problems. Whereas the direct approach can be used to formulate element properties for only the simplest element shapes the variational approach can be employed for both simple and sophisticated element shapes.

A third and even more versatile approach to deriving element properties has its basis entirely in its mathematics and is known as the weighted residual approach. The weighted residual approach begins with the governing equations of the problem and proceeds without relying on a functional or a variational statement. This approach is advantageous, because it thereby becomes possible to extend the FEM to problems where no functional is available.

A forth approach relies on the balance of thermal and/or mechanical energy of a system. The energy balance approach (like the weighted residuals approach) requires no variational statement and hence broadens considerably the range of possible applications of the FEM.

3.2.2 Steps of the FEM

Regardless of the approach used to find the element properties, the solution of a continuum problem by the FEM always follows an orderly step by step process. To summarise in general terms how the FEM works, the steps can be listed as follows:

1. *Descretize the Continuum:* The first step is to divide the continuum or solution region into elements. A wide variety of element

shapes may be used as shown in Figure 3.2. Different element shapes may be employed in the same solution region. The number and the type of elements to be used in a given problem are the matters of engineering judgement. The experience of other analysts can be used as guidelines.

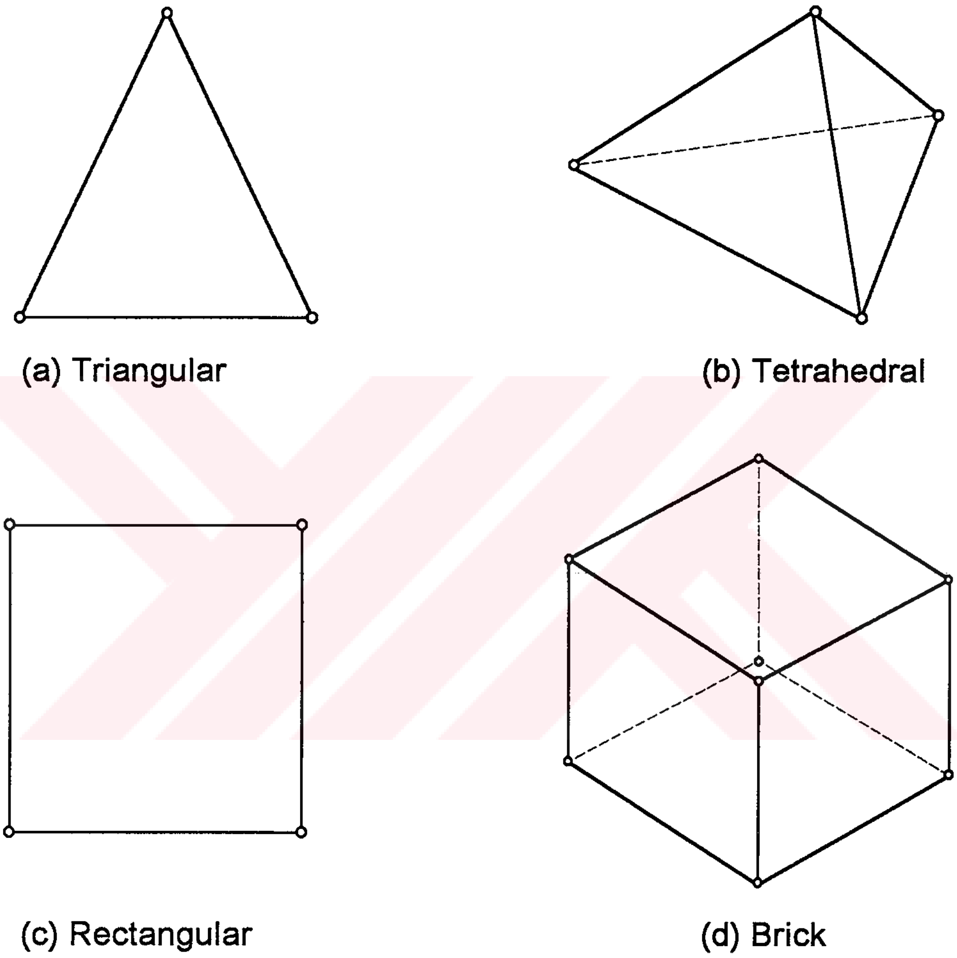

Figure 3.2 Some Element Shapes Used in Finite Element Analysis.

2. *Select Interpolation Functions:* The next step is to assign nodes to each element and then choose the type of interpolation function to represent the variation of the field variable over the element. The field variable may be a scalar, a vector, or a higher order tensor. Often,

polynomials are selected as interpolation functions for the field variable, because they are easy to integrate and differentiate. The degree of polynomial chosen depends on the number of the nodes assigned to element, the nature and number of unknowns at each node, and certain continuity requirements imposed at the nodes and along the element boundaries. The magnitude of field variable as well as the magnitude of its derivatives may be the unknowns at the nodes.

3. *Find the Element Properties:* Once the finite element model has been established (that is, once the elements and their interpolation functions have been selected), the matrix equations expressing the properties of the individual elements can be constructed. One of the four approaches just mentioned can be used, i.e. the direct approach, the variational approach, the weighted residual approach or the energy balance approach. The variational approach is often the most convenient one, but for any application the type of approach used depends entirely on the nature of the problem.

4. *Assemble the Element Properties to Obtain the System Equations:* To find the properties of the overall system modelled by the network of elements, all the element properties must be "assembled". In other words, the matrix equation which expresses the behaviour of the entire solution region of the system is constructed. The matrix equations for the system have the same form as the equations for an individual element except that they contain many more terms because they include all nodes.

The basis for the assembly procedure stems from the fact that, at a node where elements are interconnected, the value of field variable is the same for each element sharing that node. Assembly of the element equations is a routine matter in finite element analysis and usually done by computers.

Before the system equations are ready for solution, they must be modified to act for the boundary conditions of the problem.

5. *Solve the System Equations:* The assembly process of preceding step gives a set of simultaneous equations which can be solved to obtain the unknown nodal values (displacements of the nodes) of the field variable. If the equations are linear, a number of standard solution techniques can be used. If the equations are non-linear, their solution is more difficult to obtain.

6. *Make Additional Computations if Desired*: Sometimes, the solution of the system of equations may be used to calculate other important parameters. For example, using the nodal values of displacements, stress distributions and shear stresses in the members can be calculated.

3.2.3 Range of Applications

Application of FEM can be divided into three main categories depending on the nature of the problem to be solved. In the first category, all the problems are known as equilibrium problems or time independent problems. The majority of applications of the FEM fall into this category. For the solution of equilibrium problems in the solid mechanics area, it is necessary to find the displacement distribution or the stress distribution, or perhaps the temperature distribution for a given mechanical or thermal loading.

Second category is the so-called eigenvalue problems of solid and fluid mechanics. These are steady-state problems whose solution often requires the determination of natural frequencies and modes of vibration of solid and fluids. Examples of eigenvalue problems involving both solids and fluid mechanics appear in all kind of engineering applications.

Third category is the multitude of time-dependent or propagation problems of continuum mechanics. This category is composed of problems which result when the time dimensions is added to the problems of the first two categories.

3.2.4 Background Needed for Effective Use of Finite Element Computer Programs

The user of a finite element program is dependent on the detailed knowledge about theories, algorithms, and assumptions behind the program for the proper selection of models and algorithms as well as for monitoring the solution process. There are also many practical problems whose solution may require modifying (may be slightly) the program. Therefore, the effective evaluation and use of finite element programs require some knowledge of the following:

1. Basic finite element theory. Many texts and monographs have been written on the subject[38-42].

2. Mathematical modelling and formulation of the engineering and applied science problems included within the scope of the program.

3. Numerical algorithms used in the program and their efficiency. These include solution of linear (and non-linear) algebraic equations, extraction of eigenvalues, and temporal integration techniques.

4. Software engineering tools such as data base management techniques, programming languages, decomposition of the program into functional modules, and structured programming concepts.

3.2.5 Available Finite Element Computer Programs

Every branch of engineering is a potential user of the finite element method. The range of possible application of the finite element method extends to all engineering disciplines, but civil and aerospace engineers concerned with stress analysis are the most frequent users of the method. Major aircraft companies and other organisations involved in the design of structures have developed elaborate finite element computer programs. Many of these special purpose programs are proprietary.

The significant advances made in finite element technology, coupled with the rapid developments in computer hardware and software, provided the foundation from which general purpose finite element programs have evolved. After many years of development, a wide variety of finite element programs are currently being used in industry for the solution of a wide variety of practical problems. By the mid-1980s, there were about 500 user oriented and several thousand research oriented finite element program systems. Most of them known by the trade names such as; ABAQUS, ADINA, ANSYS, NASTRAN, PAFEC, etc. The potential user of a finite element system must be careful about the sorting out the existing finite element programs, and identifying the program that is best suited to his or her particular needs.

3.3 ANSYS AS A FINITE ELEMENT ANALYSIS PACKAGE

3.3.1 General Information

ANSYS[43-46] is a large scale, general purpose, finite element program used by design engineers for structural, thermal, fluid, electrical and static electromagnetic analysis. ANSYS has been used since 1970 in many industries, including nuclear, aerospace, automotive, power, transportation, biomechanics, steel, railroad, packaging, civil construction, and electrical/electronics industries. ANSYS is supported by a full-time customer-support staff in Pennsylvania and by a network of ANSYS technical support distributors in North America, Europe, Turkey, and the Far East.

3.3.2 Program Capability

ANSYS is used for finite element analysis of static, dynamic, thermal, linear or non-linear cases, and performed in two or three dimensions. ANSYS includes submodelling for detailed regions of linear and non-linear structures. In addition to many analysis capabilities, ANSYS has three main phases of finite element analysis, as preprocessing, solution and postprocessing. No additional software package is needed for generating a model or examining the analysis results.

Powerful graphics capabilities are essential for productive use of finite element analysis, and the ANSYS program is one of the first commercial FE programs to offer substantial built-in animation, translucency, and three dimensional isosurface capabilities for appropriate hardware display devices.

3.3.3 User Interface and Modelling Capability

Preprocessing for model and load creation and verification is included in ANSYS. Both mesh and loads may be generated using automatic procedures. Both can be verified graphically. On-line documentation is available for each command. ANSYS post processing supports many graphic options-hidden line, section, x-y plots, distorted shape, and contour maps of stresses or temperatures. ANSYS post processing also includes a data base language so that results can be selectively examined.

The ability to pass information between various types of design and analysis programs adds flexibility to computer aided engineering analyses. Specifically, there is a need to precisely transfer geometry data from computer aided design (CAD) packages to analysis and manufacturing. ANSYS interfaces with many CAD systems by supporting open systems.

ANSYS recognising that Non-Uniform Rational B-Splines (NURBS) mathematics is emerging as an industry standard for geometry data. Therefore, geometry data from CAD packages based on NURBS-based representation can be transferred precisely to the ANSYS program, without any inherent loss of accuracy. ANSYS also supports the Initial Graphics Exchange Specification (IGES) as the industry standard by working closely with CAD vendors to ensure the technologies are an effective tool for transferring data. IGES, includes support for complex trimmed surfaces, up to and including the NURBS representation.

The ANSYS program uses a single, centralised database for storage of all model data and solution results as shown in Figure 3.3. Model data (including solid model and finite element model geometry, materials, etc.) are written to the database using the ANSYS preprocessor. The solution works directly from information in the database. Postprocessing results data is accomplished using the postprocessors which can access the data directly from the database. Data written to the database while using one processor are available, as necessary, in the other processors.

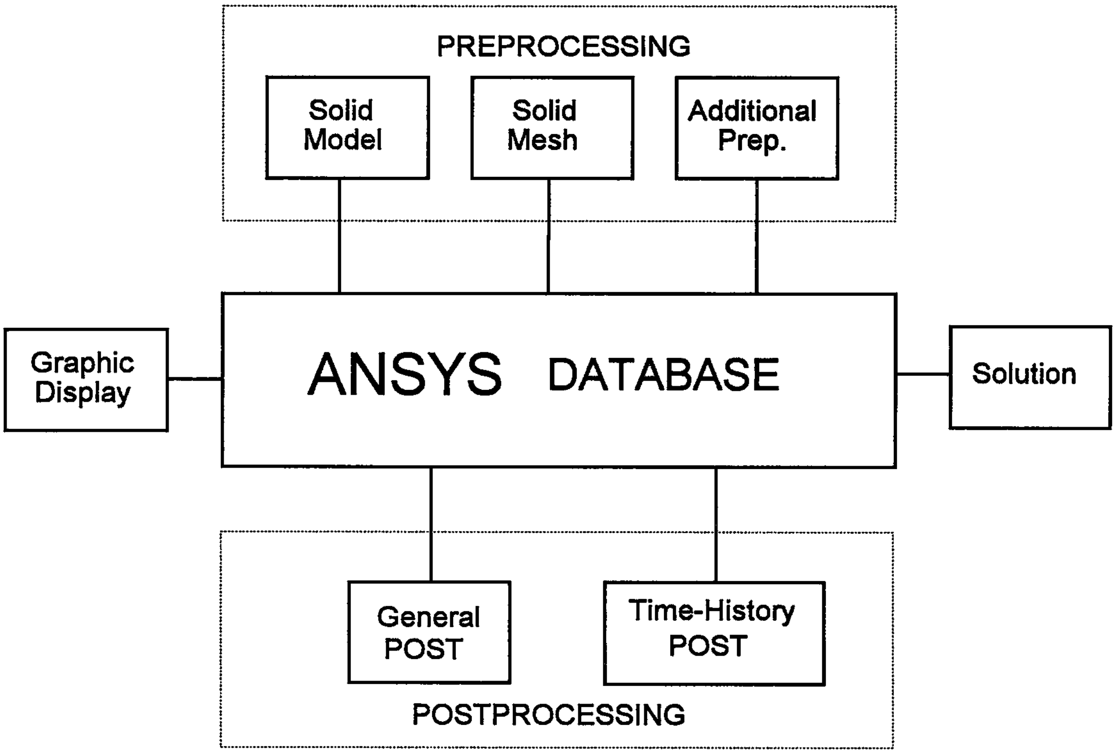

Figure 3.3 A Relational Diagram of the ANSYS Centralised Database.

The ANSYS element library consists of over 100 element types. Many have options which allow further specialisation of the element formulation in some manner, effectively increasing the size of the element library. Elements are categorised as two dimensional or three dimensional and may take the form of a point, line, area, or volume. Both linear and quadratic elements are available. Most elements allow appropriate element loading such as pressure, temperature, convection, etc.

ANSYS is able to handle up to 3000 degrees of freedom on the wave front. By using single or multi-level sub structuring, the number of possible degrees of freedom in a model is limited only by computer and time resources.

3.4 CONTACT PHENOMENON

Surface-to-surface contact is a phenomenon that occurs in most engineering applications: joints (bolted or sliding), metal forming, rolling operations, dynamic pipe whip, crash dynamics, assemblies of components, interference fit, etc. All of these problems as well as others, may be simulated with the ANSYS program. Engineers are interested in the stresses, deflections, deformations, and forces that occur due to the contact between structural parts. General contact is treated as a boundary non linearity. In the ANSYS[43] non-linear contact elements, analysis of surface-to-surface contact with large deformations, contact and separation, and sliding with friction is possible.

3.4.1 Contact Nonlinearities

Contact nonlinearities occur when two or more components (or parts of one component) come into contact with each other (or itself) during the course of the deformation process. Contact nonlinearities also occur when two components slide relative to one another. Contact is a non linearity because one or both of the following are unknown:

- The contacting area(s)
- The force transmitted, both normal and tangential directions.

General contact is represented by following the positions of points on one surface (the contact surface) relative to the points or lines or areas of another surface (the target surface).

To use the contact capability, the areas where contact might occur during the deformation must be identified. This identification is done through elements which will then track the kinematics of deformation process. There are two basic element types that may be used in analysis and they identify the type of contact conditions[43]:

- Node-to-node contact
- General surface-to-surface contact

Node-to-node contact occurs whenever a single point will come into contact with another point. The exact location of contact is presumed to be known beforehand. Only small amounts of relative sliding deformation are allowed.

Surface-to-surface contact occurs when two surfaces may come into contact. The exact location of the contacting area may not be known beforehand. Large amounts of relative sliding are permitted. Also the opposing meshes do not have to have the same discretisation. The two surfaces may both be part of a deformable body or one may be a rigid surface.

3.4.2 Contact Elements

The contact elements are used to track the relative positions of the two surfaces. In two dimensions the node-to-node contact element, CONTACT12, and the node to surface contact element, CONTACT48 (planar and axisymmetric) are shown in Figure 3.4 (a) and (b)[45]. In three dimensions the node-to-node contact element is CONTACT52, and the node to surface contact element is CONTACT49, and they are shown in Figure 3.5 (a) and (b) respectively. These contact elements are finite elements that apply appropriate forces to nodes on two surfaces to account for contact and friction.

3.4.3 Contact Stiffness

In order to handle a contact analysis with the finite element method, a stiffness relationship must be established between the two contact areas when contact occurs. Otherwise, the two areas will pass through each other. This relationship is established through a spring that is put between the two contacting areas when contact occurs. The spring will deflect an amount λ such that equilibrium is satisfied[47],

$$F = k_n \lambda \tag{3.1}$$

where k_n is the spring stiffness in this equation and it is called the contact stiffness and has the unit of force/length.

The amount of penetration, or incompatibility, between the two surfaces is therefore dependent on the stiffness k_n. Ideally there should be no penetration, but this implies $k_n = \infty$. High values of k_n also leads to ill conditioning of the global stiffness matrix, as well as convergence difficulties. Practically, a high enough stiffness value is required that the contact penetration is acceptably small, but low enough that the convergence or ill conditioning problems will not occur.

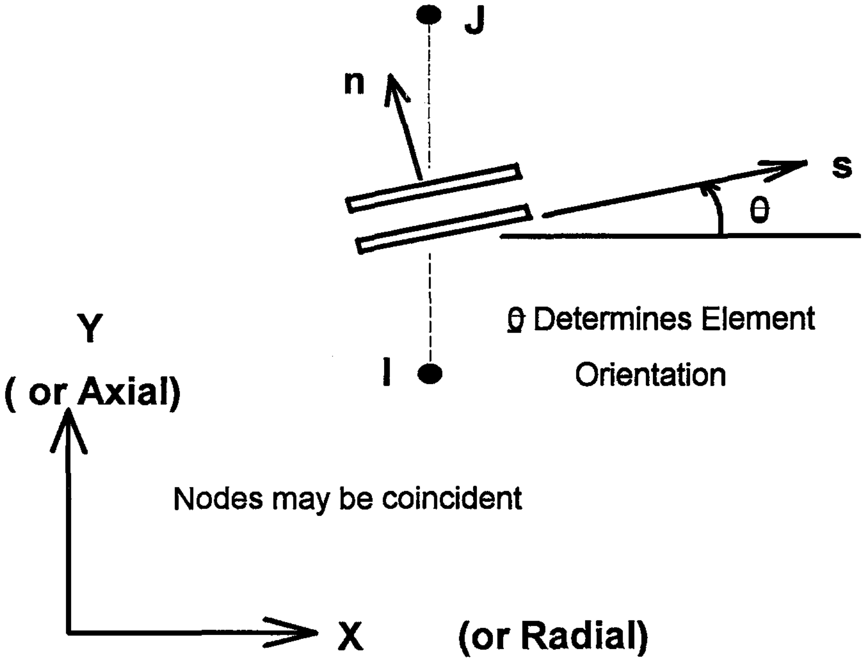

(a) Contact12

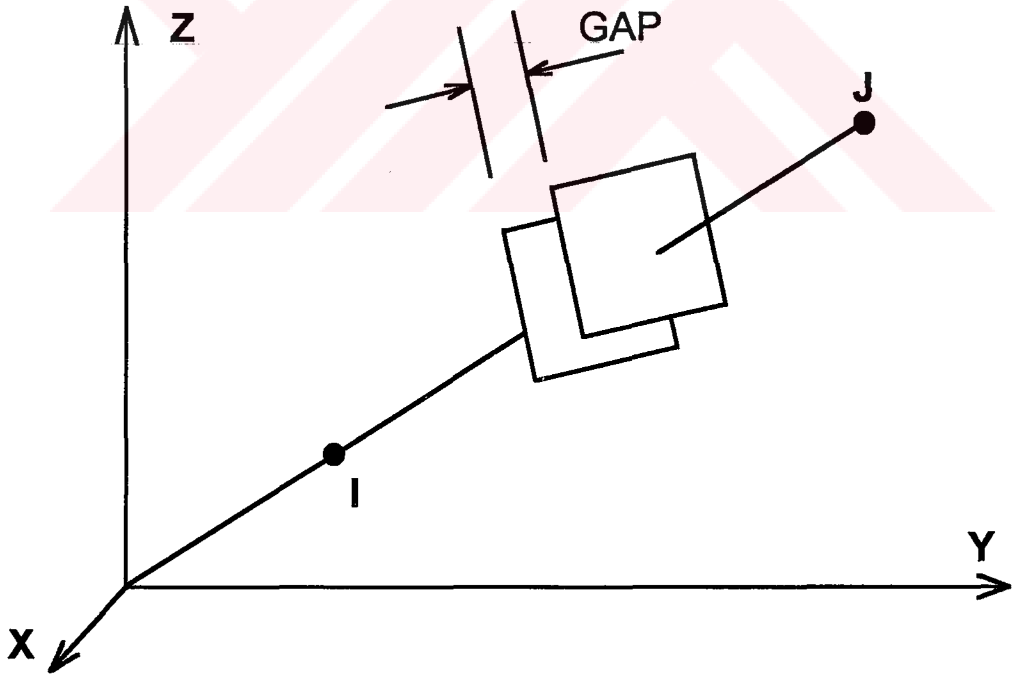

(b) Contact 52

Figure 3.4 Two and Three Dimensional Point to Point Contact Elements[45]

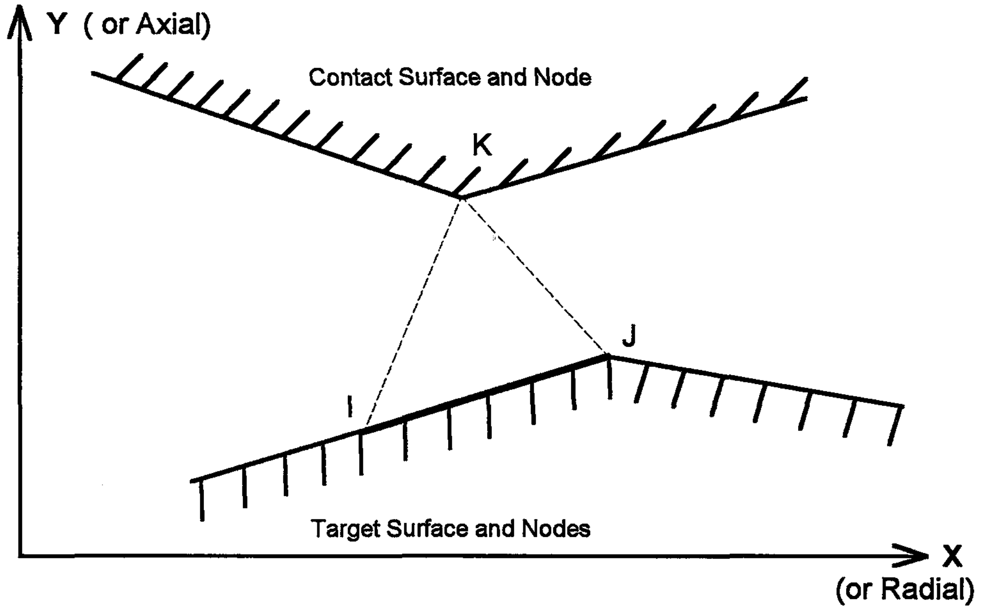

(a) Contact48

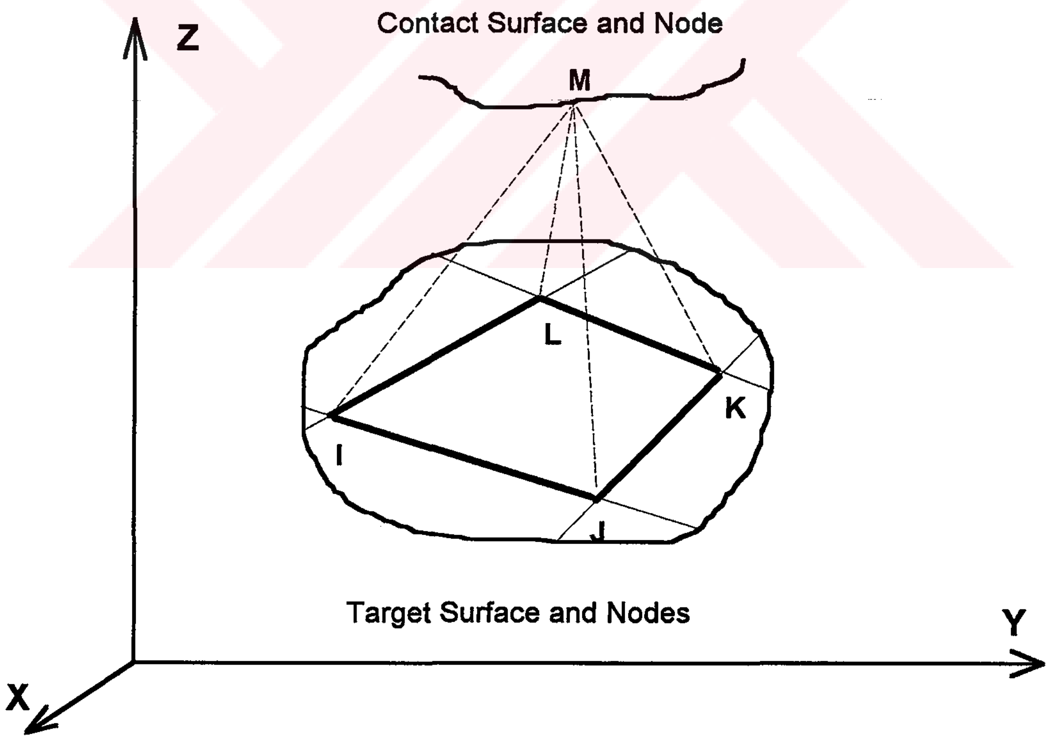

(b) Contact49

Figure 3.5 Two and Three Dimensional Point to Surface Contact Elements[45]

The value of k_n that should be used depends on the relative stiffness of the areas in contact. This stiffness may be estimated or computed from the local compliance of the components. Stiffness may be estimated using[47]

$$k_n = fEh_l \tag{3.2}$$

where f is a factor between 1 and 100, E is the elastic modulus of contacting material, and h_l is a measure of the characteristic contact length.

For contact between two different materials, the smaller elastic modulus of the two must be used. The contact length h_l depends on the geometry:

- For 3-D, h_l is a typical length associated with the contact area of a single contact point.
- For 2-D plain strain, 1.0 for h_l can be used.
- For 2-D plain stress, the thickness for h_l can be used.

CHAPTER IV

DESIGN
OF
MACHINE TOOL JOINTS

4.1 INTRODUCTION

The purpose of this chapter is to present briefly the design and analysis of machine tool joints. In section 4.2 general requirements of machine tool joints are described. Section 4.3 is devoted to the design of the bolted joints. In section 4.4, design of welded joints for two different models and loading conditions are discussed.

4.2 MACHINE TOOL JOINTS

A machine part is comprised of body parts and joint elements. A joint is defined as a break in the continuity of a machine structure. Joints are required in machine tools for assembling, manufacturing, functional reasons, transportation purposes and also for transmitting forces or torque between machine parts. Main joint types are: fixed and sliding joints. Fixed joints can be obtained by welding the components or assembling the components by bolts. They are named as welded joints and bolted joints respectively.

The main requirements for machine tool joints are: stiffness, stability and wear resistance[48,49]. Of course, in the case of fixed joints, only the static and dynamic stiffness is important. In this study only static rigidity will be considered for both fixed and sliding joints.

The joints have a great influence on the relative position between the theoretical machining point on the work piece and the tool tip point. On the lathe, for example, the main joints that define the relative position mentioned above are: headstock, tail stock, saddle to the bed and cross slide or compound box connected to the saddle. In this case four or five connections are involved. For other types of machines a similar analysis could be made, and in the load path, a large number of joints would be obtained. Levina and Nazarov[50] have analysed the deflection of single column jig-borer in three directions X, Y and Z. The deformations in the joints were of 63.6%, 67.5% and 76.5% respectively, while the deformations of the column, spindle, bearing etc., were only 36.4%, 32.5% and 23.5%.

Levina[2] reported similar results from experimental studies in lathes, vertical boring and turning mills and vertical milling machines where again 60 to 90% of total measured deflections are due to the joints itself. Therefore, careful considerations must be given in the design of joints.

4.3 BOLTED JOINTS

The design of a bolted joint requires determination of the number and the size of bolts as well as dimensions of the members to satisfy both sealing and strength requirements. That is, there must not be joint separation and static or fatigue failure of bolts under working load. In other words, there must always exist compression load on the members and the maximum load on the bolt must not be greater than the safe load.

If a preload is applied to the joint a tensile load on the bolt and a compressive load on the members is induced. When an external load is applied on a preloaded connection, tensile load on the bolt will increase while some of the compression load on the members will be relieved. The manner of load sharing is dependent on the stiffness of the bolt and the member. The bolt and member stiffness, k_b and k_m, must be determined accurately to have an agreement between the theoretical analysis and the actual behaviour of joints. Because, overestimation of member stiffness will result smaller load on the bolt than the actual case which may result shorter fatigue life than expected while underestimation of the member stiffness will result smaller load on the members than the actual case which may result separation of the joint although not expected.

The stiffness of the bolt is calculated by considering it, as a bar in simple tension.

$$k_b = \frac{AE_b}{L} = \frac{\pi E_b d^2}{4L} \tag{4.1}$$

4.3.1 Member Stiffness With Finite Element Method

Determination of the member stiffness, however, is complex because the compression spreads out between the bolt head and the nut and the compressed area is not uniform as shown in Figure 4.1.

By using FEM, a computer program is prepared to determine member stiffness directly from the given joint geometry. In order to evaluate the effect of joint geometry upon member stiffness, a number of models having different geometry were created. A practical formula is suggested for the determination of the member stiffness of bolted joints which may consist of members made from different materials and with different thicknesses. Finite Element Analyses were performed on a VAX/VMS system using developed Finite Element Program written in FORTRAN.

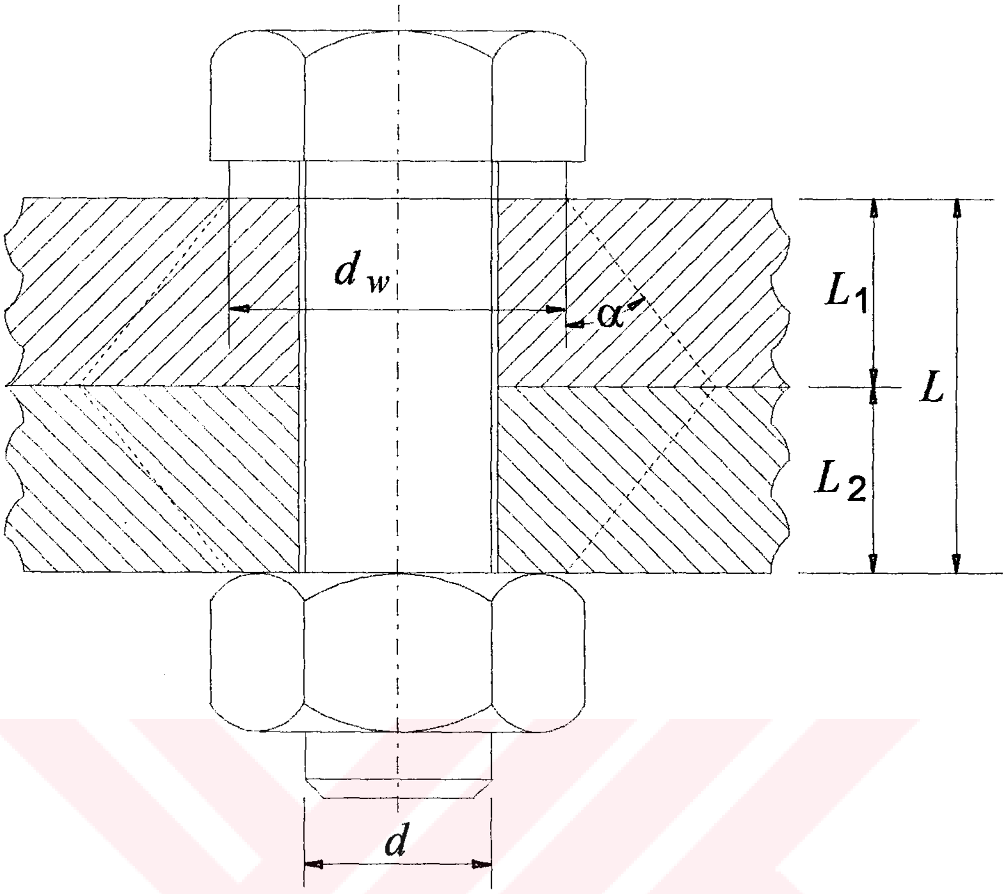

Figure 4.1 A Typical Bolted Joint

The developed program is based upon the displacement element method. Program is capable to analyse two dimensional elasticity, axisymmetric and sticking contact problems. Bolted joint is assumed as axisymmetric due to the geometry and loading. It has also been assumed that the slippage does not occur at the interface between the members, i.e. friction caused by the preload is considered to be sufficient to prevent slippage at the interface. The symmetry axis and the symmetry plane of the joint are shown in Figure 4.2. This symmetry reduce the joint model from three dimensional model to two dimensional model and from the whole cross section to the half of the joint. The finite element model of the joint has been obtained by dividing the initial regions of Figure 4.3 into the required size and number of elements. Joints are modelled by solid ring elements with a quadrilateral cross section and four noded quadrilateral elements. Although, in general, a model with eight noded quadrilateral elements gives more accurate results with less number of elements, in modelling bolted joints, four noded elements are used to illustrate the efficiency of the program developed.

While the model is being established, bolt, bolt head and nut have been removed from the model by putting their effects through the washer as uniform compressive loading. The compressive load is assumed to act from the annular area of the washer whose outside diameter is, $d_w = 1.5d$. The washer is assumed to be perfectly rigid and its elastic modulus is taken about thousand times higher than that of the members in order to obtain uniform displacement of the nodes at the washer interface. Symmetric boundary conditions are applied due to symmetry plane. It is obvious that, symmetry plane does not move under load in z-direction, but there is no constraint in the member in r-direction on the symmetry plane. This analysis gives the conical stress distribution in the member in addition to displacements at nodes, stresses at gaussian points and average stresses at nodes.

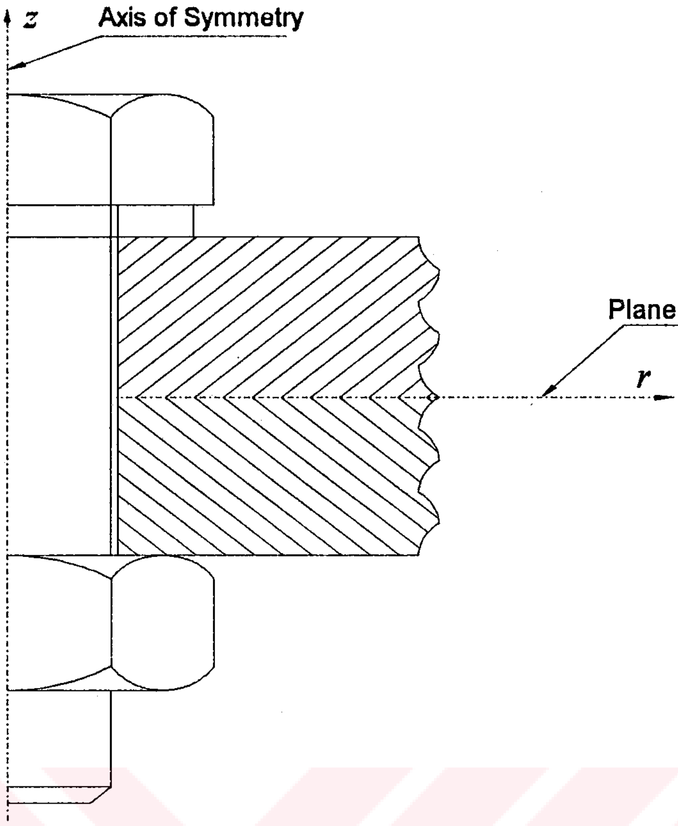

Figure 4.2 Symmetries in a Bolted Joint

As suggested by Maruyama et al.[51], the member radius is taken as at least three times greater than that of the hole radii to remove end effects. Because of the nature of FEM, the accuracy of the results depends on the mesh generation of the model. The convergence is verified by performing analyses with a coarse and a fine meshed model. Refinement of the model is continued until the difference between the results of last two analyses is less than one per cent. The final refined model contains 627 nodes, and 598 four noded elements and this model was used throughout the analysis.

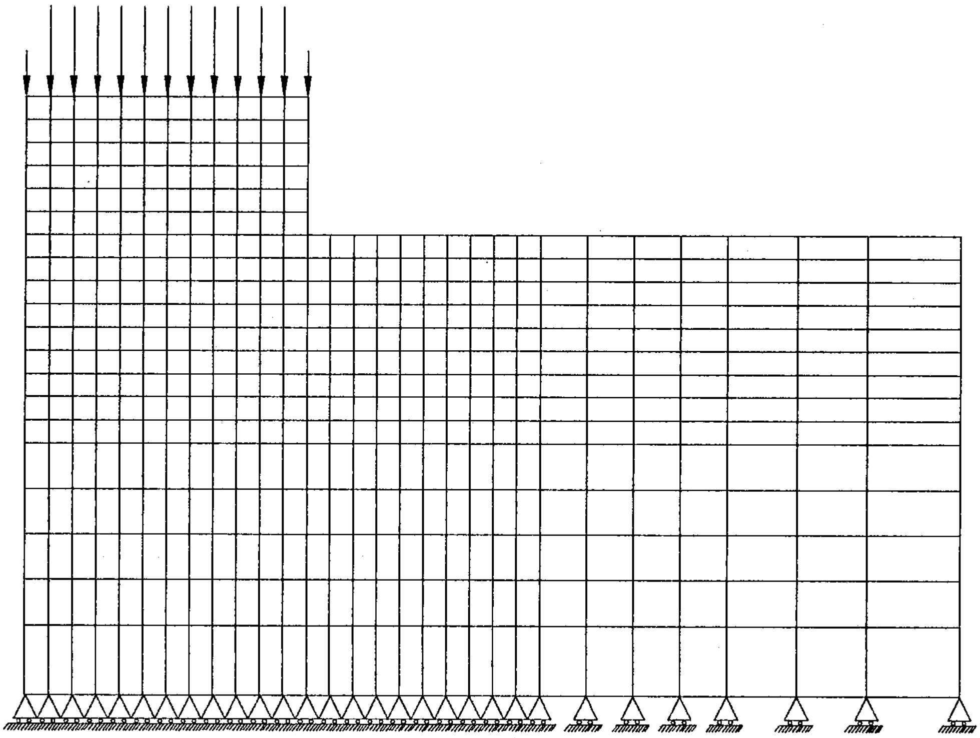

Figure 4.3 Finite Element Model of Bolted Joint Members

4.3.2 Examples

The grip length L, the material properties E and ν of the members, the bolt diameter d, and the pressure applied to the annular area of the washer are the input data to the FE program. Analyses are performed for joints made of steel, copper, cast iron or aluminium or any combination of these. Properties of these materials are given in Table 4.1. The member materials were assumed to be linearly elastic and homogeneous isotropic for each case. A constant pressure of 17.24 MPa is applied over the annular area of the washer to obtain a reasonable compressive load on the members. This particular value is used to compare the results with the results obtained by Wileman et al.[34] who had used the code ANSYS. The total load which is required to calculate member stiffness later, is equal to the applied pressure times annular area of the washer. The stiffness, k_m, is calculated by dividing the total load to the deflection of the node at the uppermost corner of the member in the model in Figure 4.3.

Table 4.1 Properties of Materials Used in the Bolted Joints

Material Used	Modulus of Elasticity, E (GPa)	Poisson's Ratio, ν
Steel	206.8	0.291
Aluminium	71.0	0.334
Copper	118.6	0.326
Cast Iron	100.0	0.211

4.3.2.1 Effects of Aspect Ratio(d/L)

In order to evaluate the effect of joint geometry on the member stiffness, two groups of models having different geometry were created. In the first group, the grip length, L, is taken as 24 mm (L_1=12 mm, L_2=12 mm), and the bolts with diameters range from 2.5 to 72 mm containing almost all standard bolt diameters are tested. Member stiffness variations with respect to d/L ratio are shown in Figure 4.4. Also, from the finite element results, the individual member stiffness, k_1 and k_2, are determined and then member stiffness of joints which might consist of members having different materials is calculated from Equation (4.2) and the results are plotted in Figure 4.5.

$$\frac{1}{k_m} = \frac{1}{k_1} + \frac{1}{k_2} \tag{4.2}$$

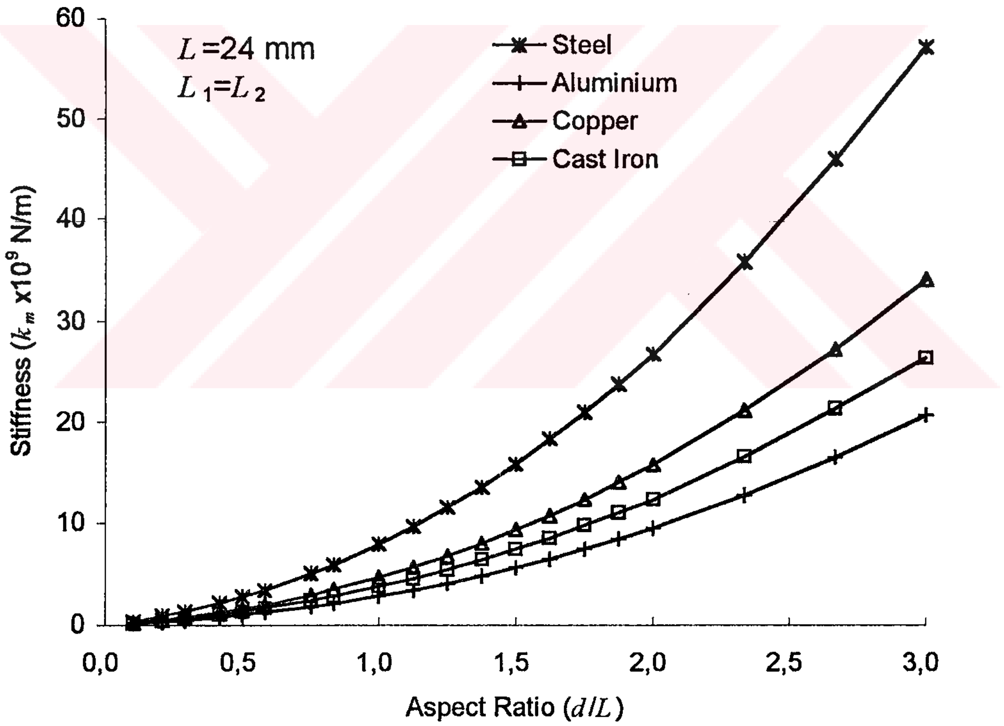

Figure 4.4 Stiffness Variations with d/L for Different Materials

4.3.2.2 Effects of Member Thickness(L)

In the second group, the effect of different member thicknesses on the member stiffness is investigated. Joints with different individual member thicknesses of 12, 16, 20, 24, 28, 32, 36, 40, 44, 48, 52, 56 and 60 mm were analysed for bolt diameters of 12, 18, and 24 mm. After determining individual member stiffness k_1 and k_2, the member stiffness, k_m, of the joints are calculated by using Equation (4.2) and the results are plotted in Figure 4.6.

4.3.3 Results

As shown in Figure 4.4, stiffness is almost directly proportional with the modulus of elasticity of the member material. The stiffness is related to the thickness of the members and the diameter of the bolt in a non-linear manner. A through study was performed by Wileman et al.[34] to obtain an equation of stiffness which would fit best with the results obtained from their finite element analysis. This equation is given in Table 2.2 and it takes into consideration only the joints with the members which are made from the same material and with equal thicknesses.

Additionally, Wileman's equation showed large deviation from FE analysis when $d/L>2$. This equation is modified to include the effects of

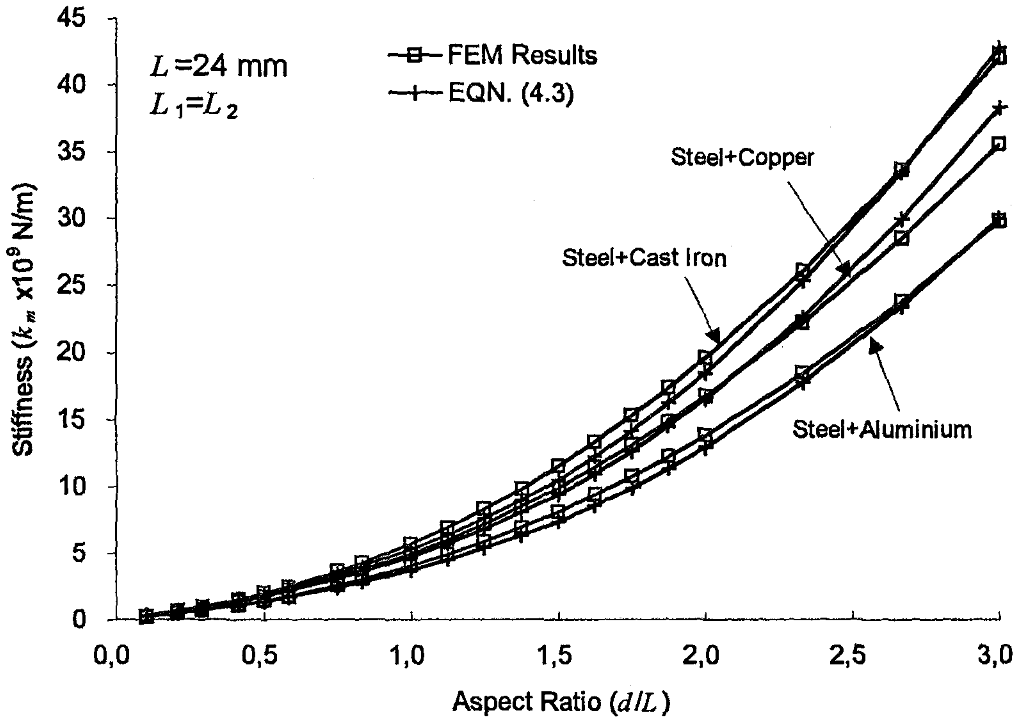

Figure 4.5 Stiffness of Joints which Consists of Members Having Different Materials

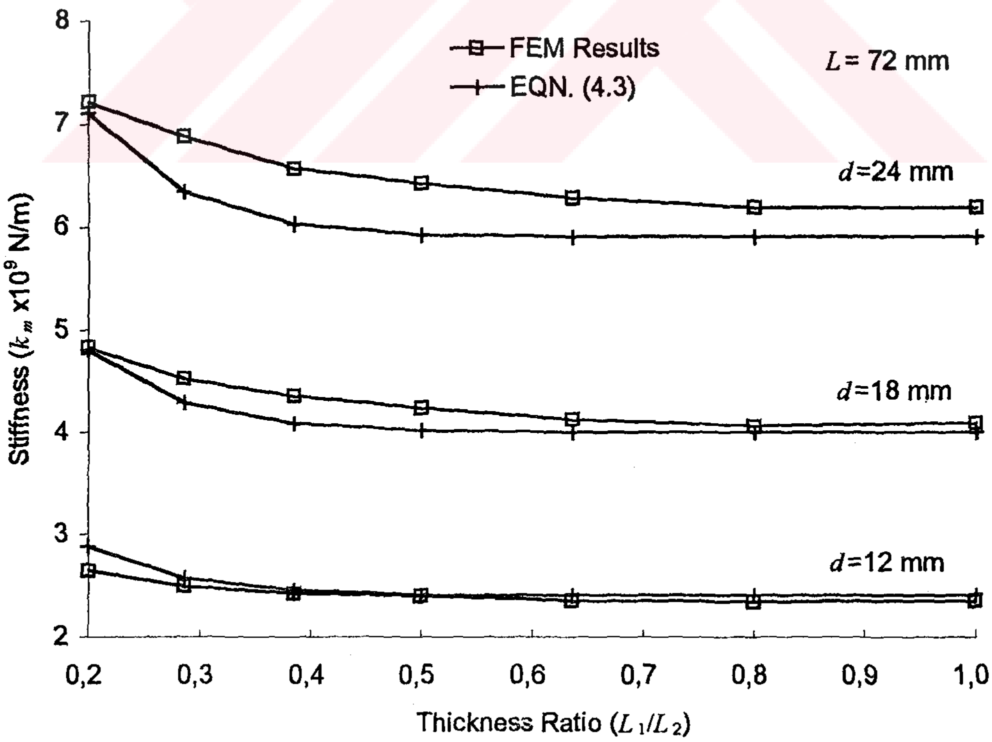

Figure 4.6 Stiffness Variations with respect to Thickness Ratio

different materials and thicknesses. After trying certain functional relationships, the following expression is chosen to fit the data obtained from finite element analysis.

$$k_m = \frac{\pi}{2} d E_{eq} e^{(\frac{\pi}{5}-\beta_1)d/L} \frac{1}{1-\beta_2} \tag{4.3}$$

where $E_{eq}= E_1 E_2 /(E_1+E_2)$and $\beta_1= (0.1d/L)^2$ is the correction factor for d/L and $\beta_2= (1-L_1/L_2)^8$ is the correction factor for thickness ratio (L_1/L_2). In Equation (4.3) $L_1/L_2 \leq 1$ and the member with smaller thickness is to be considered as the first member. This equation includes individual member thicknesses and the ratio of bolt diameter to grip length besides the bolt diameter and modulus of elasticity of member materials. The effect of Poisson's ratio of the materials can not clearly be evaluated but as Choudhury[52] suggested, its effect is ignored in obtaining the stiffness expression.

4.3.4 Discussions

As seen in Figure 4.7, the results of Equation (4.3) are very close to FEM results. The agreements of the results of this equation with FEM results were also illustrated in Figures 4.5 and 4.6 for the joints which consist of members having different materials and different thicknesses respectively.

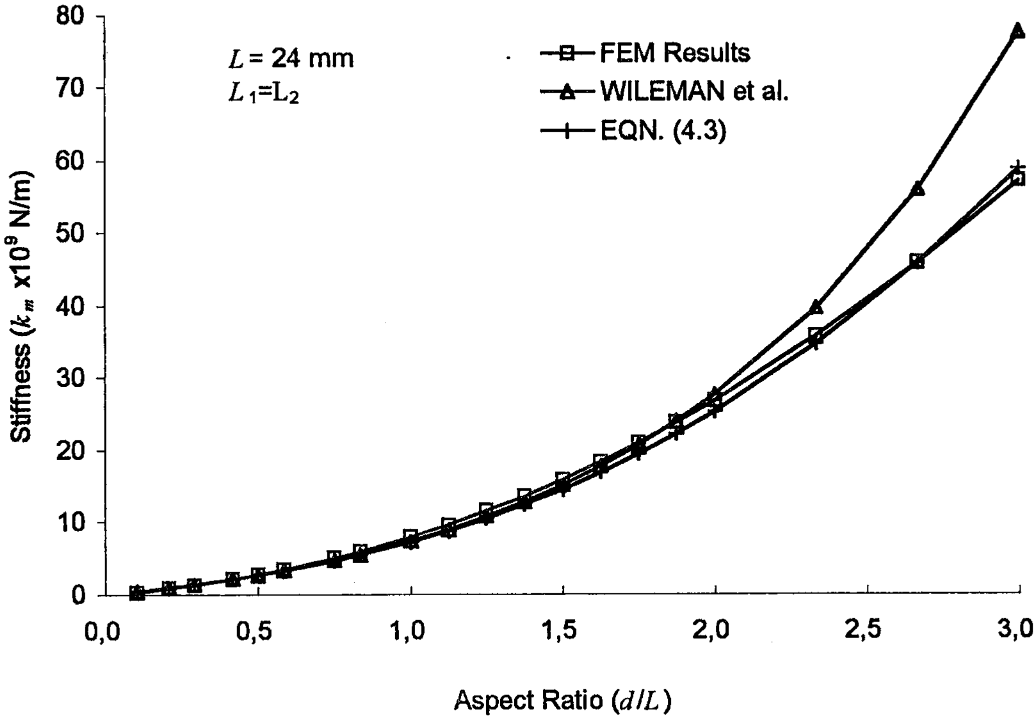

Figure 4.7 Comparisons of results of FEM, Wileman's Formula and Equation (4.3)

It was also noted that, the results of Equation (4.3) also fit the experimental results of Yıldırım[32] and Maruyama et al.[51]. For a particular joint (d= 8 mm, L= 36 mm, L_1= 8 mm, L_2= 28 mm, E_1= E_2= 206.8 GPa), Yıldırım[32] found after experiments k_m= 1.633x10^9 N/m and Equation (4.3) gives k_m= 1.603x10^9 N/m. For a joint consisting of steel members having a hole diameter of 25 mm and a grip length of 50 mm, Maruyama et al.[51] found k_m after experiments as 5.54x10^9 N/m and Equation (4.3) gives k_m as 5.55x10^9 N/m.

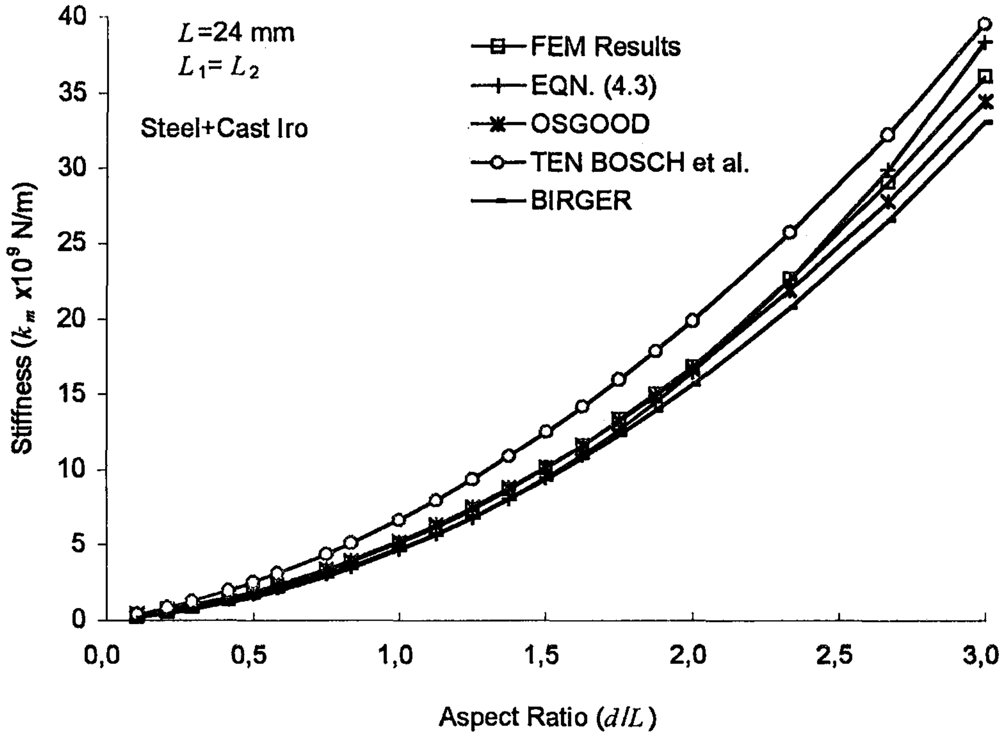

Figure 4.8 Comparisons of Results of FEM, Equation (4.3) and Previous Studies for Different Member Materials

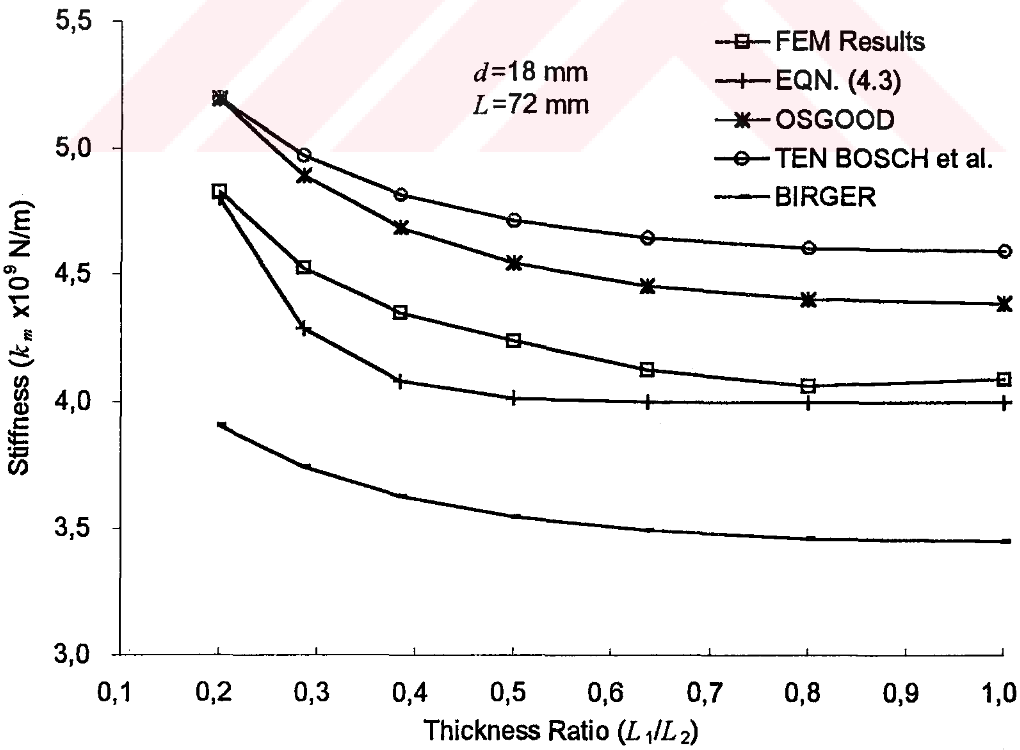

Figure 4.9 Comparisons of Results of FEM, Equation (4.3) and Previous Studies for Different Thickness Ratios

Figures 4.8 and 4.9 show comparison of stiffness calculated from Equation (4.3) and FEM results by using Equation (4.2) with those resulting from some of the previous studies. In both Figures, it was noticed that Osgood's results closely agree with the Finite Element results. The differences in the results are mainly due to different values of the cone angle estimation in their analysis. Osgood's estimation of 30° for the cone angle seemed to be more realistic than the others.

In the present study of the bolted joints, the surface qualities of the members are not considered, but it is assumed that there will be adequate preload on the joint which will clamp the members together nicely to prevent slippage between them. These assumptions might sometimes be violated in practical applications. If that is the case, a factor of safety must be introduced in the design of bolted joints.

4.4 WELDED JOINTS

Welding is one of the first process considered in joining machine elements. It has certain practical advantages and flexibility which are not to be had in other method of joining. In most cases, saving in manufacturing time, cost and weight and general improvement in appearance are obtained by proper use of welding, especially for the joining of sheet metal parts.

When the determination of stress distribution in welded joints is not possible with theoretical methods, a numerical analysis method like FEM can be used. In this study, two types of fillet welded joints are analysed. The first one is an axially loaded lapped joint with fillet welds and the second one is a cantilever beam welded to a support by fillet welds at top and bottom. In the analysis, the base metal, strap metal and weld metal were assumed to be linearly elastic, isotropic and homogeneous isotropic. The finite element model of the joints has been obtained by dividing the initial coarse FE models into required size and number of elements. Welded joints are modelled with two dimensional 4-noded structural solid elements.

4.4.1. Example 1: Lapped Welded Joint

Schematic view of the lapped welded joint model is shown in Figure 4.10. The base metal is joined with two parallel strap plates by fillet welds. In the welded joint model, length of weld legs, the thickness of strap plate and thickness of the base plate were all taken to be equal; and represented as h_w, and depth of the joint (into the paper) is two times of h_w. As shown in Figure 4.10, the analysed model is symmetric about both x and y axes. Thus, only one quarter of the joint was modelled. In symmetry planes, symmetric boundary conditions were applied and plain stress was assumed.

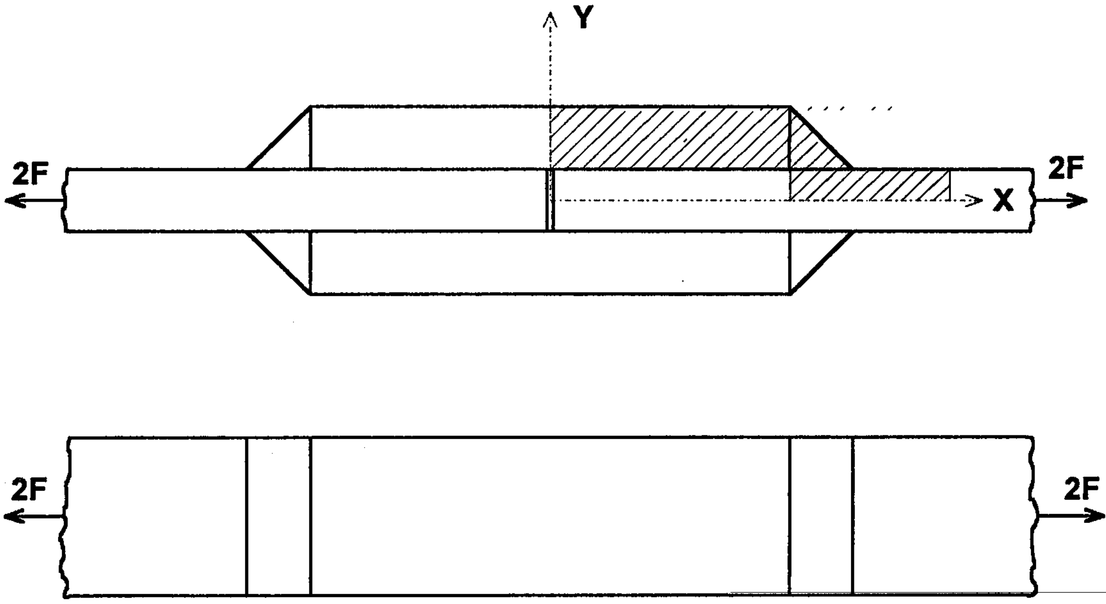

Figure 4.10 Schematic View of the Lapped Welded Joint

Parametric dimensions, symmetric boundary conditions and loading points of coarse FE model of the same welded joint is shown in Figure 4.11.

In this specific example the dimensions were taken as

h_w= 15 mm

L_1= $2h_w$

L_2= $2h_w$

Material properties are

E= 206.8 GPa

ν= 0.293

and the applied force is

F= 500 N

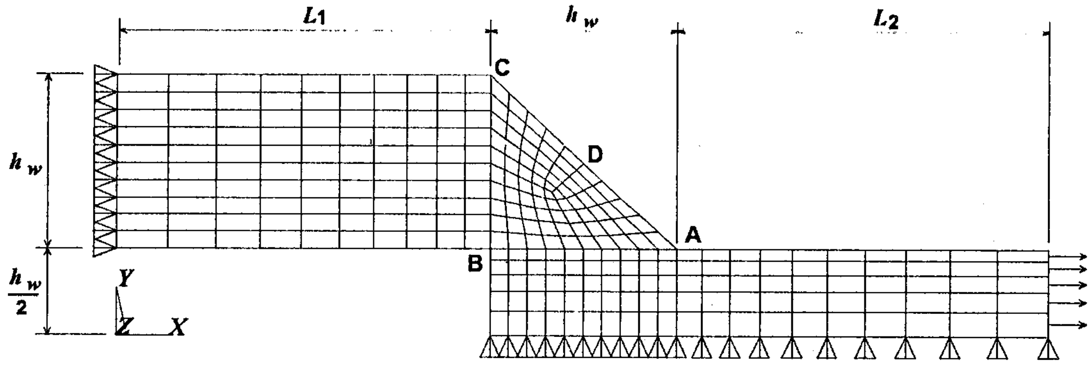

Figure 4.11 Finite Element Model of the Lapped Welded Joint

4.4.1.1 Results

The deformed shape of the model is shown in Figure 4.12. For analysis and design purposes, it is convenient to use the von Mises stresses. The stress contours for von Mises stresses are given in Figure 4.13. The maximum von Mises stress occurs at point A.

In a weldement, the welded region is the most critical region from stress distribution point of view. Principal stresses; σ_1 and σ_2 and, maximum shear stress; τ_{max}, are plotted along lines BA, BC and BD. Stresses along these lines are compared with the nominal stress; σ_0, which is calculated as

$$\sigma_0 = \frac{F}{A} \tag{4.4}$$

where F is the applied force in Newton, and A is the cross-sectional area of the welded joint in meter squares. Thus, the theoretical nominal stress; σ_0, for the data given above comes out to be 500/(0.0075*0.03)= 2.22 MPa.

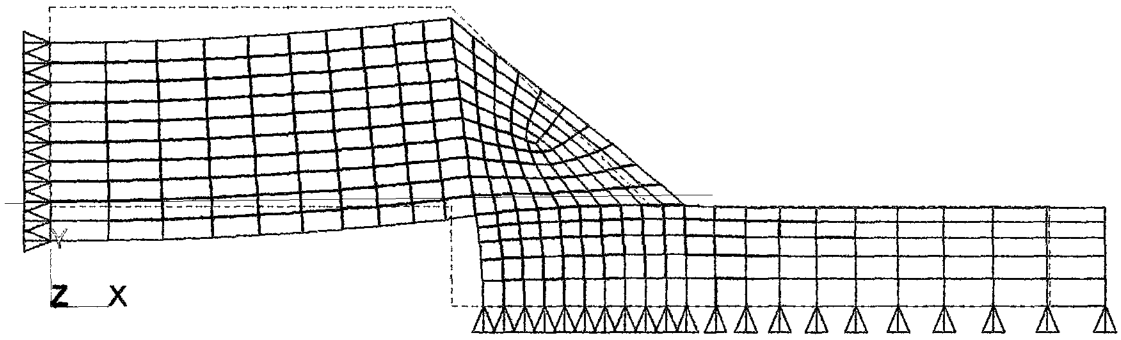

Figure 4.12 Deformed Shape of the Lapped Welded Joint

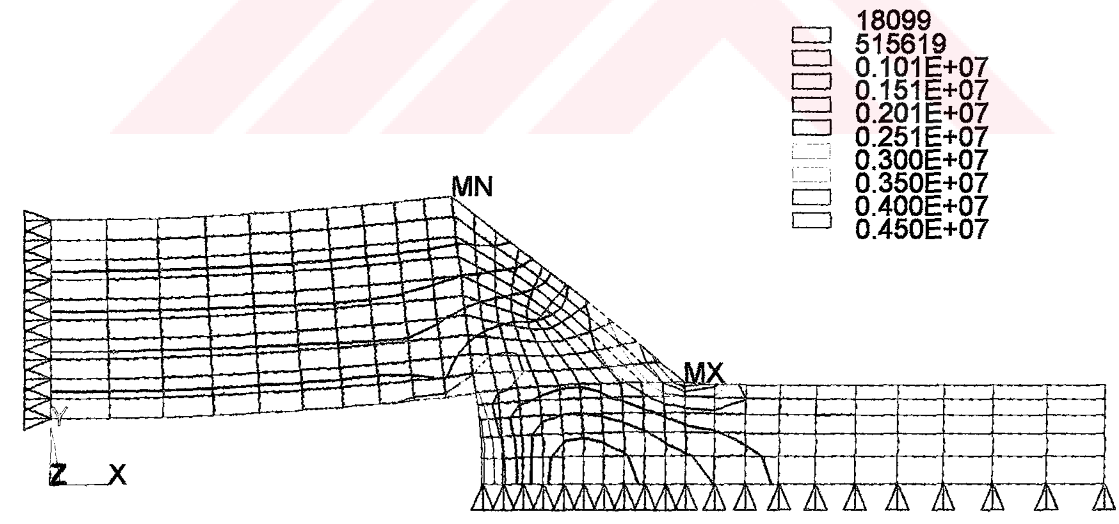

Figure 4.13 Von Mises Stress Contours (for Example 1)

The principal stresses along the line BA are plotted in Figure 4.14. Maximum principal stress; σ_1, occurs at point A as 6.07 MPa and it is 2.73 times of the nominal stress, σ_0. This is the maximum principal stress which occurs in the whole welded region.

The stress distributions along line BC are given in Figure 4.15. Along that vertical line BC the maximum stress occurs at point B. Maximum principal stress, σ_1, occurs also at point B with a value of 1.98 MPa and it is only 0.89 times of σ_0.

The stress distribution across throat area of a welded joint is of particular interest, because designers and stress analysts usually assume that failure will occur in the throat in determining the strength of a weld.

The stress distribution across the throat of the first welded joint model is given in Figure 4.16. Along the throat line BD of the welded joint, maximum normal stress, σ_x, occurs at point B as 1.97 MPa and, it is 0.89 times of σ_0. Maximum principal stress, σ_1, occurs at point B as 1.98 MPa and at point D as 1.94 MPa and it is 0.89 and 0.87 times of σ_0 respectively. Minimum principal stress, σ_2, occurs near point B as -1.98 MPa and it is -0.89 times of σ_0.

Maximum shear stress, τ_{max}, across the throat line takes the value of 1.88 MPa at point B and 0.97 MPa at point D. In terms of the nominal shear stress; σ_0, it is 1.69 and 0.87 times the nominal shear stress respectively. But, the resulting largest maximum shear stress, τ_{max}, occurs along the line BA (at point A) as 2.55 MPa and it is 2.3 times the nominal shear stress.

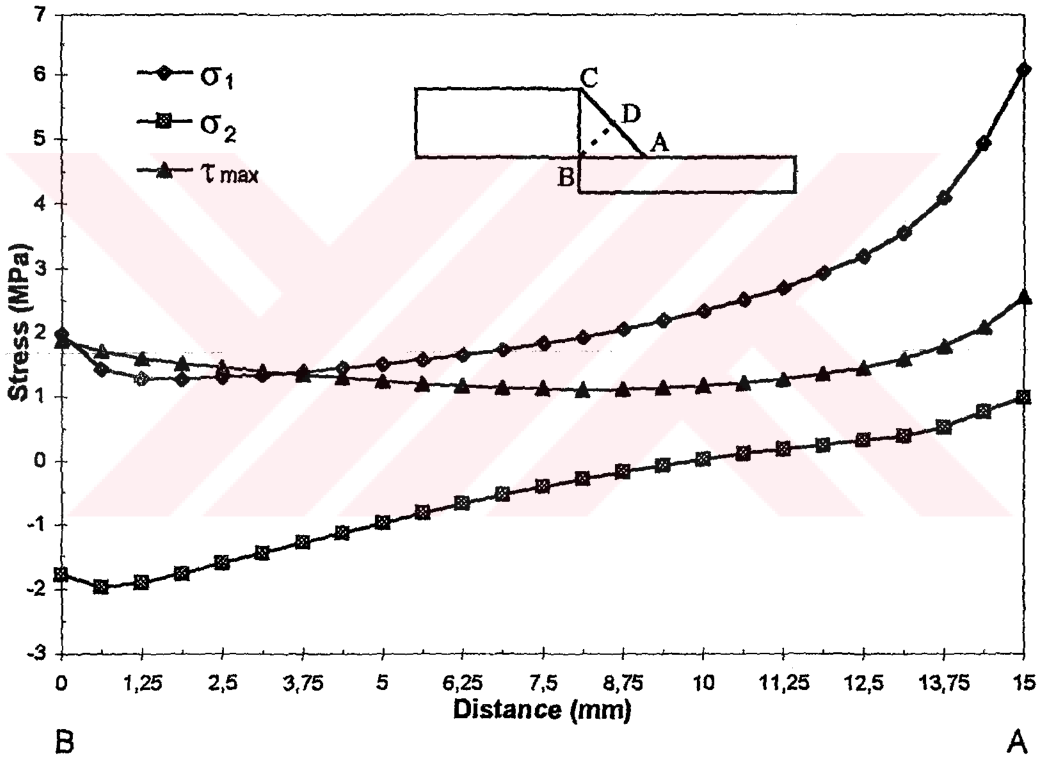

Figure 4.14 Stress Distributions Along Line BA (for Example 1)

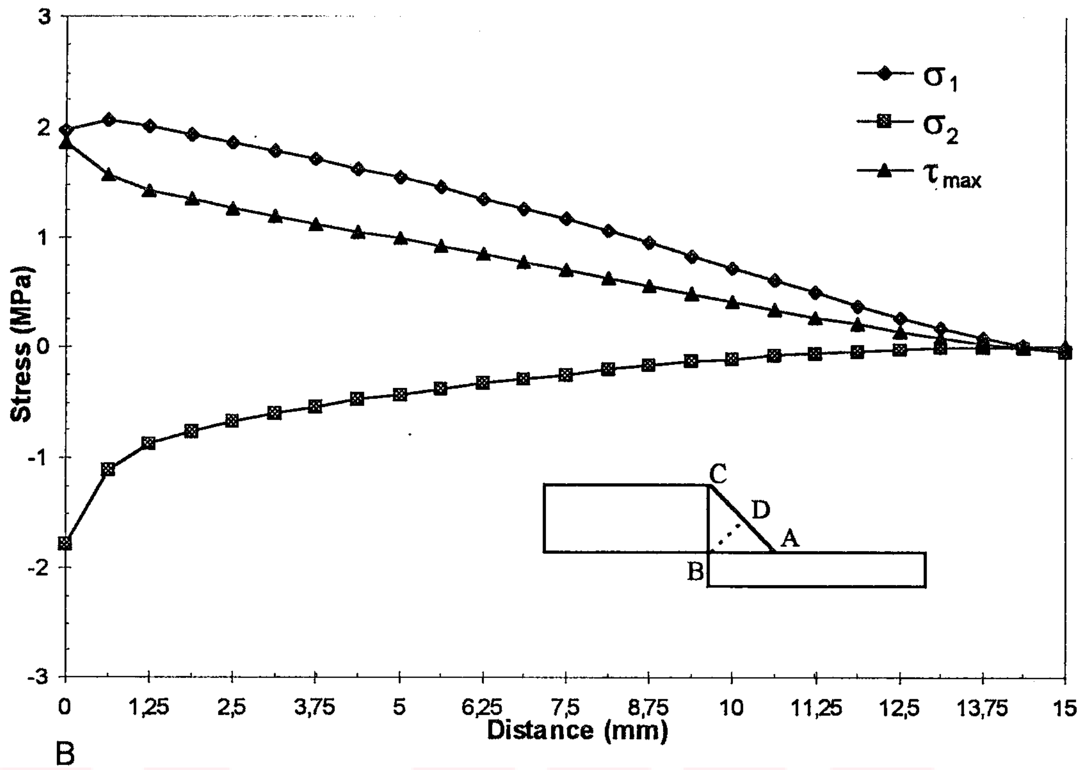

Figure 4.15 Stress Distributions Along Line BC (for Example 1)

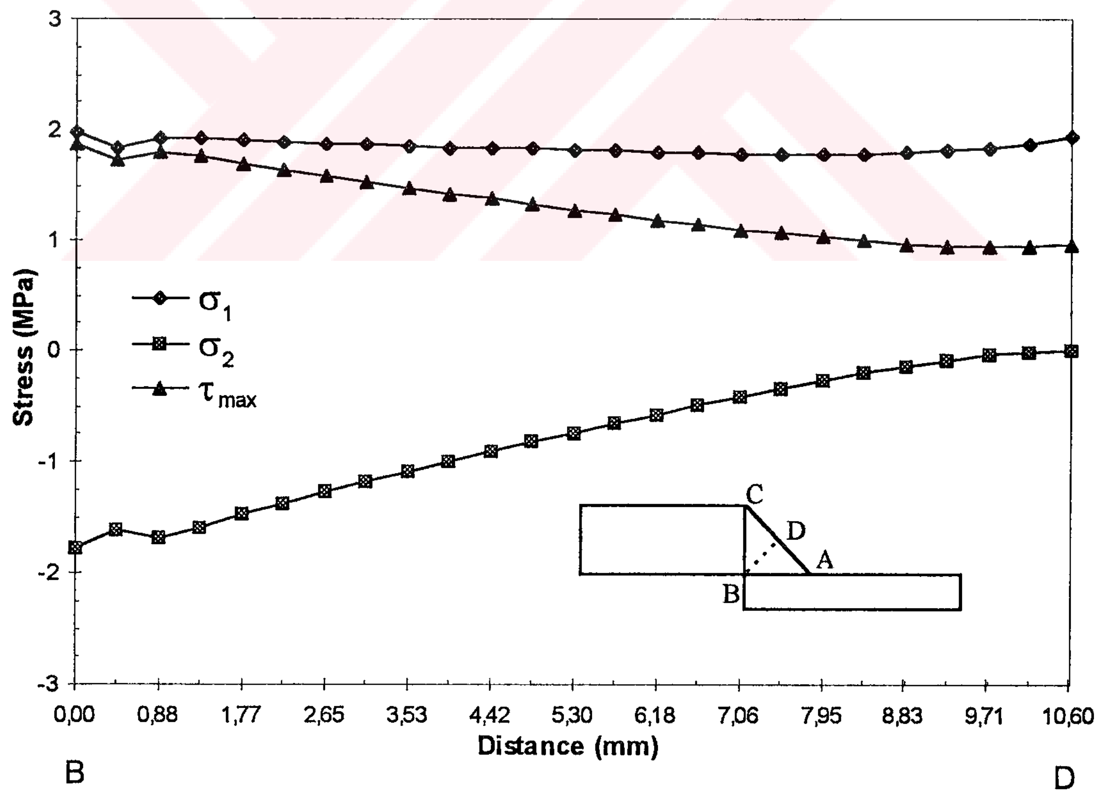

Figure 4.16 Stress Distributions Along Line BD (for Example 1)

4.4.2. Example 2: Cantilever Beam Welded Joint

The second welded joint model is shown in Figure 4.17 as a cantilever beam welded to a support by fillet welds at top and bottom. In this model too, the length and thickness of the welded cantilever beam is taken as the function of the length of weld leg; h_w, and depth of the joint (into the paper) is two times of h_w. For this example too, plain stress was assumed.

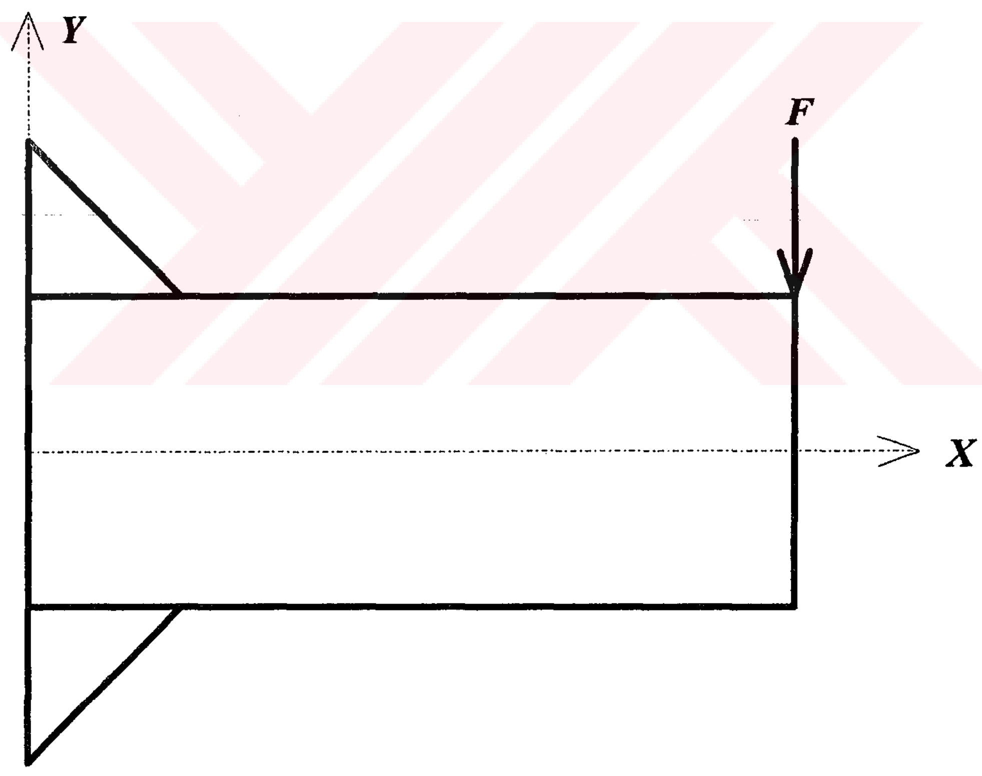

Figure 4.17 Cantilever Beam Welded Joint

Parametric dimensions and loading points of coarse FE model of the joint is shown in Figure 4.18.

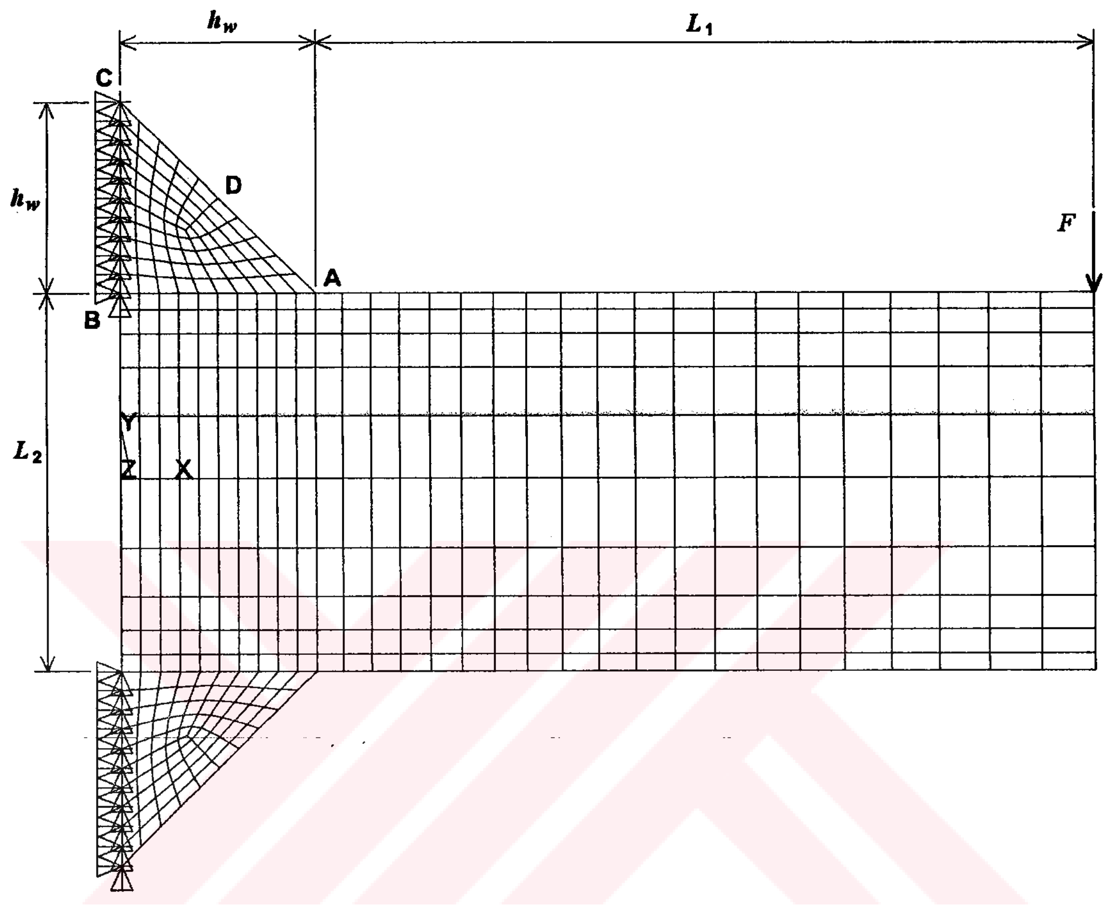

Figure 4.18 Finite Element Model of Cantilever Beam Welded Joint

The dimensions are taken as

h_w= 15 mm

L_1= $4h_w$

L_2= $2h_w$

Material properties are the same with the first example;

E= 206.8 GPa

ν= 0.293

and the applied force is

F = 1000 N

4.4.2.1 Results

The deformed shape of the second welded joint model is shown in Figure 4.19. The stress contours for von Mises stresses are given in Figure 4.20. The distribution of stress contours are similar for upper and lower welds, but the stress values for the upper weld are a little bit higher than the lower weld. So, the principal stresses; σ_1 and σ_2, and maximum shear stress; τ_{max}, are plotted along lines BA, BC and BD of the upper weld. Stresses along these lines are compared with the principal stresses or the maximum shear stress. The primary shear stress; τ_{xy}, and normal bending stress; σ_b, which are used in determining the principal stresses or the maximum shear stress are calculated as

$$\tau_{xy} = \frac{F}{A} \tag{4.5}$$

where F is the applied force, in Newton and A is the cross-sectional area of the weld in shear and

$$\sigma_b = \frac{Mc}{I} \tag{4.6}$$

where M is reaction moment as the result of the applied force F, c is the maximum distance from neutral axis for bending stresses and I is the moment of inertia of the welded joint.

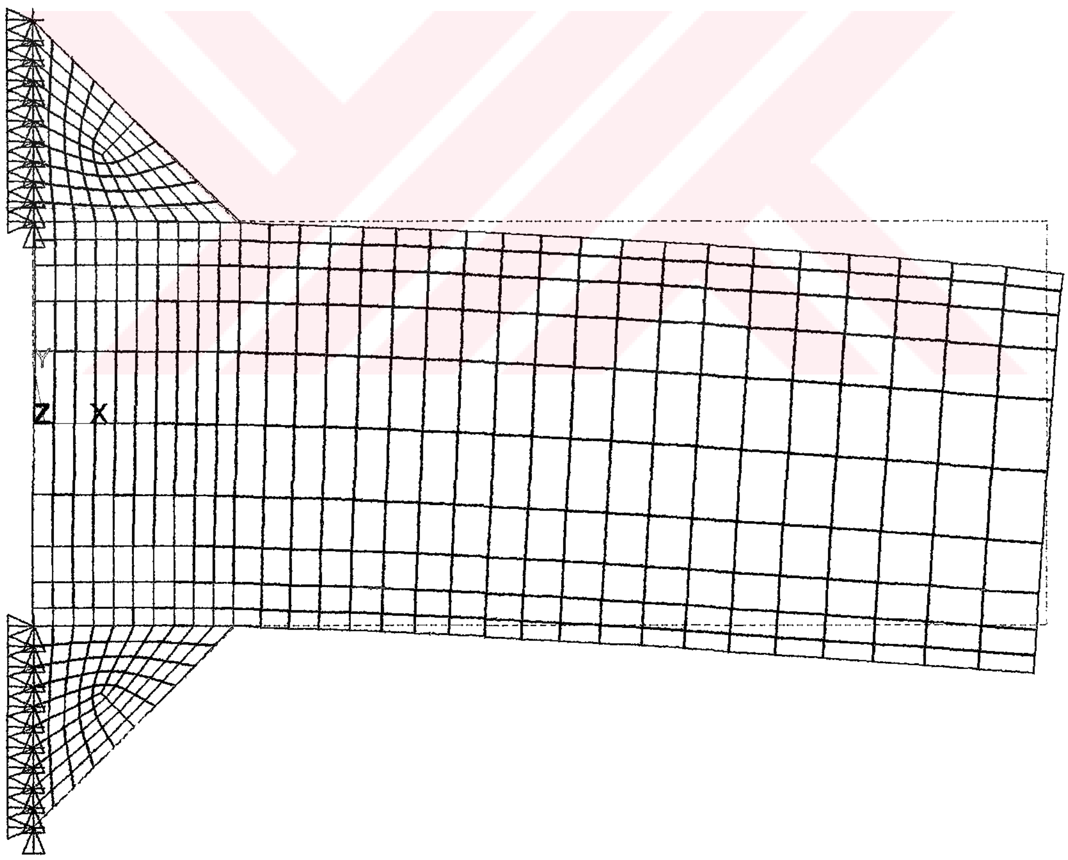

Figure 4.19 The Deformed Shape of Cantilever Beam Welded Joint

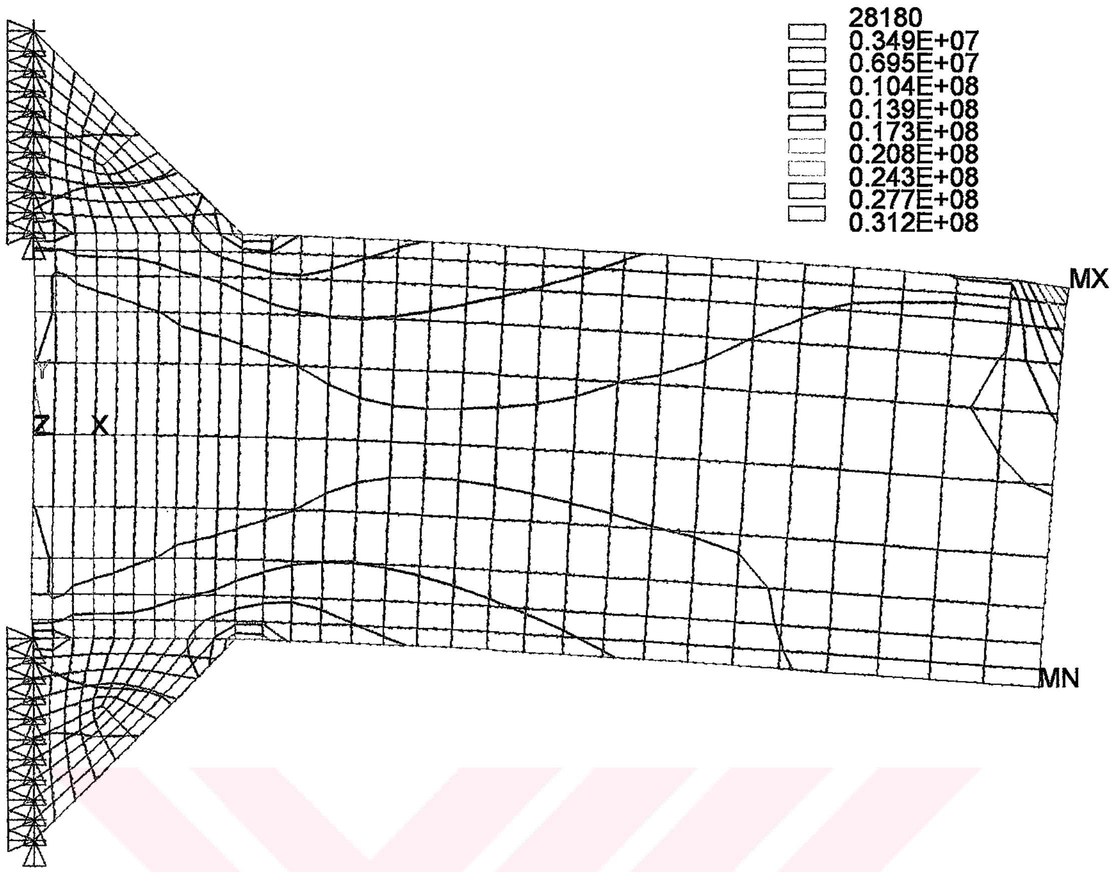

Figure 4.20 Von Mises Stress Contours (for Example 2)

The principal stresses along the line BA are plotted in Figure 4.21. The maximum principal stress; σ_1, occurs at point A as 27.42 MPa and it is 4.23 times the calculated principal stress. This is the maximum principal stress which occurs in the whole welded region for this example.

The stress distributions along line BC are given in Figure 4.22. Along that vertical line BC the maximum stress occurs at point B. Maximum principal stress, σ_1, occurs also at point B with a value of 21.26 MPa and it is 3.28 times the calculated value.

The stress distributions across the throat line are given in Figure 4.23. Along the throat line BD, the maximum principal stress; σ_1, occurs at point B.

Maximum shear stress, τ_{max}, across throat line occurs at point B as 7.69 MPa and, at point D as 1.57 MPa. In terms of the nominal stress; σ_0, it is 2.31 and 0.47 times the calculated stresses respectively. The resulting largest maximum shear stress, τ_{max}, occurs along line BA at point A (in Figure 4.21) as 11.43 MPa and it is 3.43 times the calculated maximum shear stress.

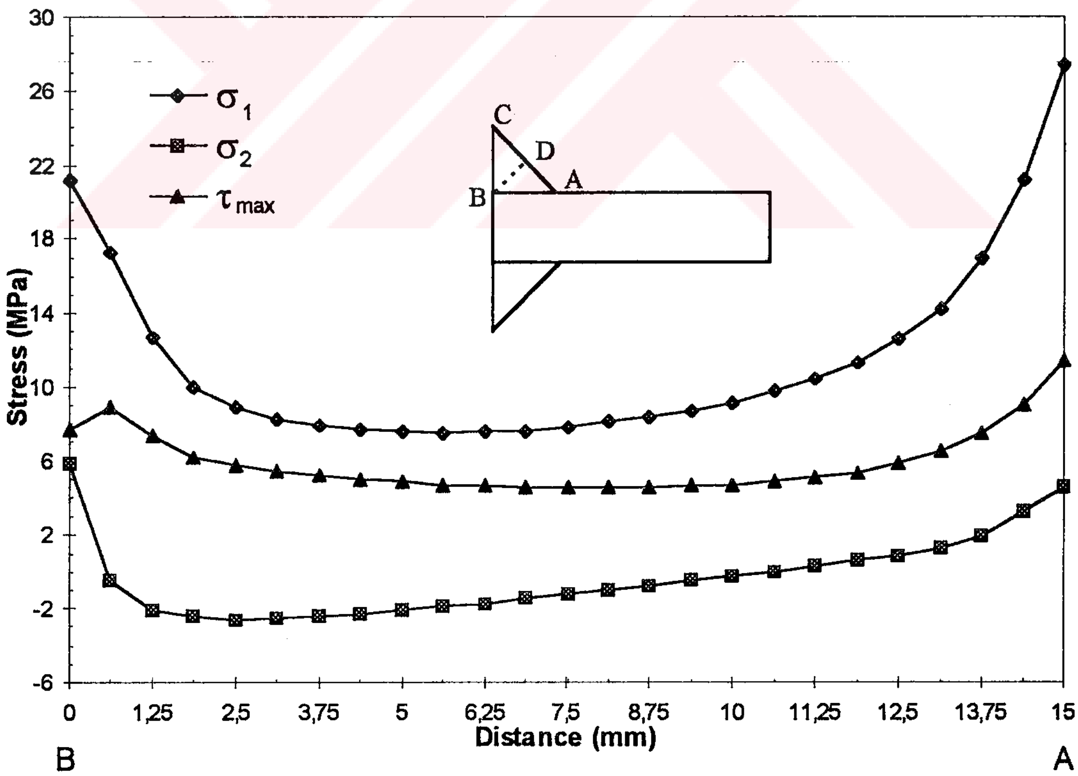

Figure 4.21 Stress Distributions Along Line BA (for Example 2)

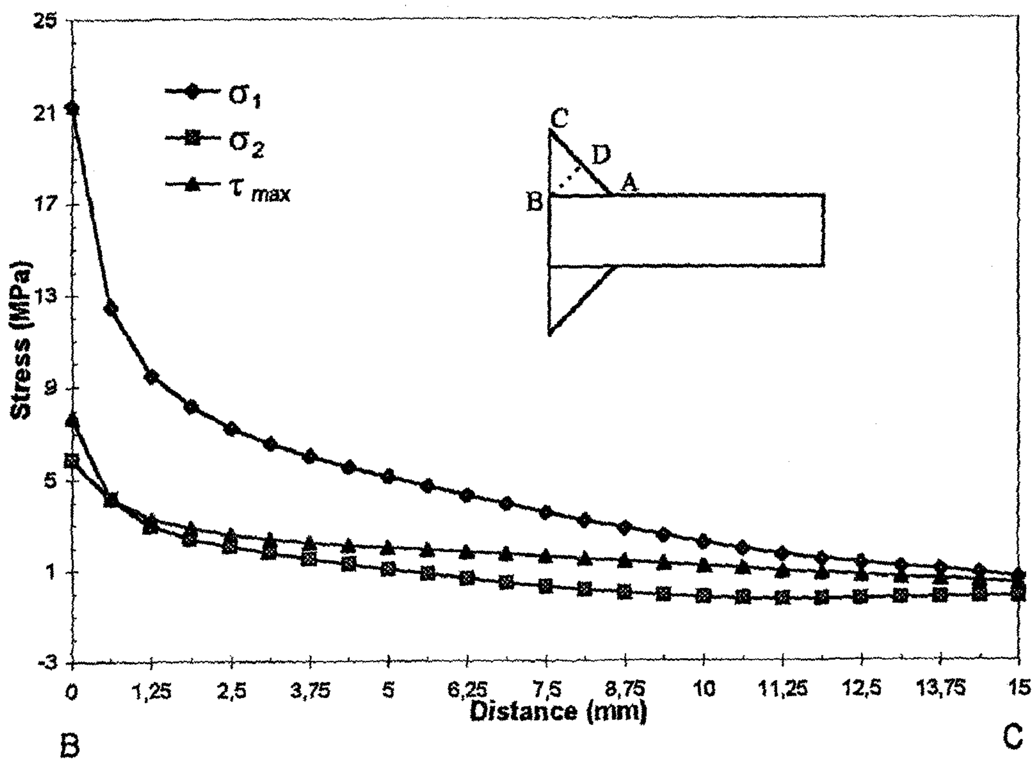

Figure 4.22 Stress Distributions Along Line BC (for Example 2)

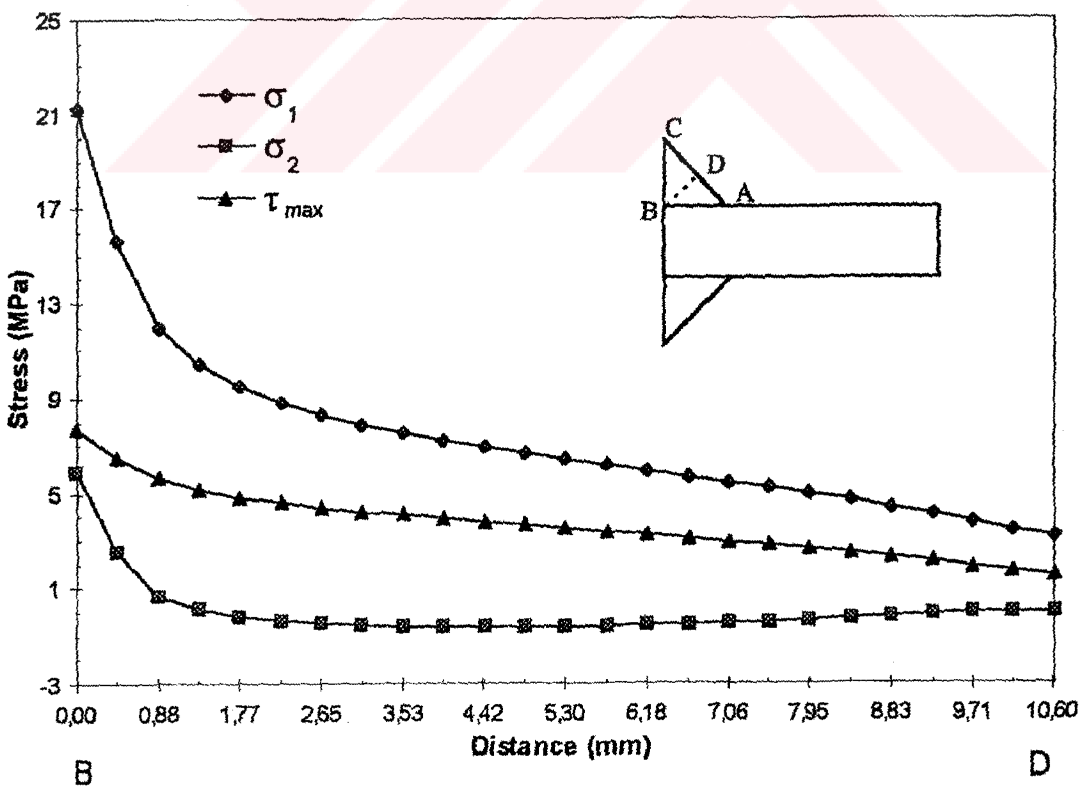

Figure 4.23 Stress Distributions Along Line BD (for Example 2)

4.4.3 Discussions

It can be concluded from Figures 4.14-16 and 4.21-23 that the maximum stresses occur at point A; for both examples. The method most often used for the design of welded joints is to assume that the throat section is in shear.

The resulting largest maximum shear stress, τ_{max}, across throat area occurs at point B. It is 1.88 MPa and 1.69 times of σ_0 for the first example. But for the second example, it is 7.69 MPa and 2.31 times of calculated maximum shear stress. On the other hand, maximum shear stress, τ_{max}, along line BA occurs at point A. It is 2.55 MPa and 2.3 times of σ_0 for the first example and it is 11.43 MPa and 3.43 times of the calculated value for the second example.

In literature, during the design of lapped fillet welds the average stress in throat area is taken as $1.414\sigma_0$, and it is assumed that the stress is uniformly distributed over the entire area[53]. The maximum shear stress values obtained at point A are 2.3 and 3.43 times the nominal values for the first and second examples respectively. There is a ratio of about, (2.3/1.414)= 1.63 and (3.43/1.414)= 2.43 between the calculated and theoretically suggested values of the maximum shear stresses in two examples. It is quite clear that the design stress values for the fillet welded joints like above models, must be increased from the value given in literature ($1.414\sigma_0$) to be able to design a safe weldement.

CHAPTER V

DESIGN PRINCIPLES
OF
MACHINE TOOL SLIDEWAYS

5.1 INTRODUCTION

The basic function of slideway in a machine tool structure is to transmit forces while permitting accurate and controlled relative movements of the machine parts. The advances made in the field of machine tools, especially after the introduction of Numerical Control, brought to light the considerable influence of slideways on the overall performance of a machine tool.

The purpose of this chapter is to explain the design principle and analysis of machine tool slideways. Section 5.2 is devoted to the functions of the slideways. Design principles of slideways are explained in section 5.3. Finite element analysis and implementation of contact stiffness to calculate contact deformation are explained in Section 5.4.

5.2 FUNCTIONS OF A SLIDEWAY

Good slideway design should ensure smooth and stable movement of the moving element of machine tool under all operating conditions. Slideways of a machine tool perform the function of guiding the moving element along the desired path, either rectilinear or circular, within the required accuracy limits to enable machining.

To achieve the required precision and productivity, the slideway configuration chosen should meet the following requirements.

1. Guidance of the moving element should be within the accuracy limits of the machine tool.

2. The axial and rotational stiffness of the sliding element should be sufficient enough to contain their deflections in the directions considered within reasonable limits.

3. The location of guiding elements with respect to the various forces acting on the element should be so chosen that the reaction forces at the sliding faces and consequently the friction force are kept at a minimum value.

4. The slideway should provide sufficient damping in the principal directions to enable maximum metal removal.

5. For consistency of performance, the effect of slideway wear on the accuracy of the machined component should be a minimum.

5.2.1 Forces on Slideways

The external forces acting on a member of a machine tool are the cutting forces with components F_x, F_y, F_z; weight of the slide W; and the feed drive force. These forces are resolved on the slideway elements as the reactions and tilting moments. If the tilting moments are zero, the pressure due to reactions will be distributed uniformly over the bearing area of the slideways. The existence of the tilting moment changes the pressure distribution and, therefore, displaces the point of application of the reaction forces. The magnitude of reaction force is also affected by the type, material, shape of slide surfaces and the application of lubricants. Acherkan[54] has specified the value of maximum pressure as 25-30 kgf/cm^2 for cast iron slideways employed by lathes and milling machines. For steel slideways, he suggested a 25 to 30 % increase in the maximum pressure value.

The forces acting and the reaction forces developed at the slideway interfaces for the cases of a centre lathe and a horizontal boring machine are shown in Figures 5.1 and 5.2 respectively.

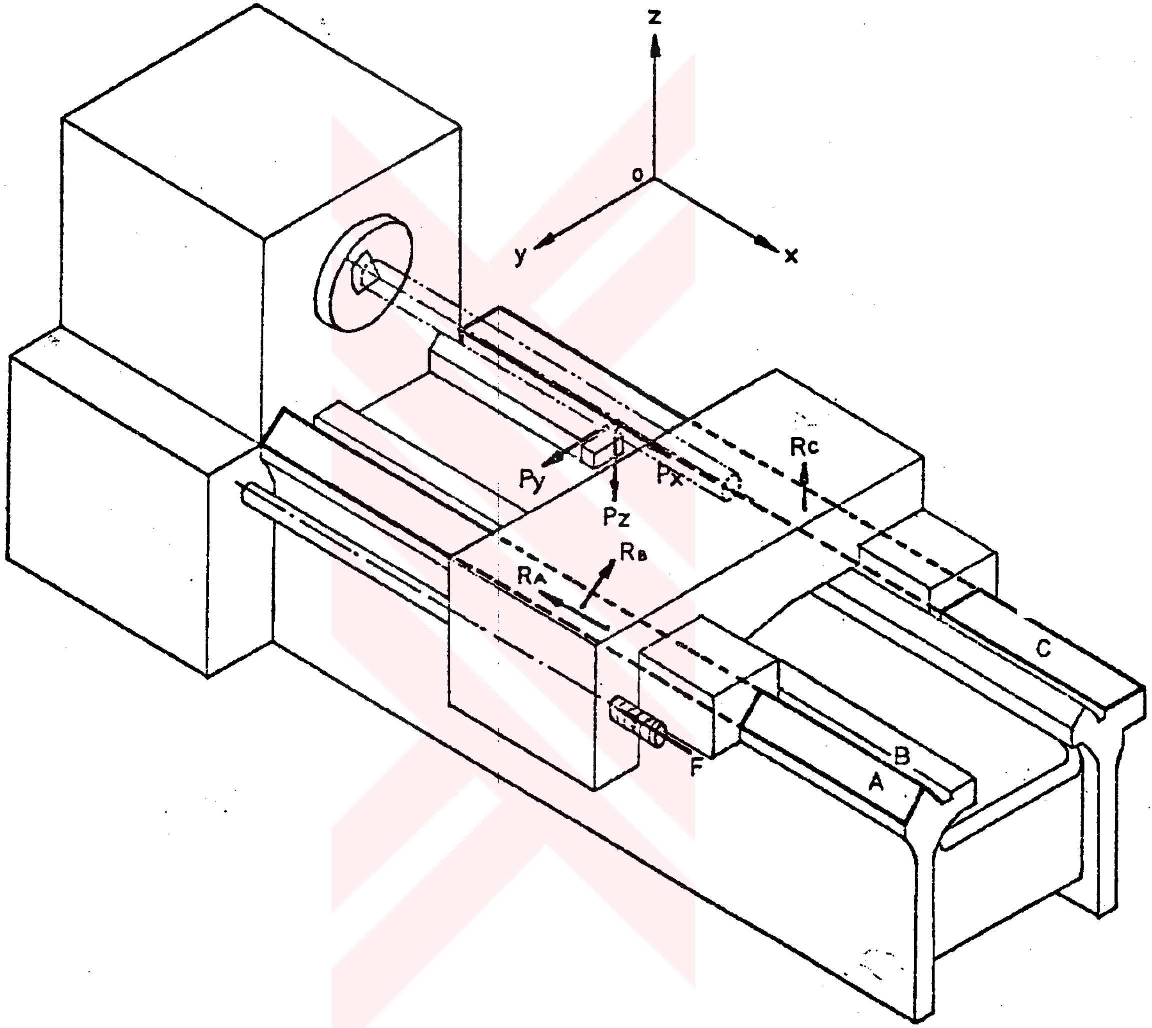

Figure 5.1 Forces on a Lathe Slideway System[55]

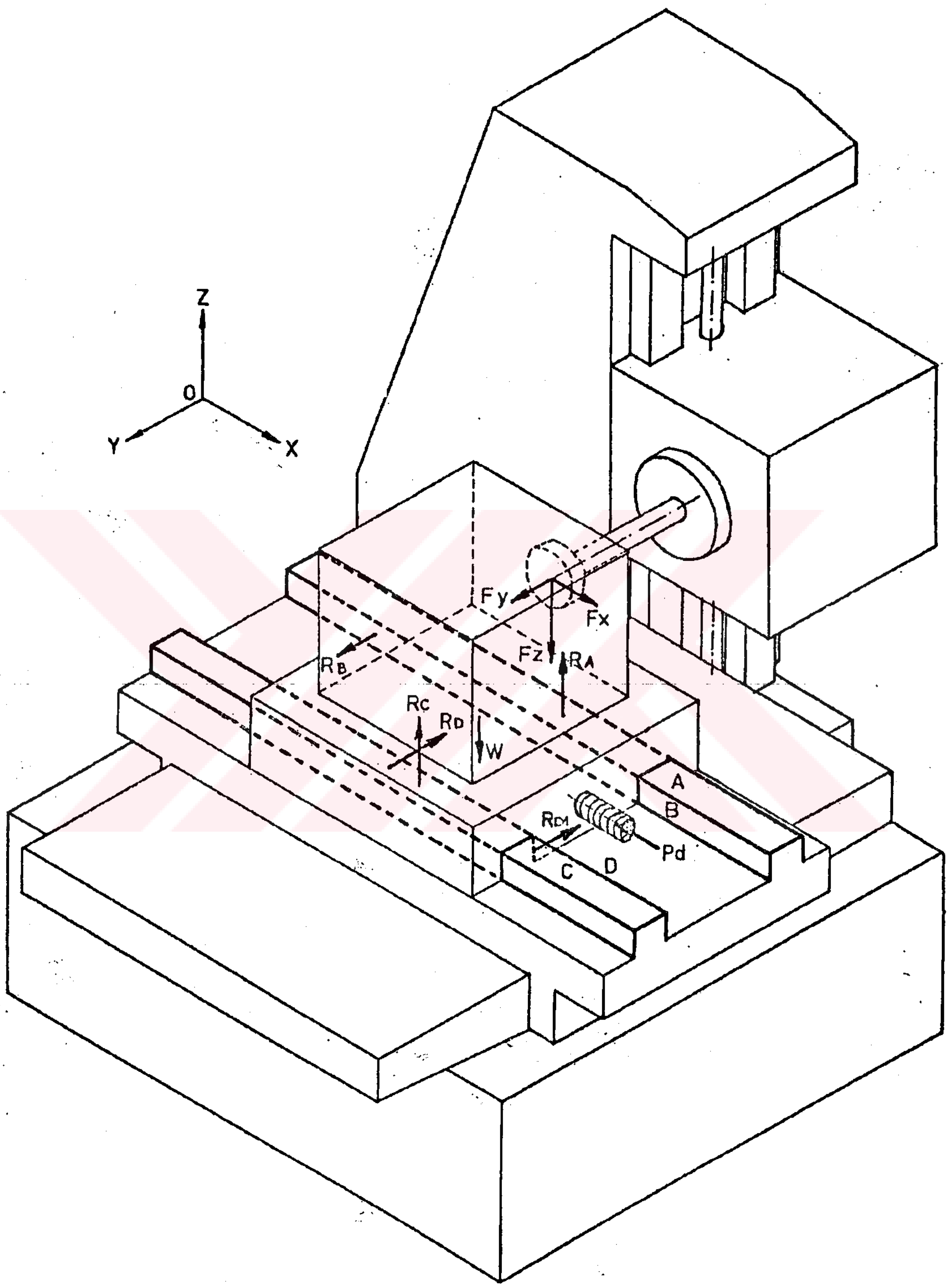

Figure 5.2 Forces on the Table Slideways of a Horizontal Boring Machine[56]

5.2.2 Slideway Configurations

For providing the necessary guidance and constraints to the moving member of a machine tool, the slideway elements may be constructed from a combination of basic configurations as shown in Figure 5.3. These can be arranged in different combinations to form the suitable slideway configuration. Vee and cylindrical guideways constrain two degrees of freedom. A combination of these elements will impose more constraints than necessary, making the structure redundant. Manufacture and assembly of such an arrangement is difficult and consequently expensive. But the distribution of wear will be more uniform, resulting in longer life.

A combination of vee and flat guideways is the most common, usually found on centre lathes, grinding machines, planing machines, and boring machines, etc. Vee is arranged with the apex upwards on lathes where speeds are low and it is necessary to prevent swarf getting trapped in the slideways. Vee is arranged with the apex upwards also in grinding machines and planing machines, where speeds are high enough to be in the hydrodynamic region and the slideway should retain lubricated.

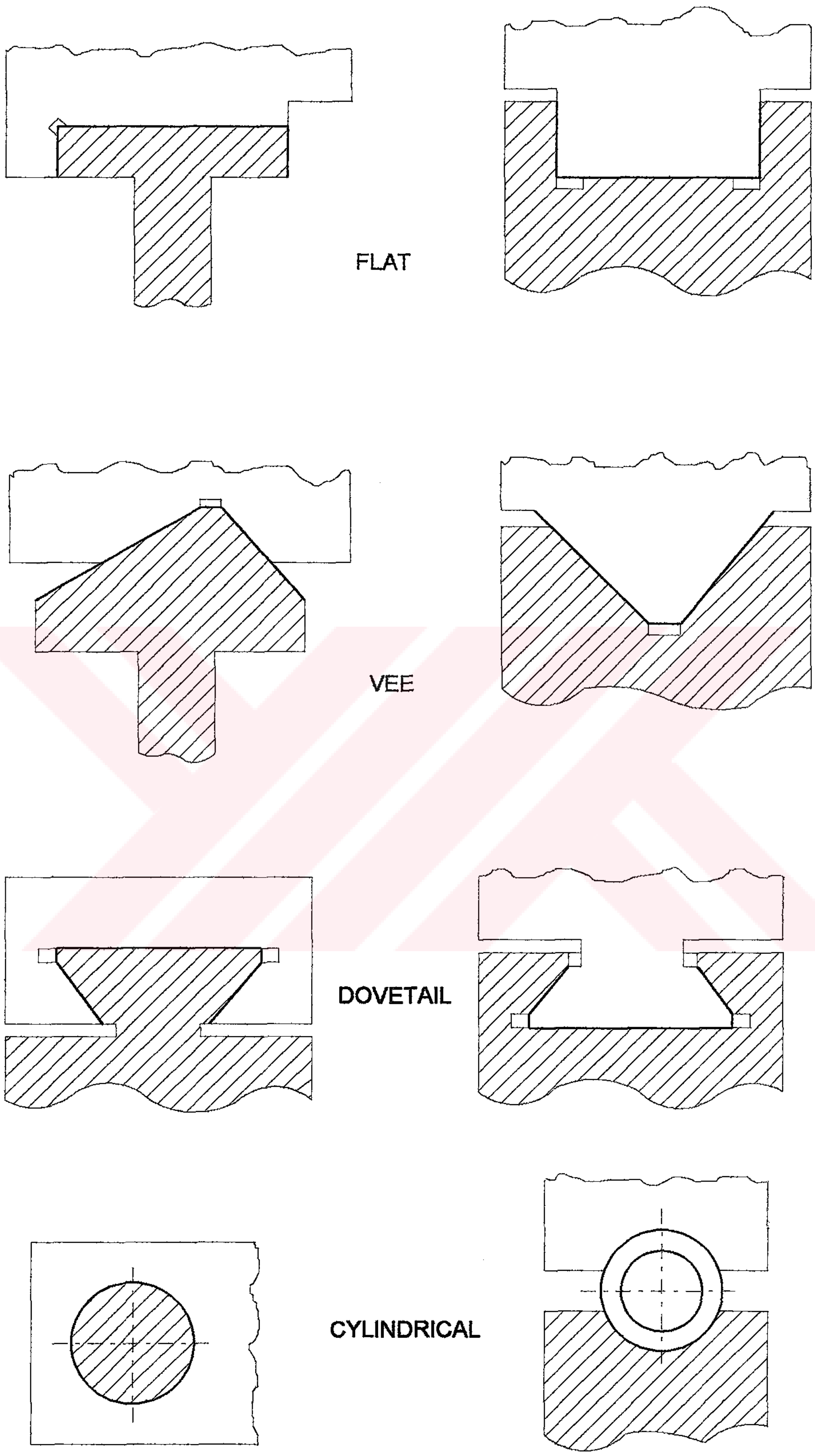

Figure 5.3 Basic Types of Slideway Guiding Elements[55]

5. 3 DESIGN PRINCIPLES OF SLIDEWAYS

Plain slideways were extensively used in all machine tools and their design was based on the following main principles.

1. The contact pressure on the sliding surfaces should be within acceptable values. Too high a contact pressure will result in a high rate of wear, whereas too low a value will seriously reduce the contact stiffness.

2. The geometry of the slideways should ensure that the effect of wear on the accuracy of the machined component is a minimum.

3. The sliding elements should be of adequate proportions to prevent excessive static deflections.

Optimum location of the slideway surfaces with respect to the system of forces acting on the machine tool will minimise the reaction forces at the sliding faces, thus reducing the friction force.

When the resultant of the friction forces and drive force do not coincide, tilting moments will be developed and friction force will increase. In extreme case, skewing of the slide can occur.

To determine deformations and pressure distribution under the static loading condition, contact elements are defined between the sliding faces of the machine tool slideways by using ANSYS Rev. 5.0A's non-linear contact elements.

5.4 FINITE ELEMENT ANALYSIS

In modelling of the slideways, the first thing to consider is the behaviour of the surfaces in contact when a force is applied to the elements. The model must be constructed such that deformations at each point in the joint and the pressure distribution at the surfaces in contact could be easily evaluated. The model must be simple, but adequate to give accurate results.

In the models, it is always necessary to consider that the contact between the surfaces is elastic. If the surfaces were assumed to be rigid, then the calculated deflection of the slideways were going to be smaller than the actual values. This error can not be neglected. For precise calculations of the deformations and pressure distributions, it is necessary to consider the compliance of the structural components surrounding the contacting surfaces. In general, qualitative influences of all factors on the behaviour of the joints are known from experiments and simple theoretical models. A method of solution taking into account all the factors in quantitative terms and permitting the calculation of the pressure distribution and deflections is still not available. For this reason ANSYS Finite Element package which can handle models with non-linear contact elements, is used for fast, and efficient analysis of both simple and relatively complex slideway geometry.

5.4.1 Contact Deformations

The accuracy of the results depends on a number of factors such as mesh density, element boundary conditions, type of analysis and contact stiffness. Among these factors the contact stiffness of the surface is a variable which should be improved during the loading process. The contact stiffness of a surface is the function of surface finish, pair of contact material and interface pressure distribution. It is obvious that the interface pressure is the most important effecting factor for the contact stiffness. The contact stiffness is large for the large mean interface pressures[37]. A new contact stiffness value must be calculated according to the new interface pressure for each element along the contacting surface during the loading steps.

For an isotropic material the following relationship is valid[21].

$$p = \frac{\lambda k_n}{10^6 l t_d} \tag{5.1}$$

where p is mean interface pressure, λ is contact deformation, l is length of a contact element, t_d is the depth of the model and k_n is contact stiffness for a contact element. From Equations (2.7) and (5.1) the following identity can be established

$$10^4 (\tfrac{\lambda}{c})^{\frac{1}{m}} = \frac{\lambda k_n}{10^6 l t_d} \tag{5.2}$$

or

$$k_n = (10^{10}) \frac{l t_d (\lambda)^{\frac{1-m}{m}}}{c^{1/m}} \tag{5.3}$$

At the initial stage of the process, a constant value is assigned to the contact stiffness for every contact element by assuming that the interface pressure is uniform along the contacting surface. Then the deformation of surface can be calculated from Equation (2.7). By using Equation (5.3) the new contact stiffness values for each element along the surface in contact can be calculated. For the next iteration, contact stiffness values are calculated from previous deformation values. This procedure is repeated until the difference in the successive deformation values are less than an allowed error.

CHAPTER VI

TWO DIMENSIONAL ANALYSIS
OF
SLIDEWAYS

6.1 INTRODUCTION

In this chapter, as an application of FEM with two dimensional contact elements, some examples of two dimensional slideways will be analysed by using the methods developed in chapter 5. General modelling of two dimensional slideways are explained in section 6.2. Two dimensional slideway examples are given in section 6.3.

6.2 TWO DIMENSIONAL MODELS OF SLIDEWAYS

Examples for flat and dovetail types of slideway models are prepared to illustrate the determination of the deformation and the pressure distribution at the contacting surfaces of machine tool slideways. PLANE42, two dimensional structural solid element which is defined by four nodes having two degrees of freedom at each node is used in modelling the body of slideways. In order to model contacting surface of the slideways, CONTACT12, the node-to-node contact element in two dimensions is used. The element has two nodes and two degrees of freedom at each node, translations in the nodal x and y directions as explained in chapter III section 3.4.

6.3 EXAMPLES

6.3.1 Example 1: 2-D Open Type Flat Slideway

Dimensions and finite element division of an open type flat slideway model is shown in Figure 6.1. Contact elements are defined between contacting surfaces along lines AB, BC, DE and EF. The lengths of AB and DE are 30 mm and, of BC and EF are 20 mm, and the depth of the joint (into the paper) is 60 mm. The load was applied at the centre; and plane stress was assumed in the analysis. The surface compliance parameters are c= 0.69 and m= 0.5 as it is defined by Back[21]. The coefficient of friction, μ, for contact elements is taken as 0.1. The materials for both fixed and sliding elements are cast iron with the modulus of elasticity of 95 GPa and Poisson`s ratio of 0.211. Mean interface pressure is obtained by dividing the total applied external load to total contact area of the joint. The deformed shape of the model for 1.6 MPa mean interface pressure is shown in Figure 6.2.

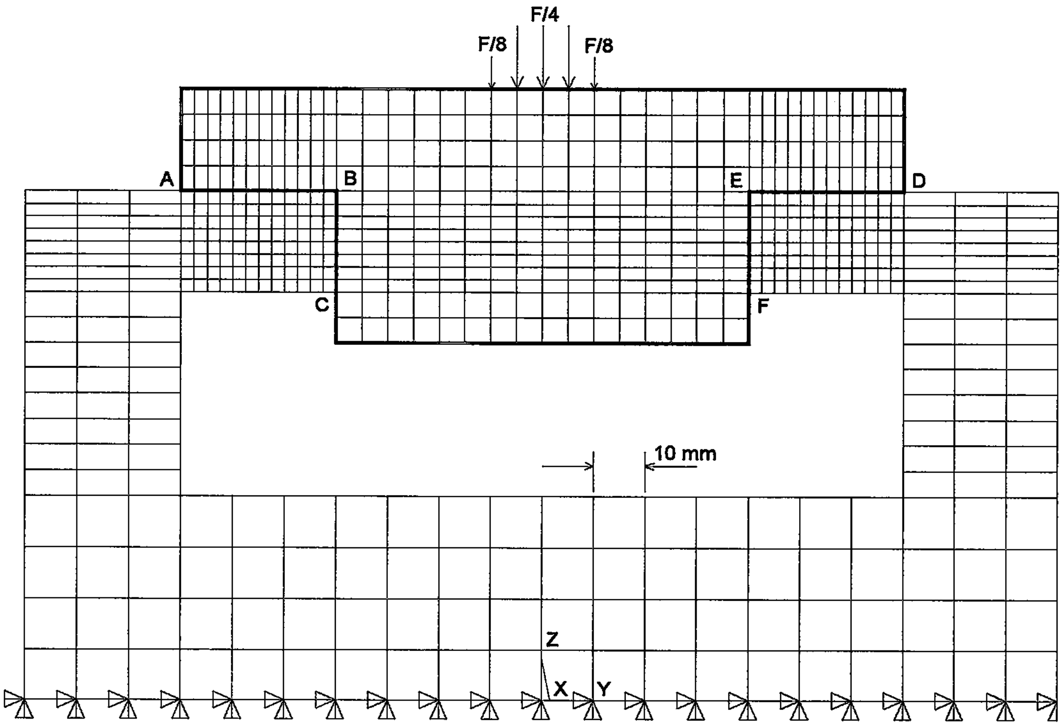

Figure 6.1 Finite Element Division of the Open Type Flat Slideway Model and Load Application Points. F is the Total External Load

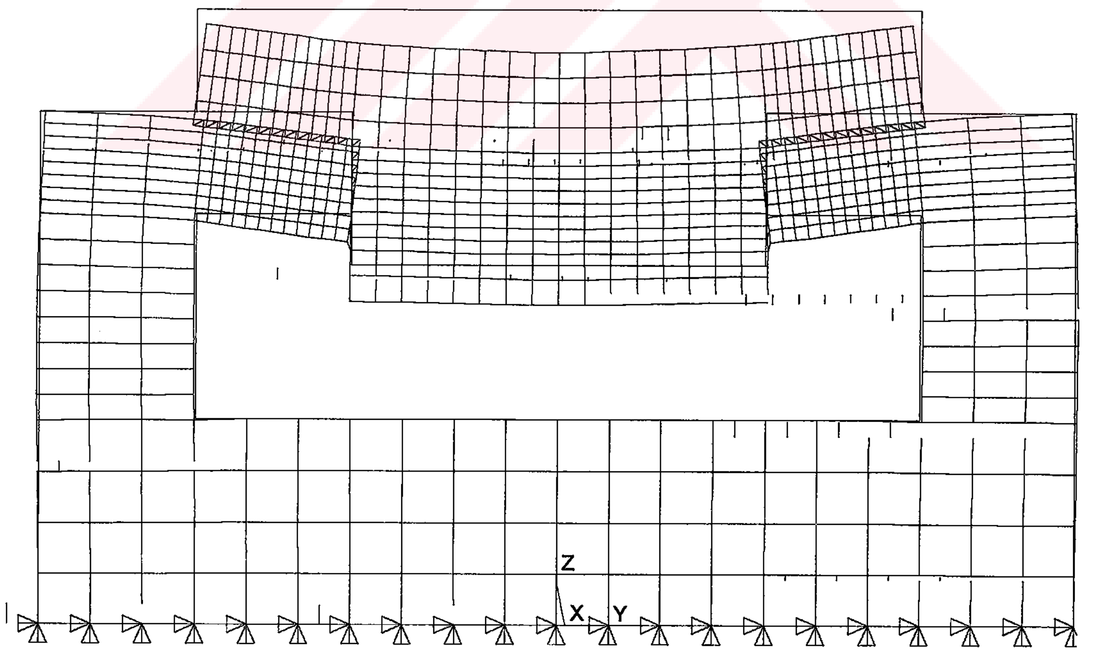

Figure 6.2 Deformed Shape of the Open Type Flat Slideway Model for 1.6 MPa Mean Interface Pressure

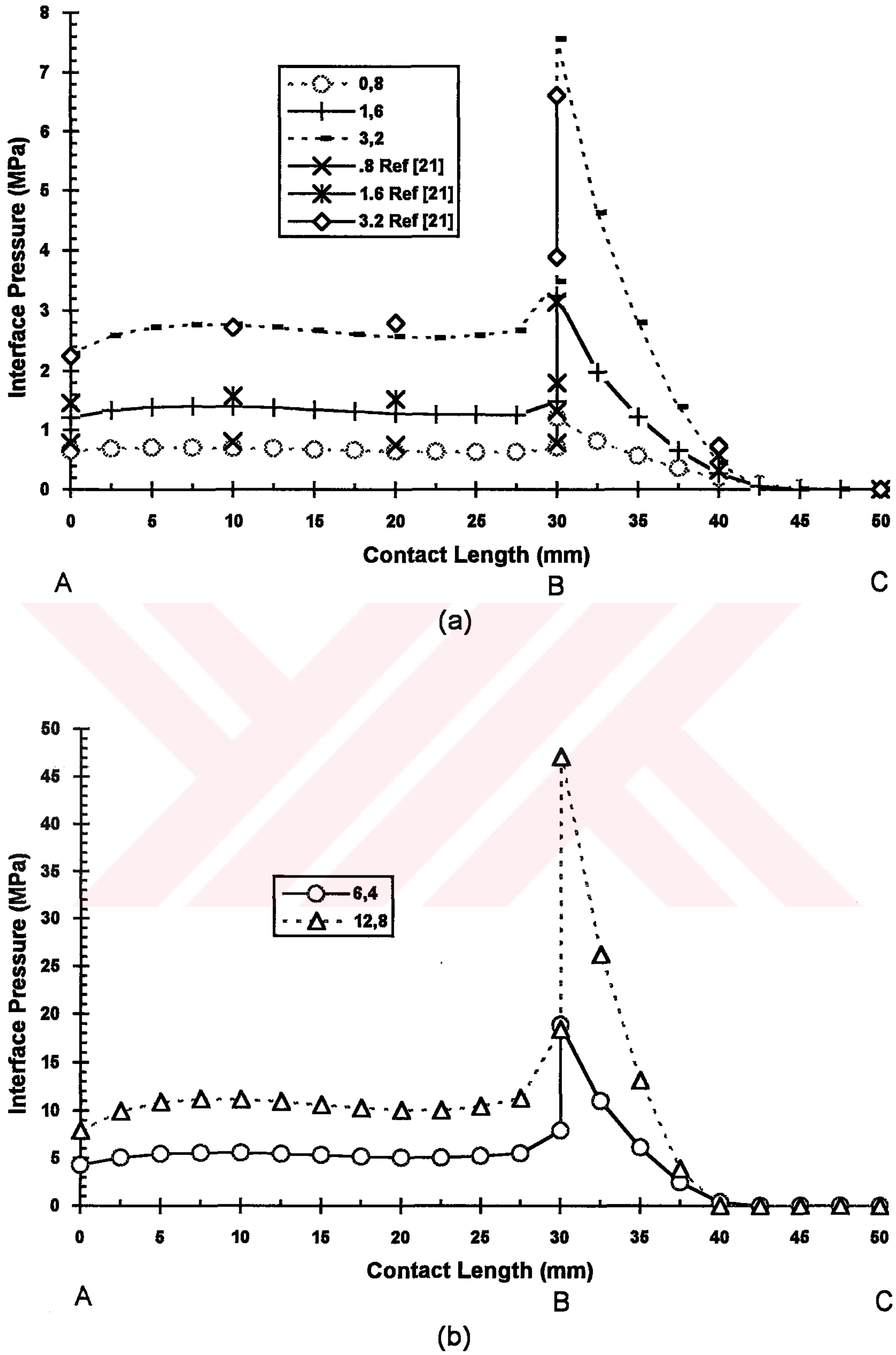

Figure 6.3 Pressure Distribution at the Contacting Surfaces of the Open Type Flat Slideway Model for Several Mean Interface Pressures

Deformations of the elements are obtained and pressures are calculated from Equation (5.1) at each pair of nodes along the contacting surfaces. Figure 6.3 (a) and (b) show the calculated pressure distribution along the faces AB and BC for several mean interface pressures. The trends of pressure distribution are similar, but for high pressures, the distribution become less uniform, because of the influence of body deformation. At low mean interface pressures, maximum interface pressure is about the same as the mean interface pressure. The ratio of maximum interface pressure to mean interface pressure increases with the mean interface pressure. And also as the mean interface pressure is increased, the contact length on BC and EF become smaller.

When the deflections at the centre of the joint are plotted against the interface pressure, the diagram in Figure 6.4. is obtained. It allows the designers to determine the required load for the allowable deflection. Non-linearity between deflections and mean interface pressure can be observed.

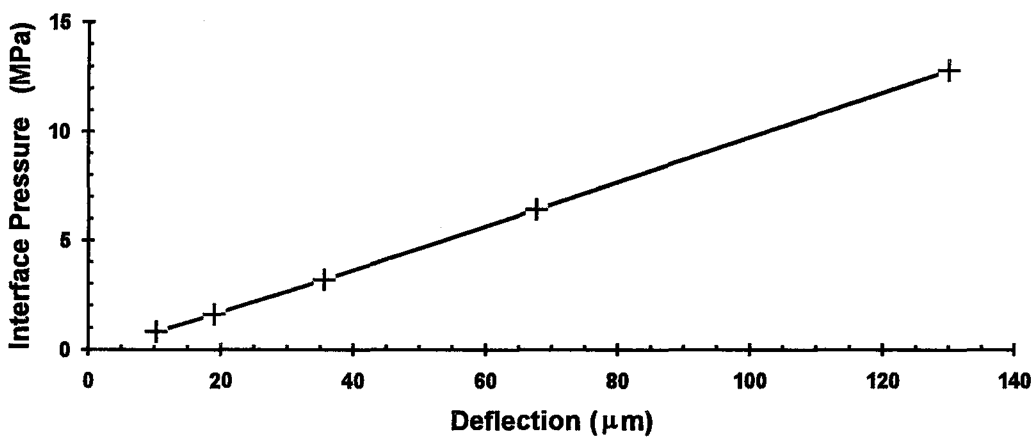

Figure 6.4 Relationship Between the Applied Interface Pressure and the Deflection at the Centre of the Open Type Flat Slideway Model

6.3.2 Example 2: 2-D Closed Type Flat Slideway

Finite element division and dimensions of second slideway model is shown in Figure 6.5. This is a typical example of closed type flat slideways. Depth of the joint, surface compliance parameters, other assumptions and material properties are the same with the Example 1. In this problem, contact elements are defined along the lines AB, CD, DE and FG, HI, IJ. The length of AB and FG is 40 mm, of CD and HI is 90 mm and of DE and IJ is 35 mm. Contact elements are not defined along the lines BC and GH because when the joint is loaded due to the deformation, a separation at this surface will be developed.

The deformed shape of the closed type slideway model is shown for 1.6 MPa mean interface pressure in Figure 6.6. The calculated pressure distribution for five mean interface pressures is shown in Figure 6.7 (a) and (b). In this example, at low mean interface pressures, the maximum interface pressure is about 1.5 times of the mean interface pressure, but at high mean interface pressures, the maximum interface pressure is about three times of the mean interface pressure.

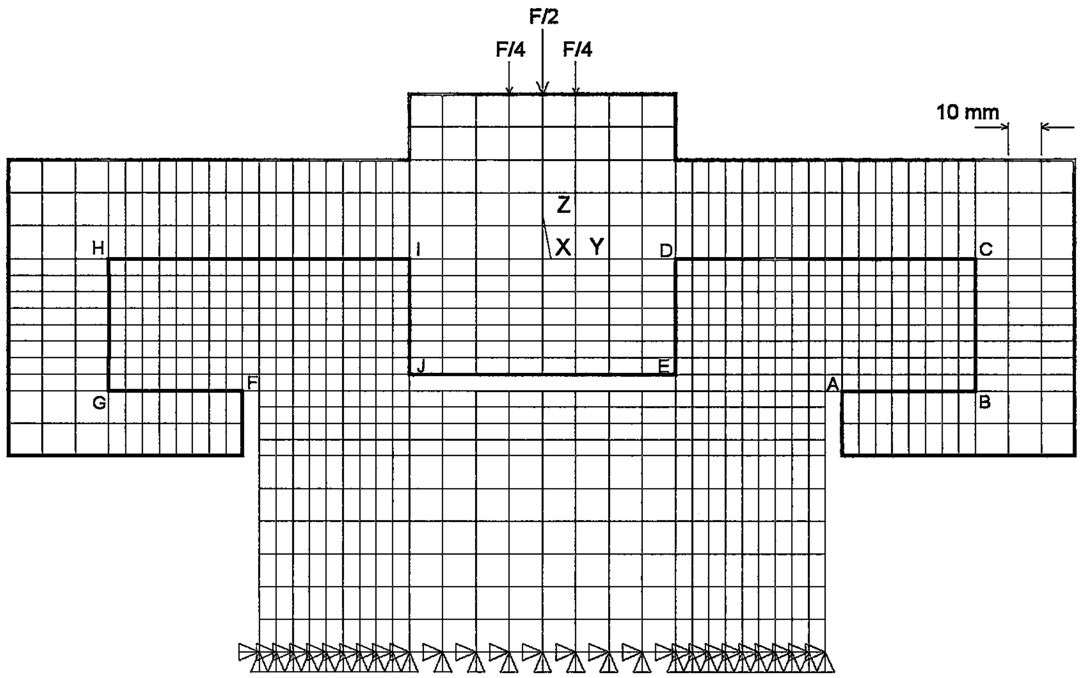

Figure 6.5 Finite Element Division of the Closed Type Flat Slideway and Load Application Points. F is the Total External Load

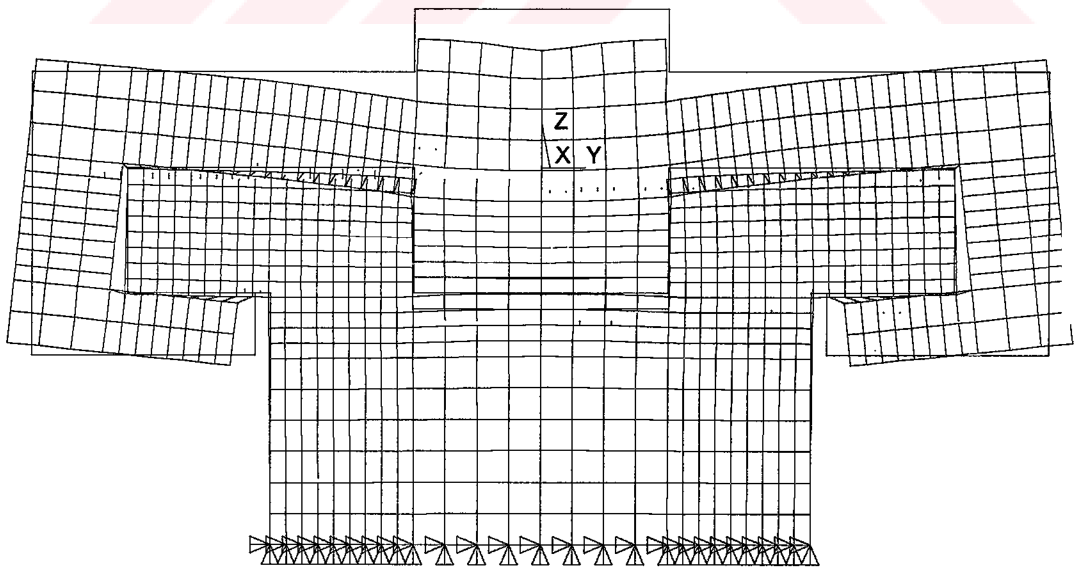

Figure 6.6 Deformed Shape of the Closed Type Flat Slideway Model for 1.6 MPa Mean Interface Pressure

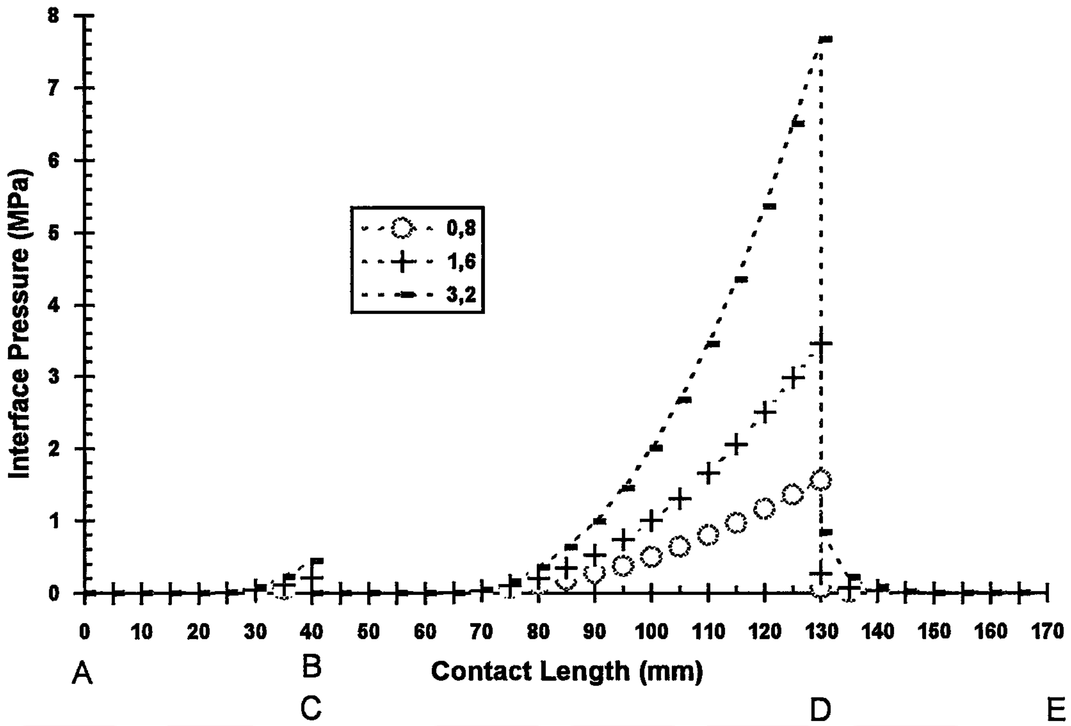

(a)

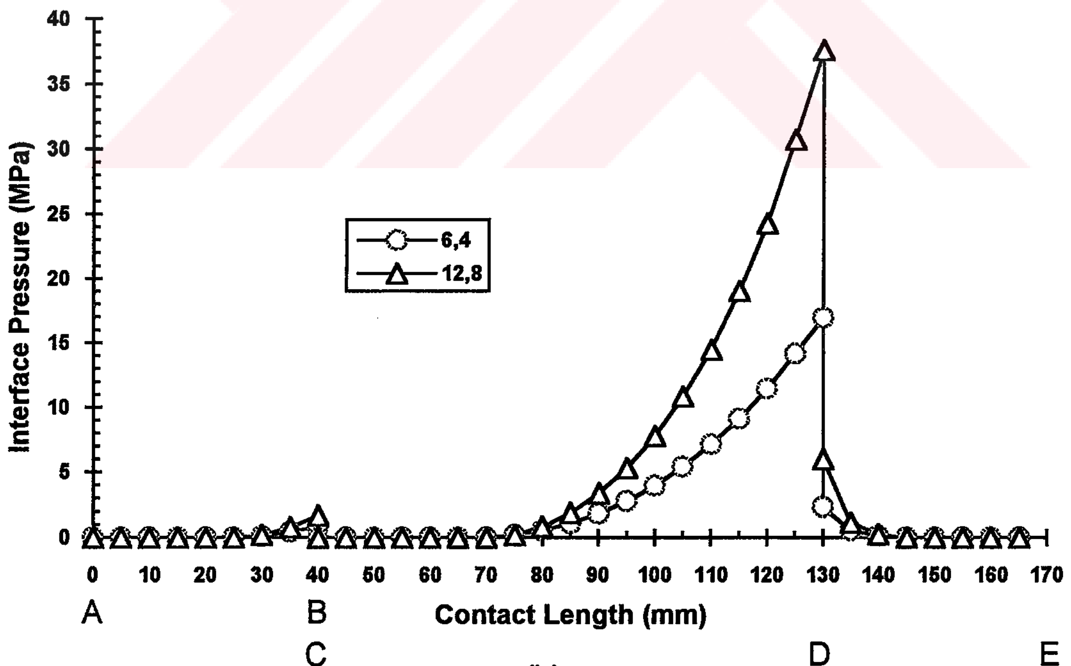

(b)

Figure 6.7 Pressure Distribution at the Contacting Surfaces of the Closed Type Flat Slideway Model for Several Mean Interface Pressures

6.3.3 Example 3: 2-D Dovetail Slideway

As the third example, finite element division and position of the loads for a dovetail slideway model is represented in Figure 6.8. The material is cast iron and surface compliance parameters are c= 0.25 and m=0.70, and the other parameters are the same with the previous examples. The length of contacting lines AB and CD is 42.42 mm.

The deformed shape of the model is shown for 1.6 MPa mean interface pressure in Figure 6.9. Figure 6.10. (a) and (b) show the calculated pressure distribution at contacting surfaces of dovetail slideway model for five different mean interface pressures. As the pressure increases, the length of contact decreases. In this example, for low mean interface pressures, the maximum pressure is about twice the mean interface pressure, but for high mean interface pressures, it is about four times the mean interface pressure.

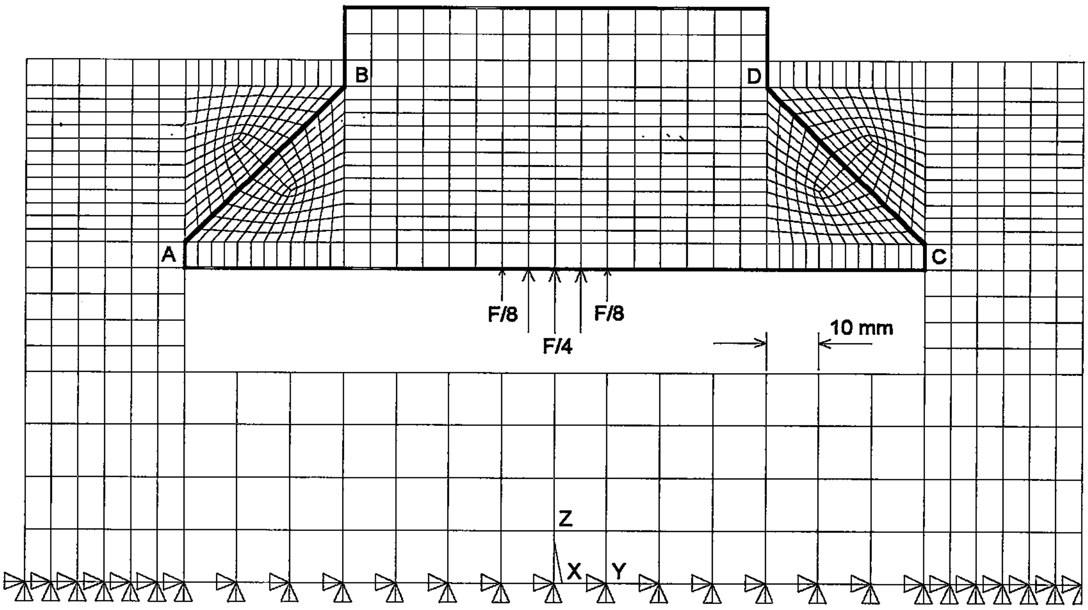

Figure 6.8 Finite Element Division of the Dovetail Slideway Model and Load Application Points. F is the Total External Load

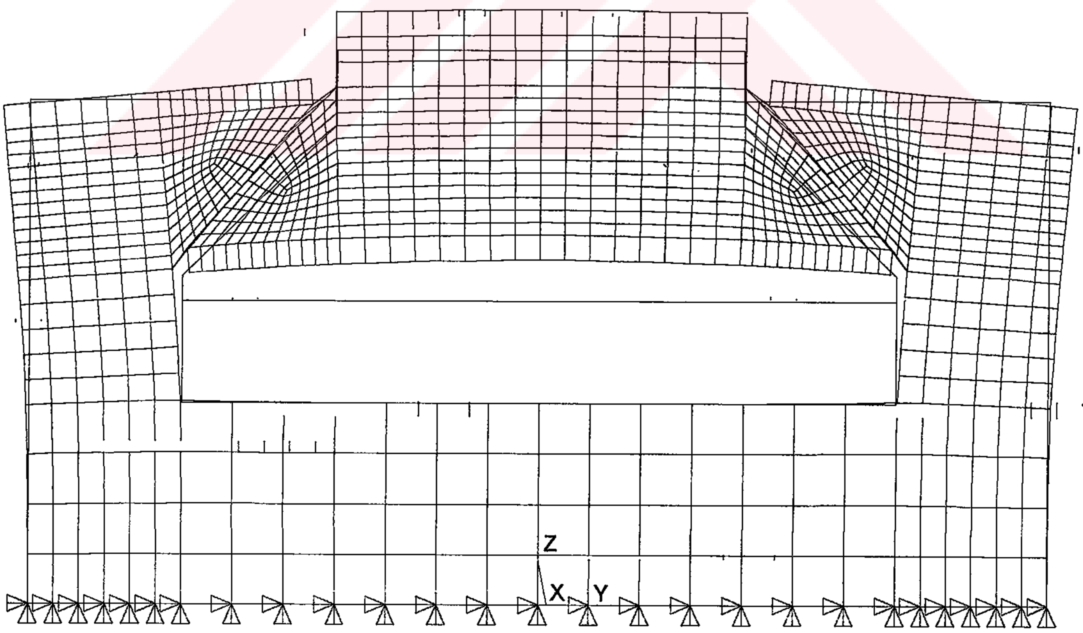

Figure 6.9 Deformed Shape of the Dovetail Slideway Model for 1.6 MPa Mean Interface Pressure

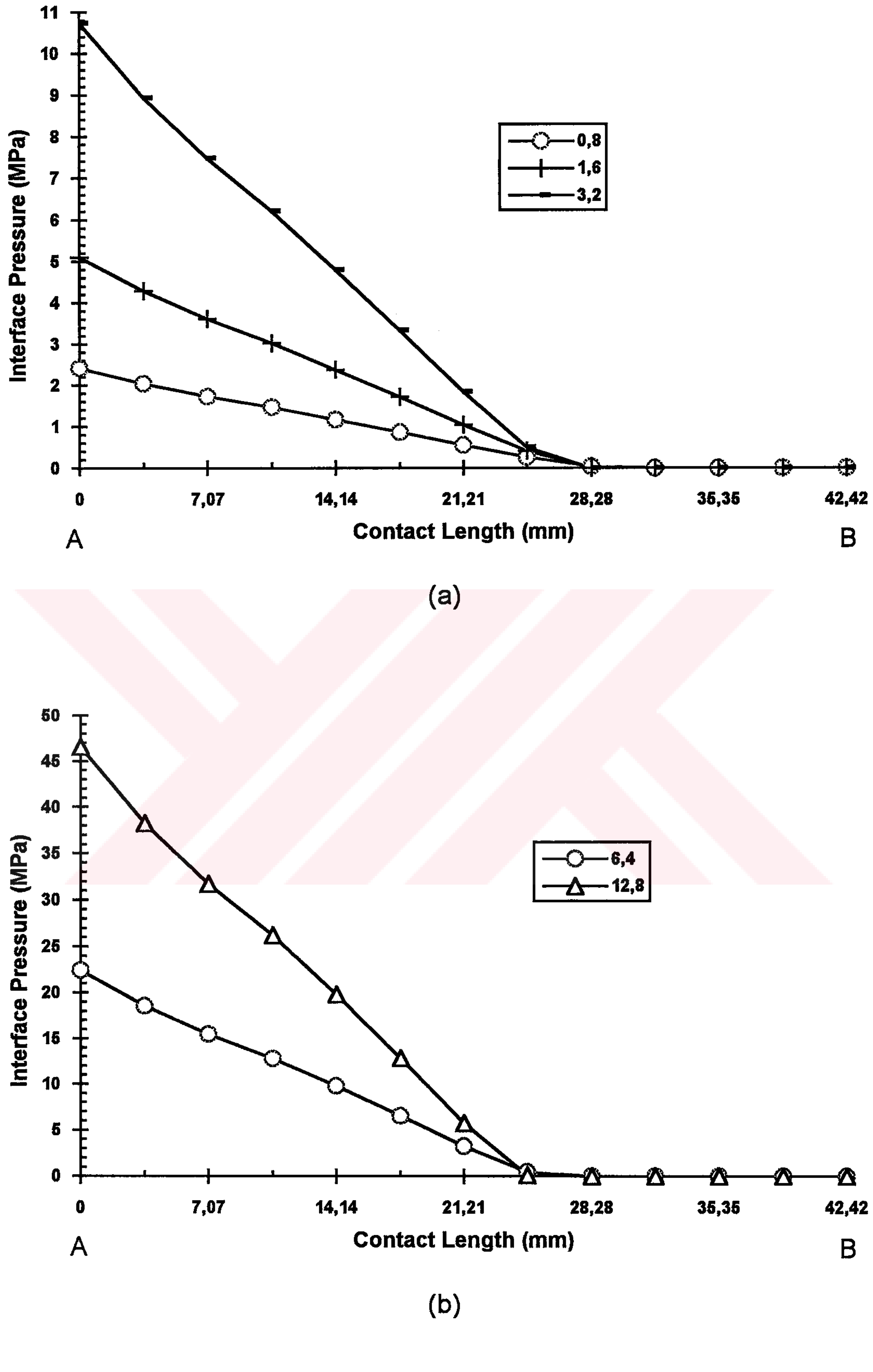

Figure 6.10 Pressure Distribution at the Contacting Surfaces of the Dovetail Slideway Model for Several Mean Interface Pressures

CHAPTER VII

THREE DIMENSIONAL ANALYSIS
OF
SLIDEWAYS

7.1 INTRODUCTION

In this chapter three dimensional models of slideways will be analysed by using the methods developed in chapter 5. Section 7.2 is devoted to the general considerations of three dimensional models of slideways. As an application of FEM with three dimensional contact elements some examples of common types of slideway models are analysed in Section 7.3.

7.2 GENERAL CONSIDERATIONS OF THREE DIMENSIONAL SLIDEWAYS

Maximum pressure on slideways have to be checked in the design process, since they considerably influence the life of slideways. They must not be higher than their permissible values which depend on the slideway material, the type of machine tool, and the machining operation.

The distribution of pressure has to be as uniform as possible along the slideway length to limit the effect of deformation of slideway surfaces on the accuracy of the workpiece, and to reduce wear of the slideway surfaces. Tilting moments are a serious treat to the uniformity of pressure distribution. The relative positions of the tip point of cutting tool and slideway surfaces have to be adjusted to minimise the effect of tilting moments. But in practice, it is not possible to eliminate tilting moments. In two dimensional models, only moments in x-axis could be included while the other components not. So, it is necessary to analyse slideways with three dimensional models to consider the effects of moments in all axis.

SOLID45, three dimensional structural solid element which is defined by eight nodes having three degrees of freedom at each node is used in modelling the body of three dimensional slideways. In order to model contacting surface of the slideways, CONTACT49, the node-to-surface contact element in three dimensions is used. The element has five nodes with three degrees of freedom at each node, translations in the nodal x, y, and z directions as explained in Chapter III section 3.4.

7.3 ANALYSES OF SLIDEWAYS WITH THREE DIMENSIONAL MODELS

Five different types of slideway examples are modelled for three dimensional analysis. First example is the same with the two dimensional models analysed in Chapter 6, an open type flat slideway. Second example is a closed type flat slideway. Third example is an open type dovetail model. Fourth example is a combined type of slideway; one side is flat and other side is a vee shape. This type of slideway is commonly used in lathes. The fifth example is chosen from an existing machine tool.

It is a small, closed type lathe which is used in student workshop of Mechanical Engineering Department of the University of Gaziantep.

7.3.1 Example 1: 3-D Open Type Flat Slideway

Dimensions and finite element division of three dimensional open type flat slideway model is shown in Figure 7.1. Three dimensional contact elements are defined between contacting surfaces of which edge views are seen as red lines in Figure 7.1. The load was applied at the centre; and two couples are applied to obtain moment about y and z axis. The surface compliance parameters and material properties are the same with the first example in Chapter 6. Mean interface pressure is obtained by dividing the total applied external load to total contact area of the slideway. To obtain 1.6 MPa mean interface pressure, the applied load in z direction is F_z= 5650 N, and moments are M_y= 75 Nm, M_z= 85 Nm. The deformed shape of the Example 1 for 1.6 MPa mean interface pressure is shown in Figure 7.2.

Figures 7.3, 7.4 and 7.5 show the normal force distribution (pressure distribution) on the contacting guideway surfaces and stress distribution on x, y and z axis for 0.4, 1.6 and 6.4 MPa mean interface pressures respectively. For different mean interface pressures, the trends of pressure distribution are similar. The values of maximum interface pressures are 0.46, 2.54 and 16.39 MPa, and they are about 1.15, 1.58 and 2.56 times of the mean interface pressures respectively.

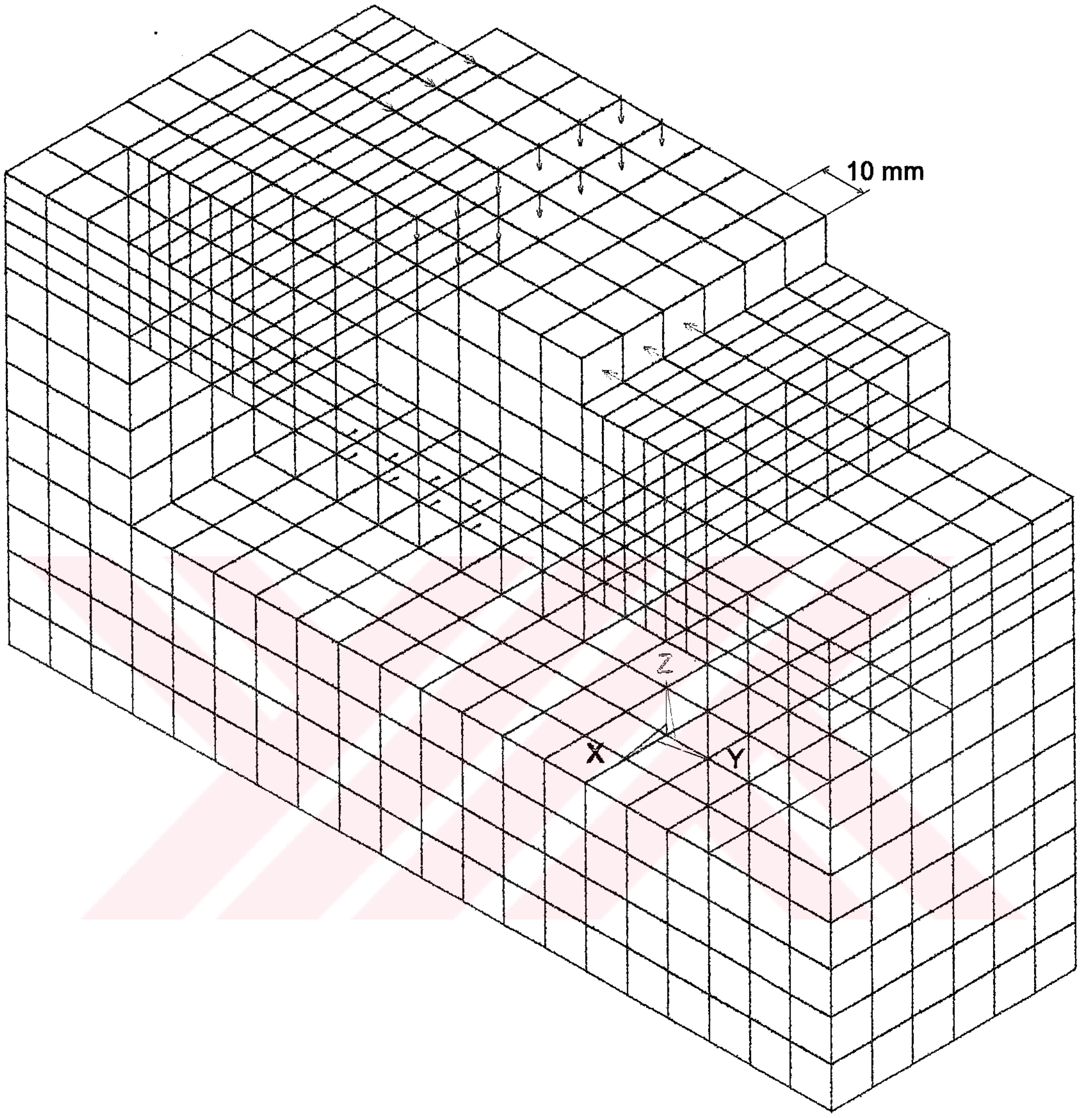

Figure 7.1 Finite Element Division of the Open Type Flat Slideway and Load Application Points

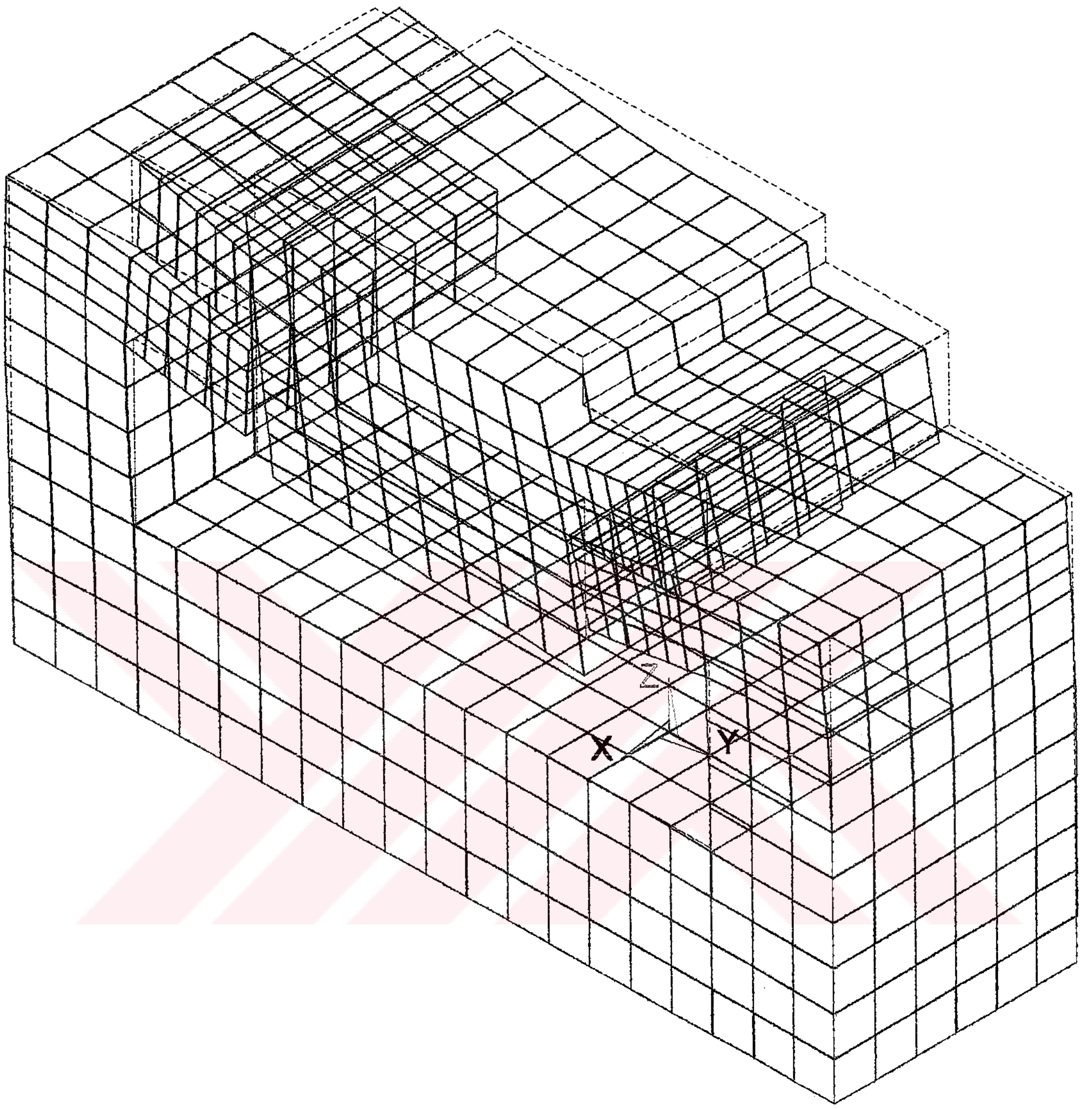

Figure 7.2 Deformed Shape of the Open Type Flat Slideway for 1.6 MPa Mean Interface Pressure.

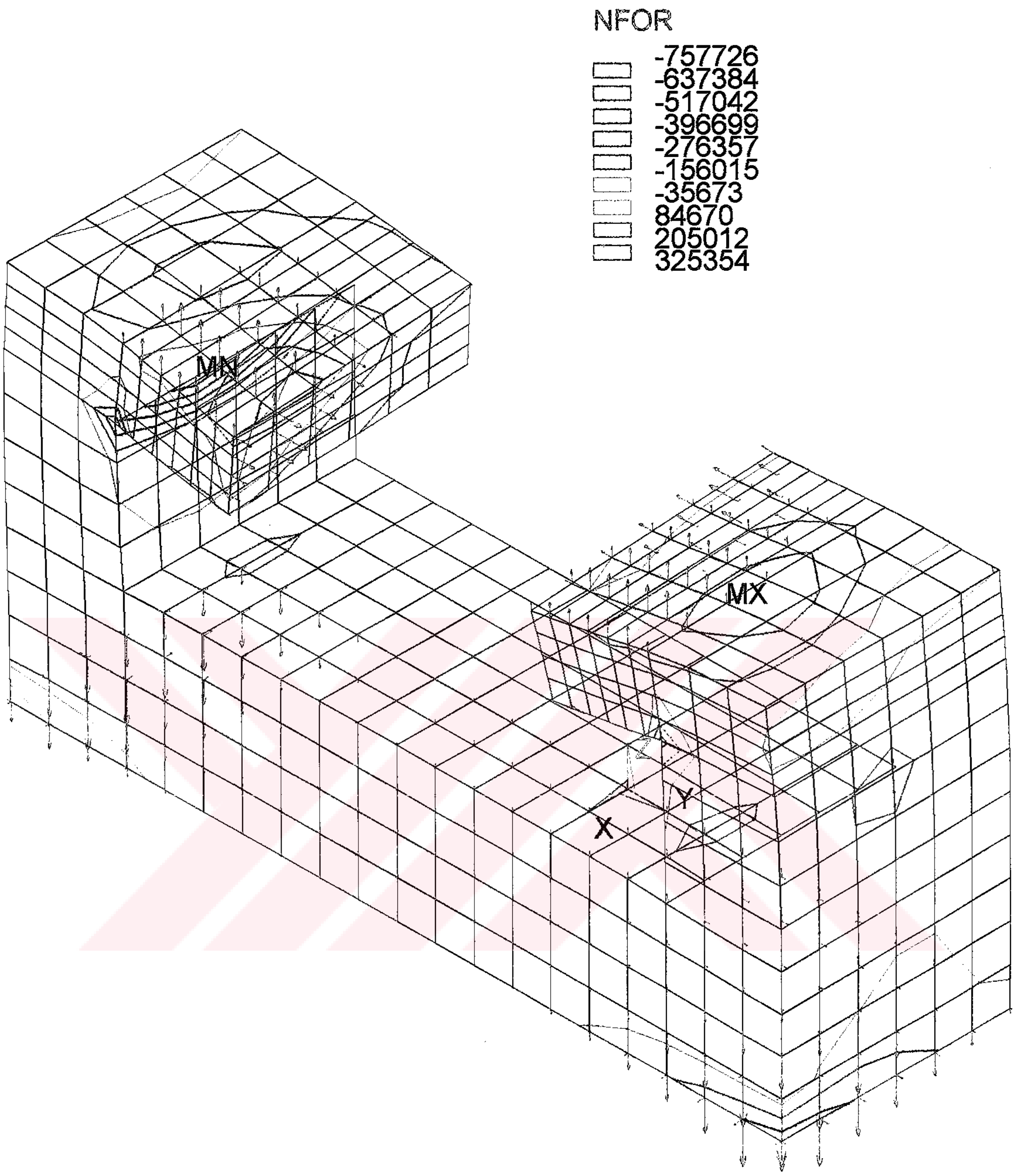

Figure 7.3 Pressure Distribution at the Contacting Surfaces and Stress Distribution in x-axis for 0.4 MPa Mean Interface Pressure (for Example 1)

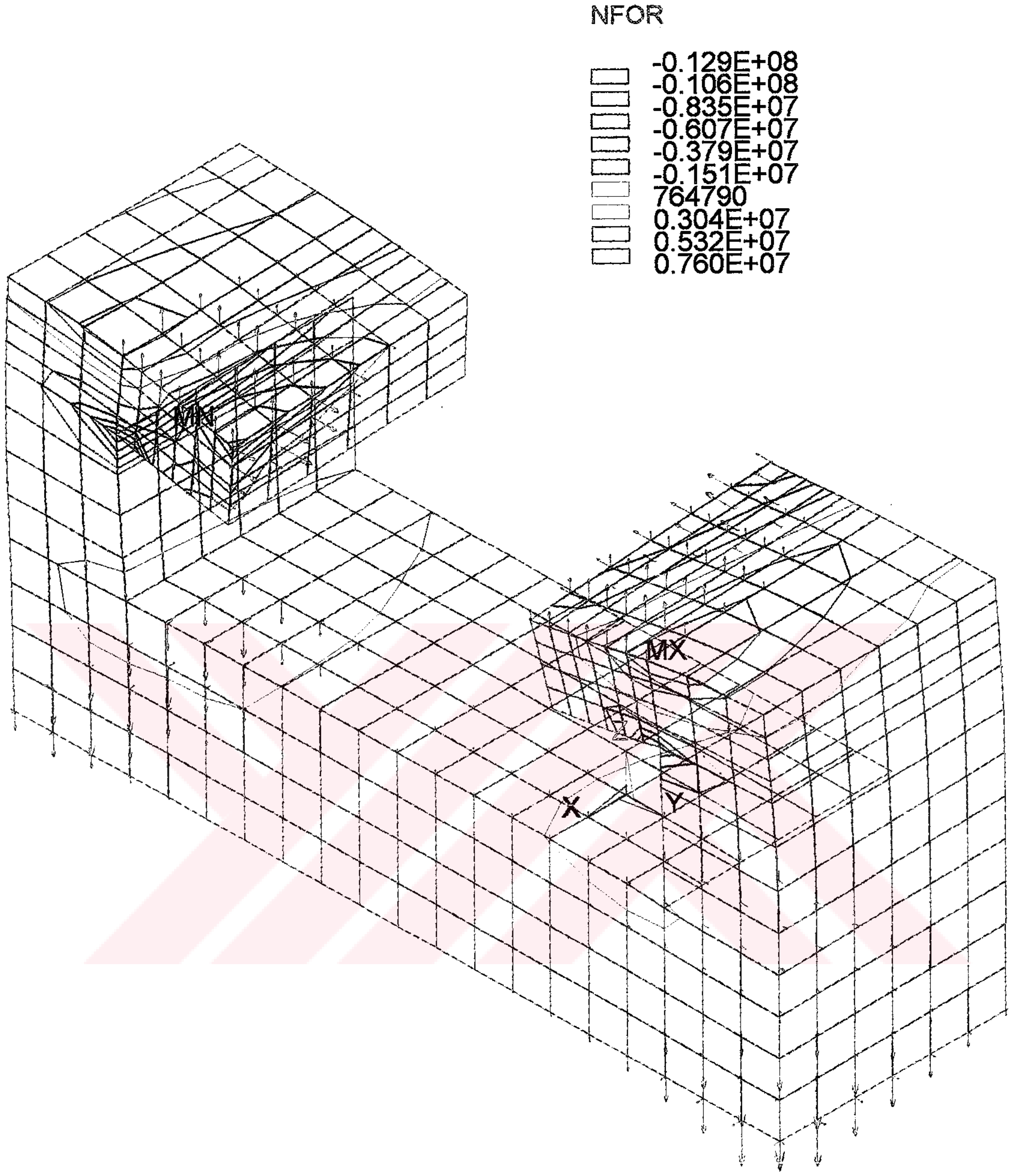

Figure 7.4 Pressure Distribution at the Contacting Surfaces and Stress Distribution in y-axis for 1.6 MPa Mean Interface Pressure (for Example 1).

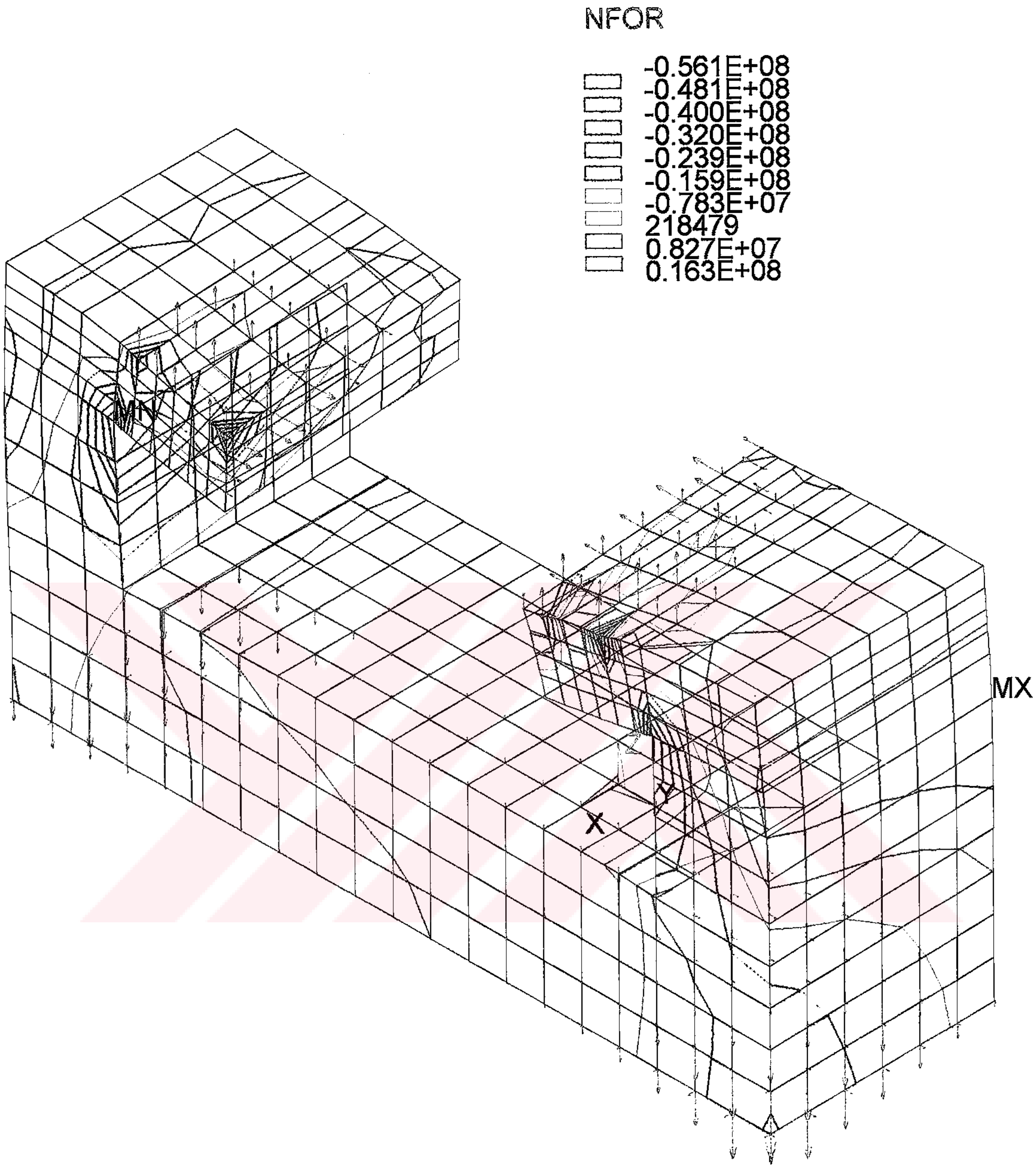

Figure 7.5 Pressure Distribution at the Contacting Surfaces and Stress Distribution in z-axis for 6.4 MPa Mean Interface Pressure (for Example 1).

7.3.2 Example 2: 3-D Closed Type Flat Slideway

Dimensions and finite element division of the second three dimensional slideway model is shown in Figure 7.6. Contact elements are defined between contacting surfaces of which edge views are seen as red lines in Figure 7.6. The load was applied at the centre; and two couples are applied to obtain moment about y and z axis. To obtain 1.6 MPa mean interface pressure, the applied load in z direction is F_z= 9417 N, and moments are M_y= 63 Nm, M_z= 71 Nm. The surface compliance parameters and material properties are the same with the second example in Chapter 6. Deformed shape of the model for 1.6 MPa mean interface pressure is shown in Figure 7.7.

Figures 7.8, 7.9 and 7.10 show the normal force distribution (pressure distribution) on the contacting guideway surfaces and stress distribution on x, y and z axis for 0.4, 1.6 and 6.4 MPa mean interface pressures respectively. The values of maximum interface pressures, for this example, are 0.47, 2.26 and 10.89 MPa and they are about 1.17, 1.41 and 1.70 times of the mean interface pressures respectively.

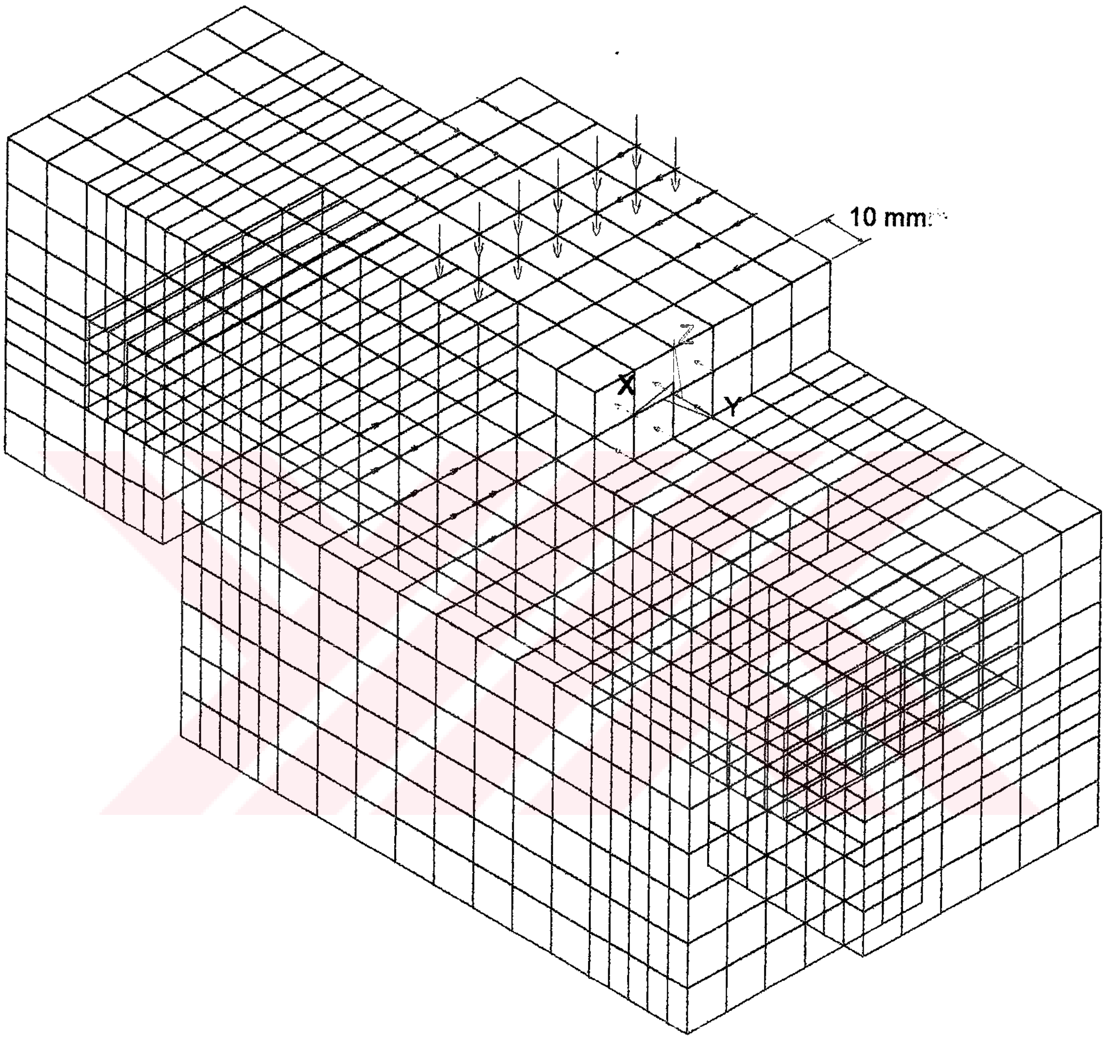

Figure 7.6 Finite Element Division of the Closed Type Flat Slideway and Load Application Points

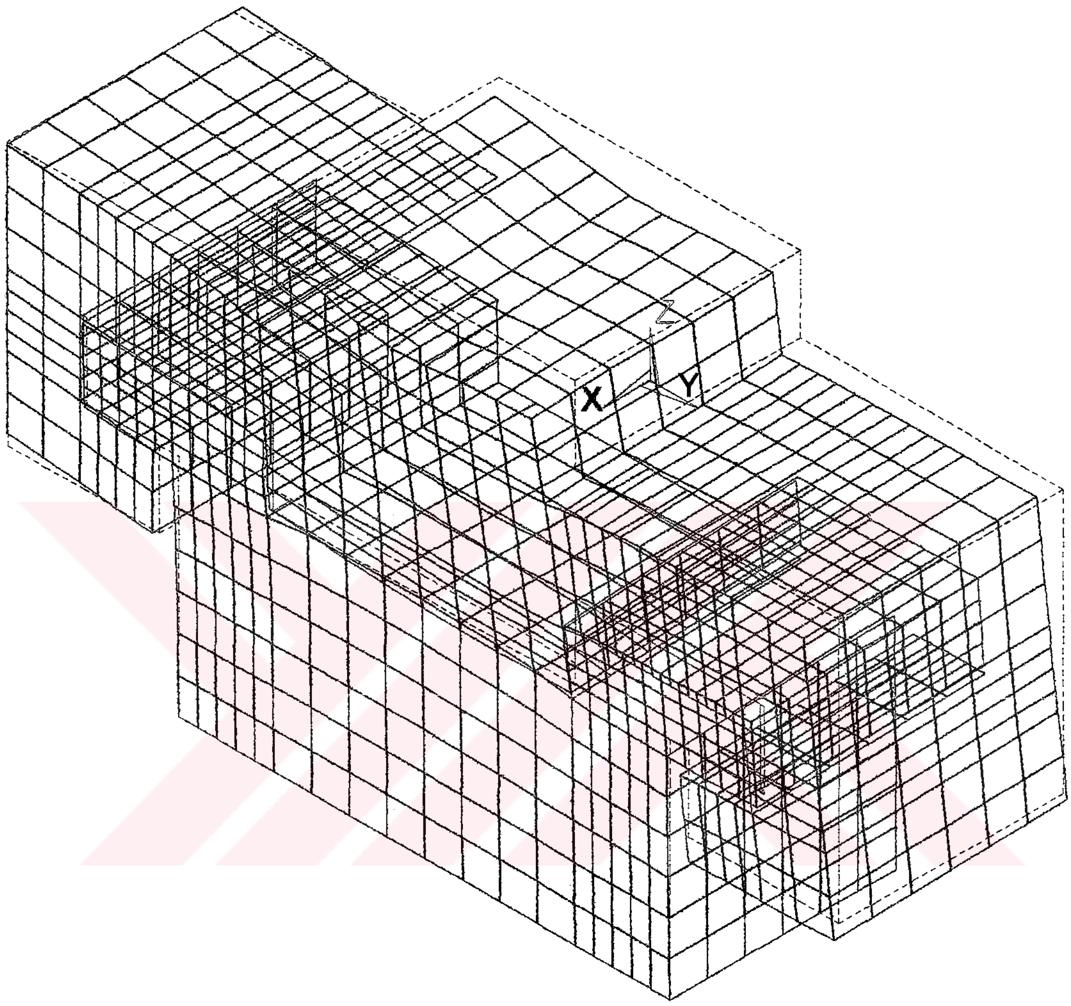

Figure 7.7 Deformed Shape of the Closed Type Flat Slideway for 1.6 MPa Mean Interface Pressure.

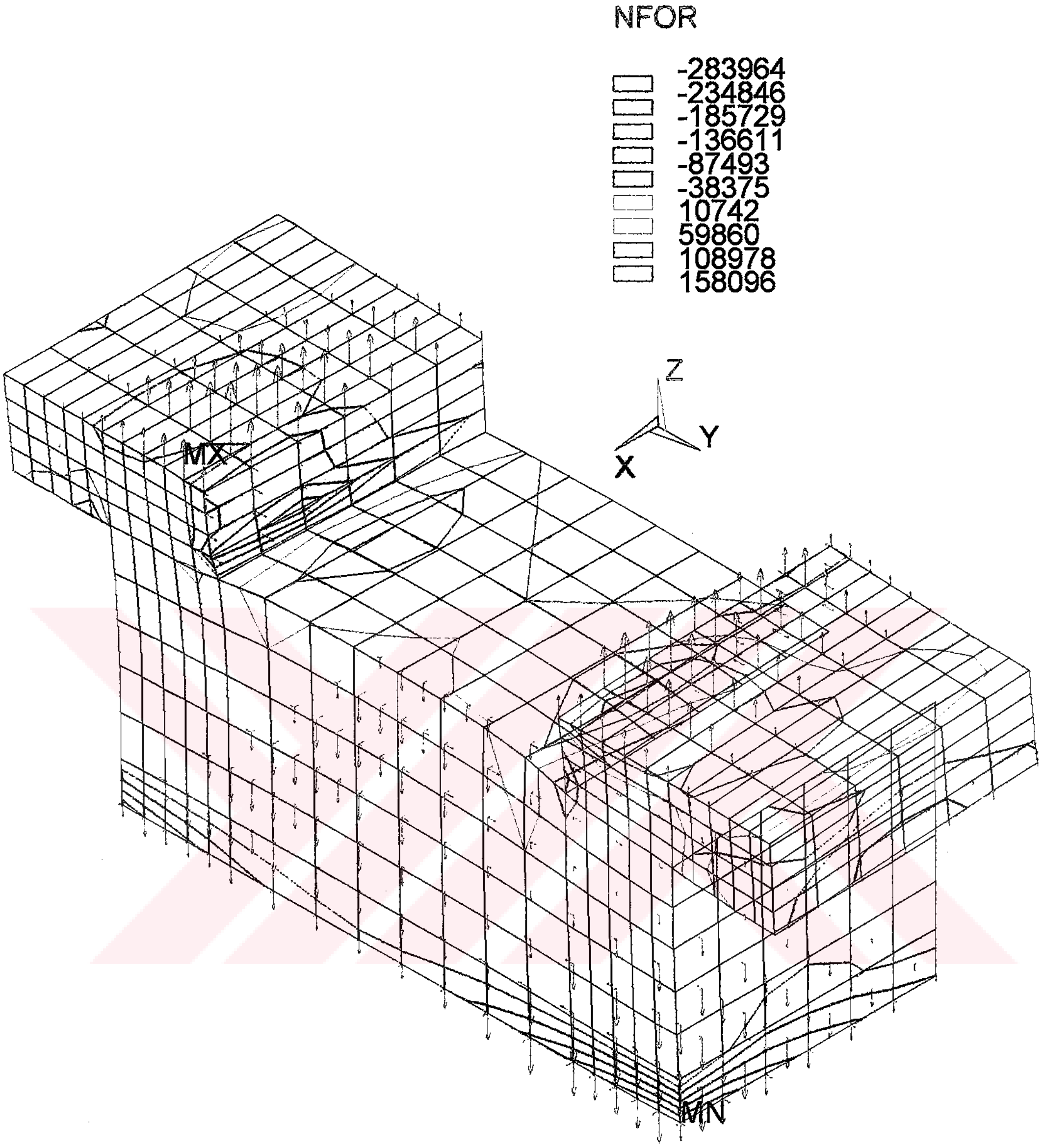

Figure 7.8 Pressure Distribution at the Contacting Surfaces and Stress Distribution in x-axis for 0.4 MPa Mean Interface Pressure (for Example 2).

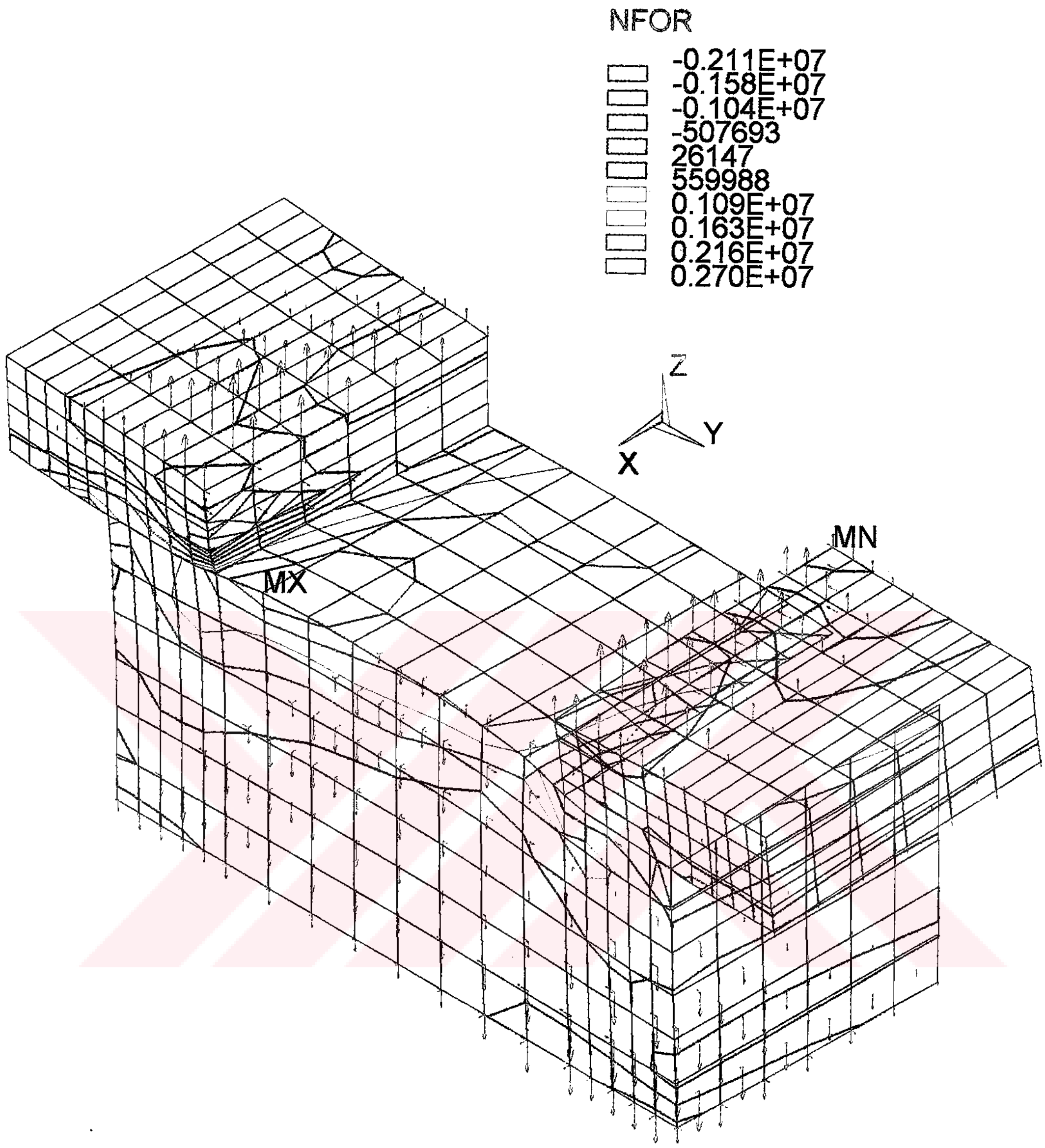

Figure 7.9 Pressure Distribution at the Contacting Surfaces and Stress Distribution in y-axis for 1.6 MPa Mean Interface Pressure (for Example 2)

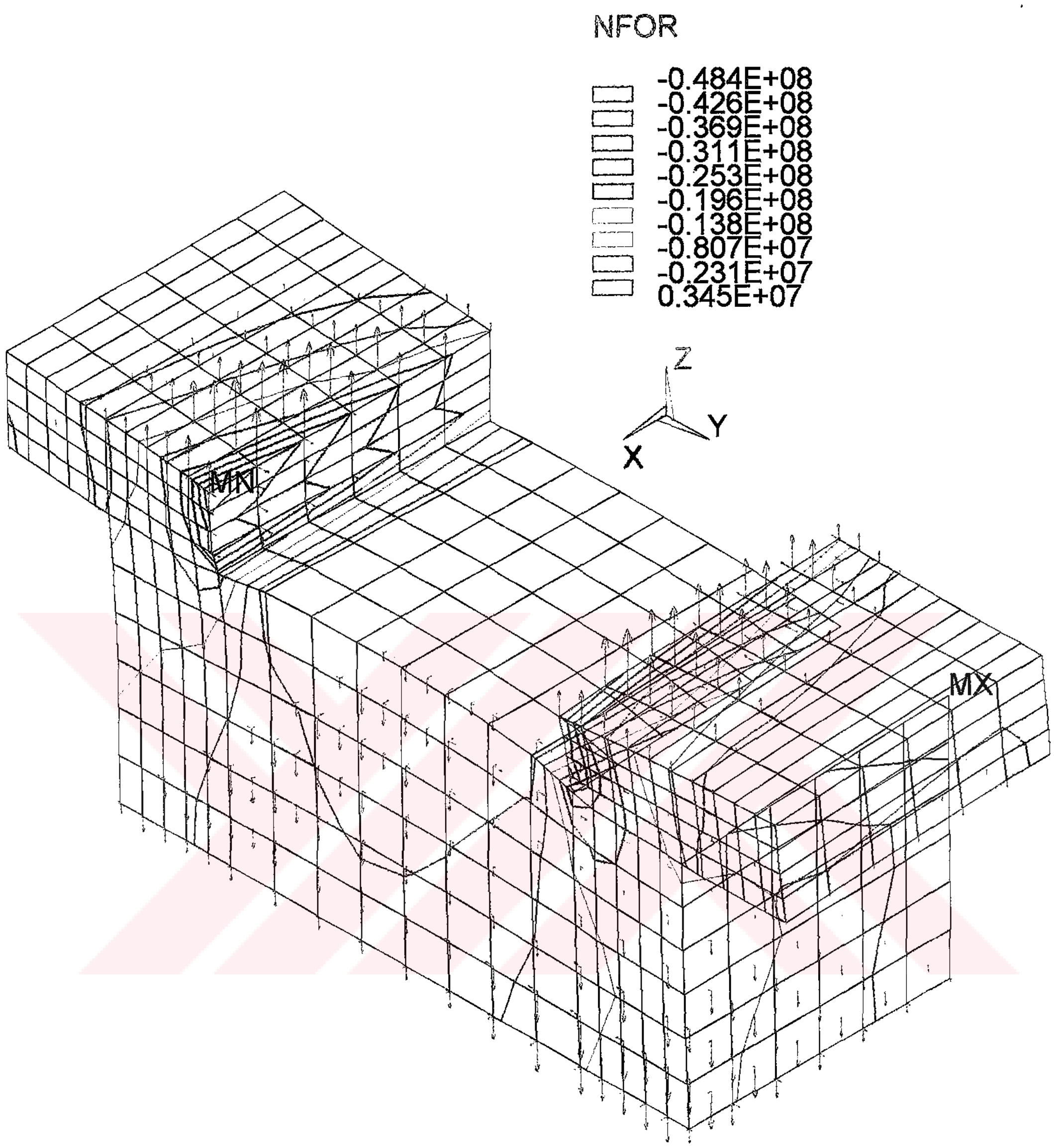

Figure 7.10 Pressure Distribution at the Contacting Surfaces and Stress Distribution in z-axis for 6.4 MPa Mean Interface Pressure (for Example 2)

7.3.3 Example 3: 3-D Dovetail Slideway

Figure 7.11 shows the dimensions and finite element division of the three dimensional dovetail slideway model. Contact elements are defined between contacting surfaces of which edge views are seen as red lines in Figure 7.11. The load was applied at the centre; and two couples are applied to obtain moment about y and z axis. To obtain 1.6 MPa mean interface pressure, the applied load in z direction is F_z= 5650 N, and moments are M_y= 37 Nm, M_z= 42 Nm. The surface compliance parameters and material properties are the same with the Example 3 in Chapter 6. Deformed shape of the model for 1.6 MPa mean interface pressure is shown in Figure 7.12.

Figures 7.13, 7.14 and 7.15 show the normal force distribution (pressure distribution) on the contacting guideway surfaces and stress distribution on x, y and z axis for 0.1, 0.4 and 1.6 MPa mean interface pressures respectively. The values of maximum interface pressures are 0.12, 0.53 and 8.79 MPa and they are about 1.18, 1.32 and 5.49 times of the mean interface pressures respectively. For low mean interface pressures, the maximum pressure is about the same with the mean interface pressure, but for high mean interface pressures, it is about five times the mean interface pressure.

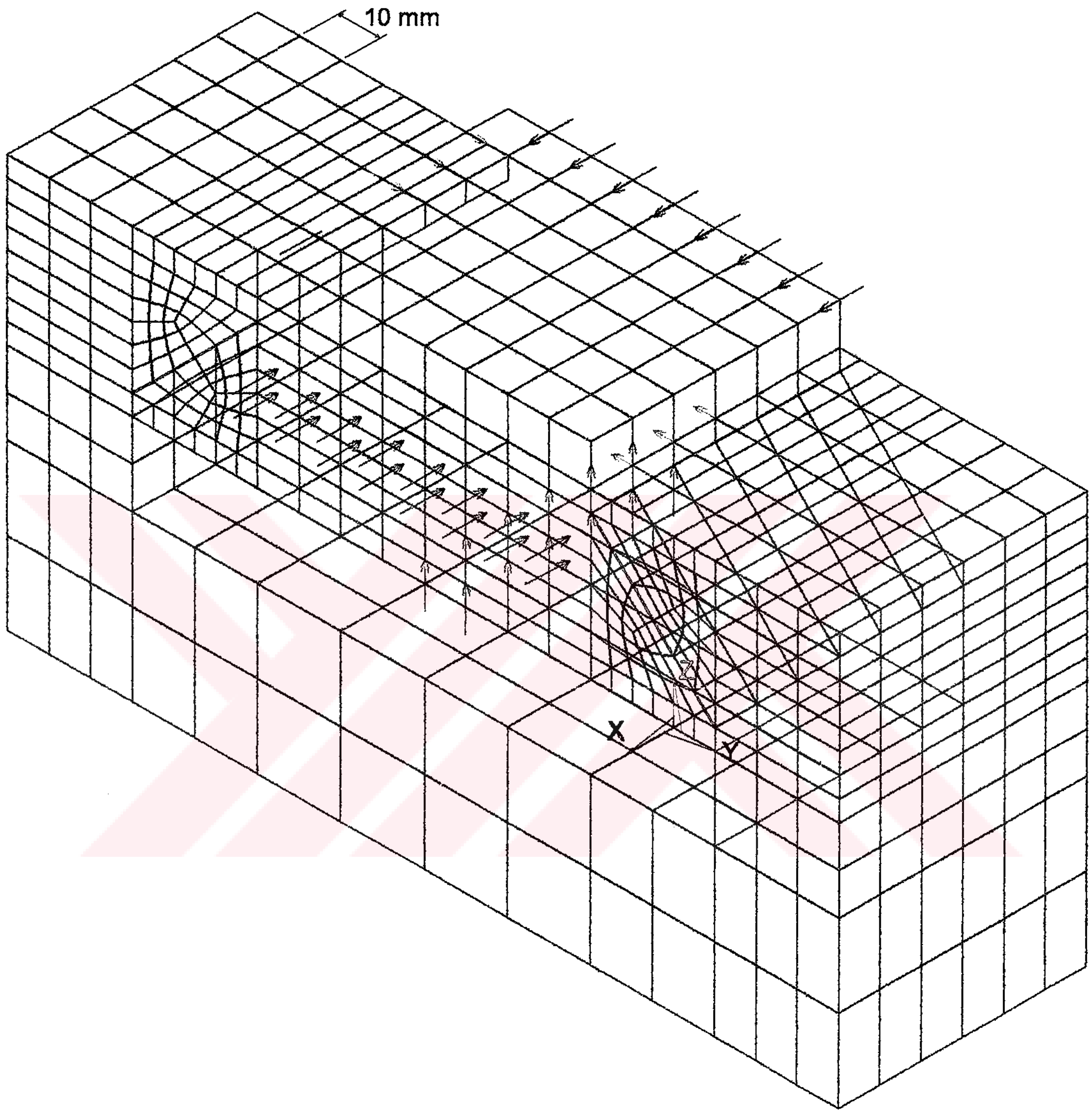

Figure 7.11 Finite Element Division of Dovetail Slideway and Load Application Points

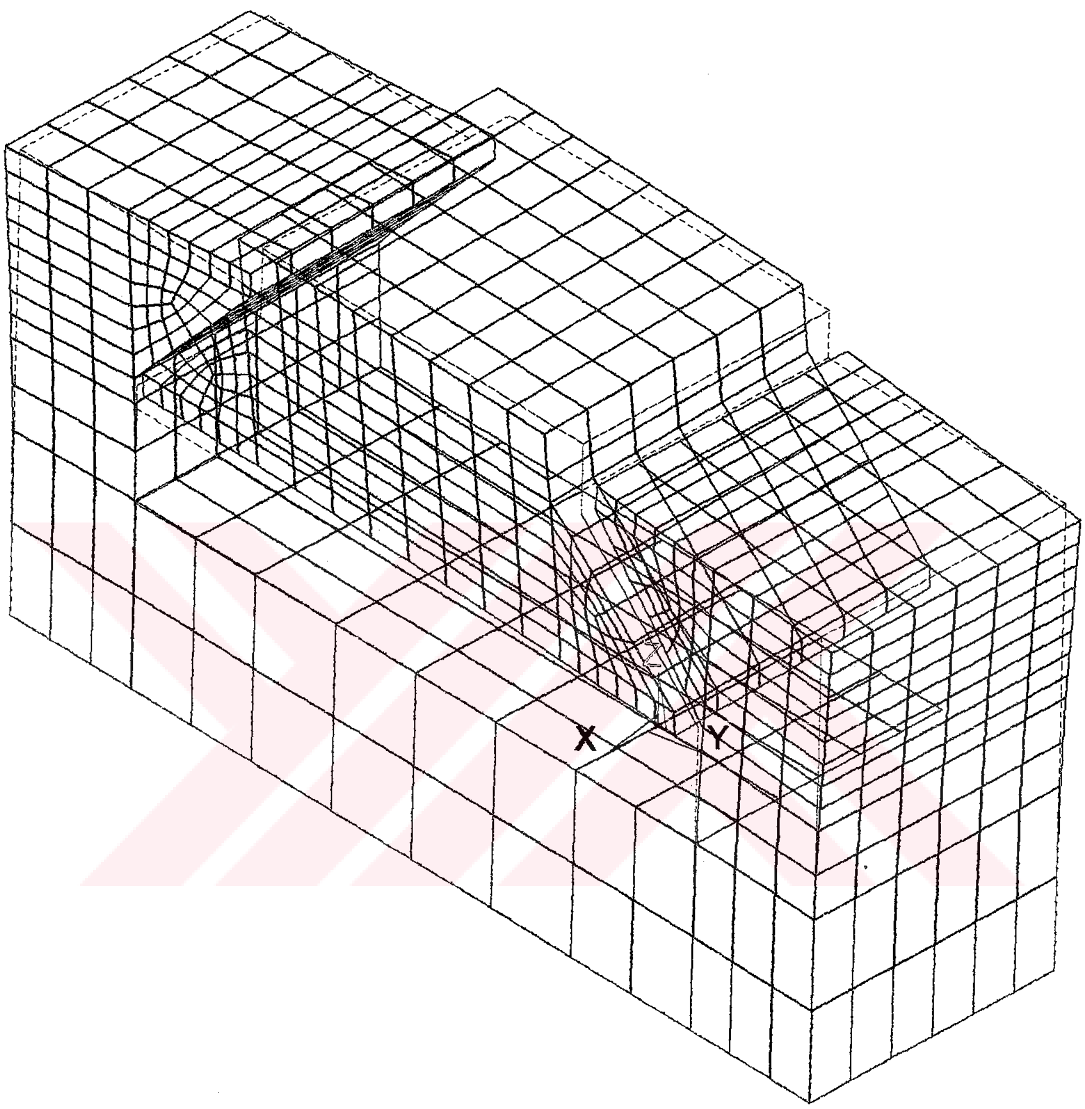

Figure 7.12 Deformed Shape of Dovetail Slideway for 1.6 MPa Mean Interface Pressure.

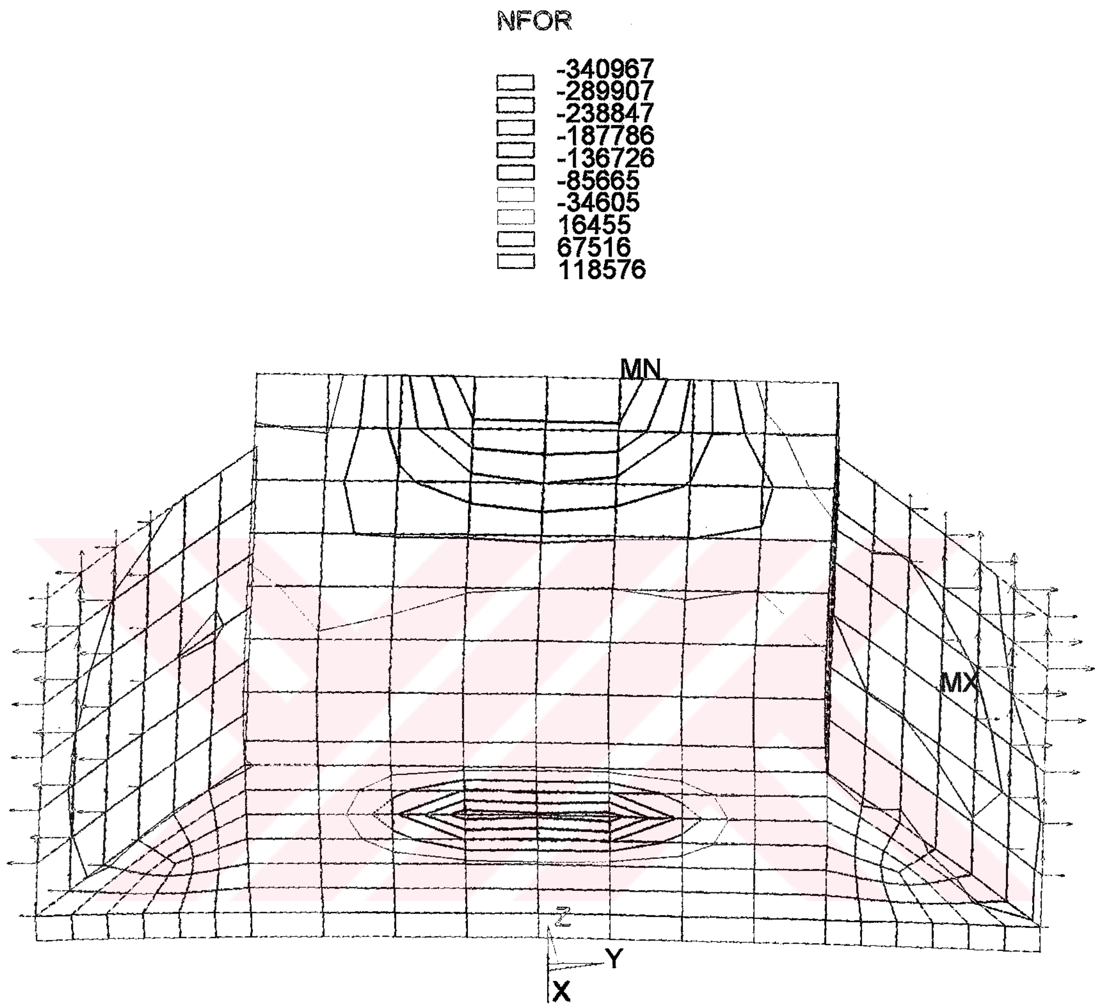

Figure 7.13 Pressure Distribution at the Contacting Surfaces and Stress Distribution in x-axis for 0.1 MPa Mean Interface Pressure (for Example 3)

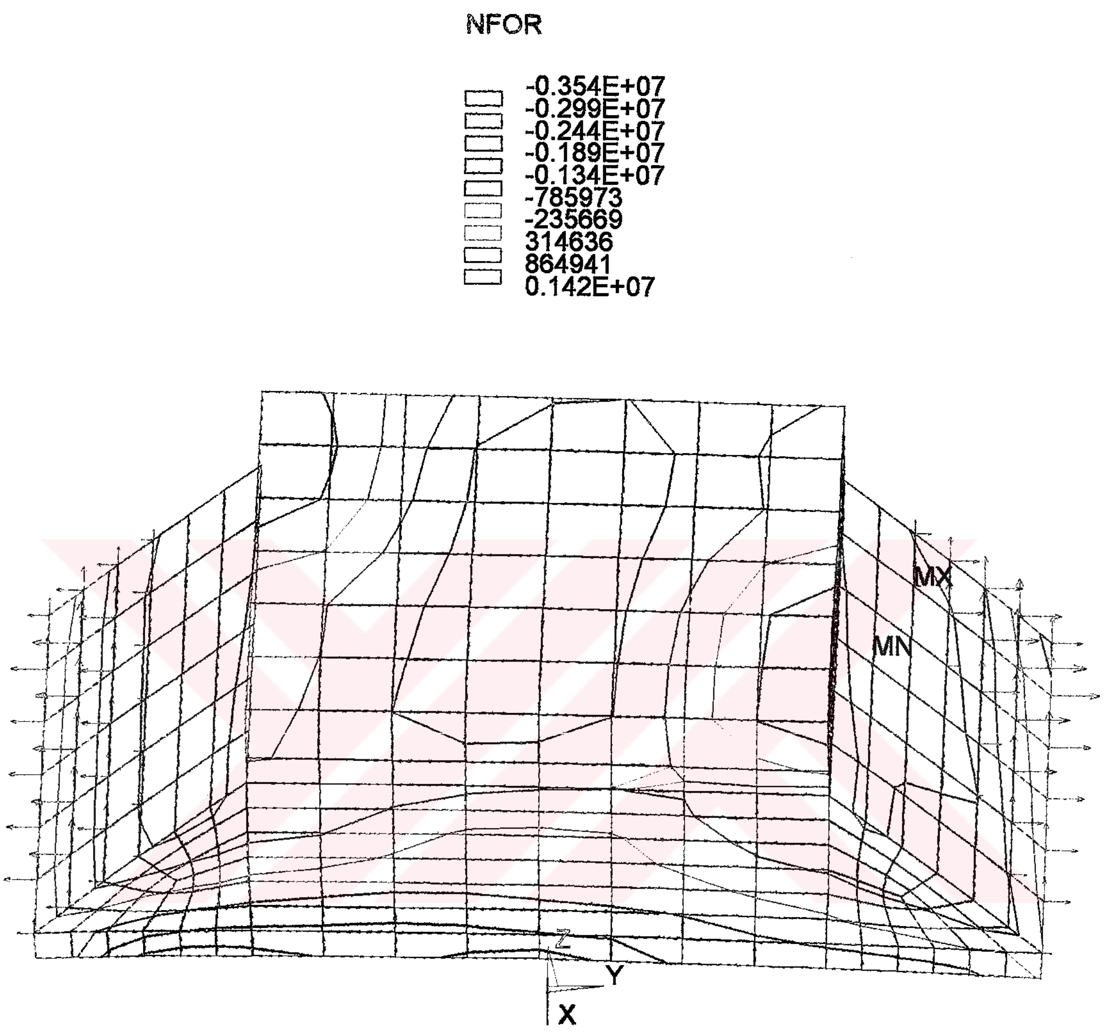

Figure 7.14 Pressure Distribution at the Contacting Surfaces and Stress Distribution in y-axis for 0.4 MPa Mean Interface Pressure (for Example 3)

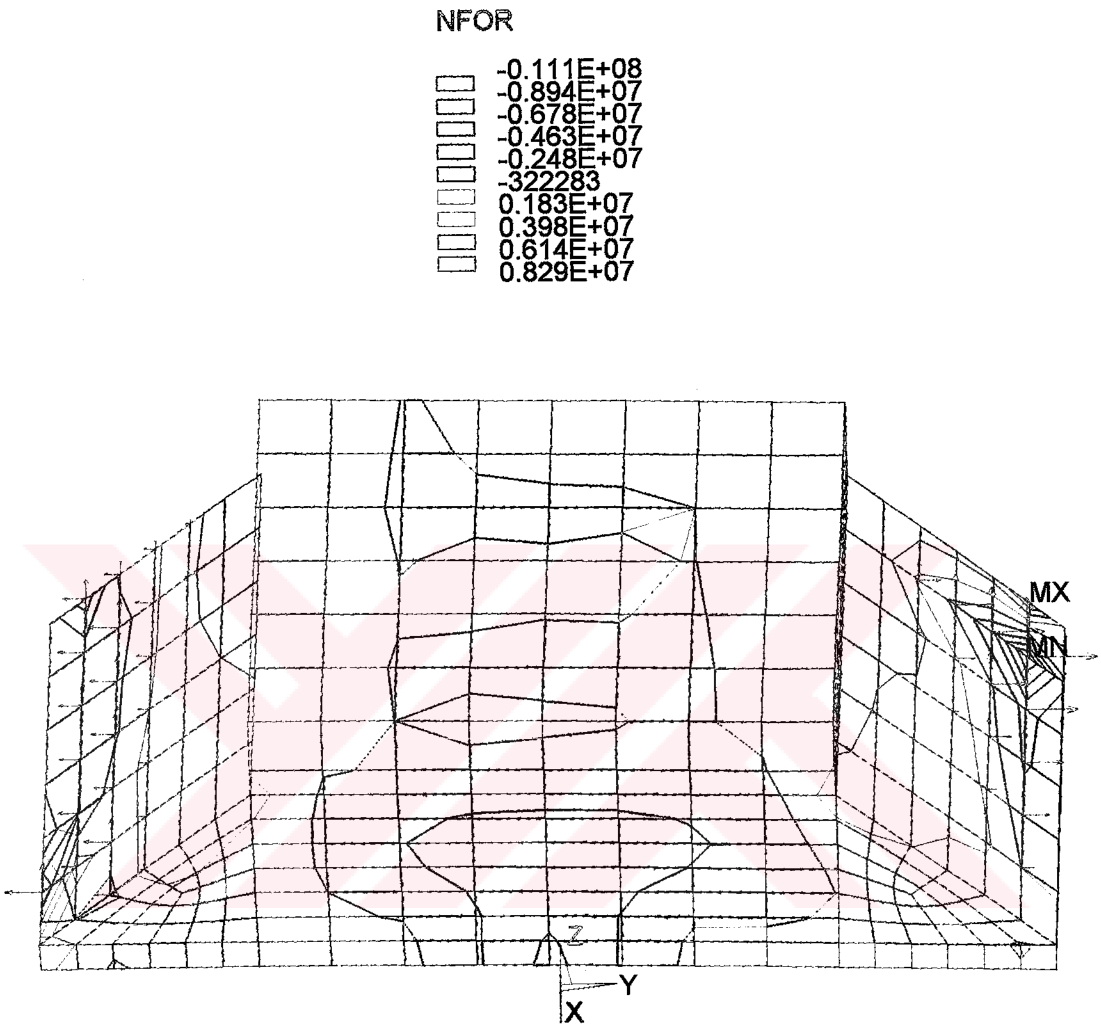

Figure 7.15 Pressure Distribution at the Contacting Surfaces and Stress Distribution in *z*-axis for 1.6 MPa Mean Interface Pressure (for Example 3)

7.3.4 Example 4: 3-D Combined Type Slideway

Dimensions and finite element division of the three dimensional combined type slideway model is shown in Figure 7.16. Contact elements are defined between contacting surfaces of which edge views are seen as red lines in Figure 7.16. The load was applied at the centre; and two couples are applied to obtain moment about y and z axis. To obtain 1.6 MPa mean interface pressure, the applied load in z direction is F_z= 11301 N, and moments are M_y= 75 Nm, M_z= 85 Nm. The surface compliance parameters and material properties are the same with the third example in chapter 6. The deformed shape of the model for 1.6 MPa mean interface pressure is shown in Figure 7.17.

Figures 7.18, 7.19 and 7.20 show the normal force distribution (pressure distribution) on the contacting guideway surfaces and stress distribution on x, y and z axis for 0. 4, 1.6 and 6.4 MPa mean interface pressures respectively. The values of maximum interface pressure, for this example, are 0.61, 3.04 and 19.28 MPa and they are about 1.53, 1.90 and 3.01 times of the mean interface pressure.

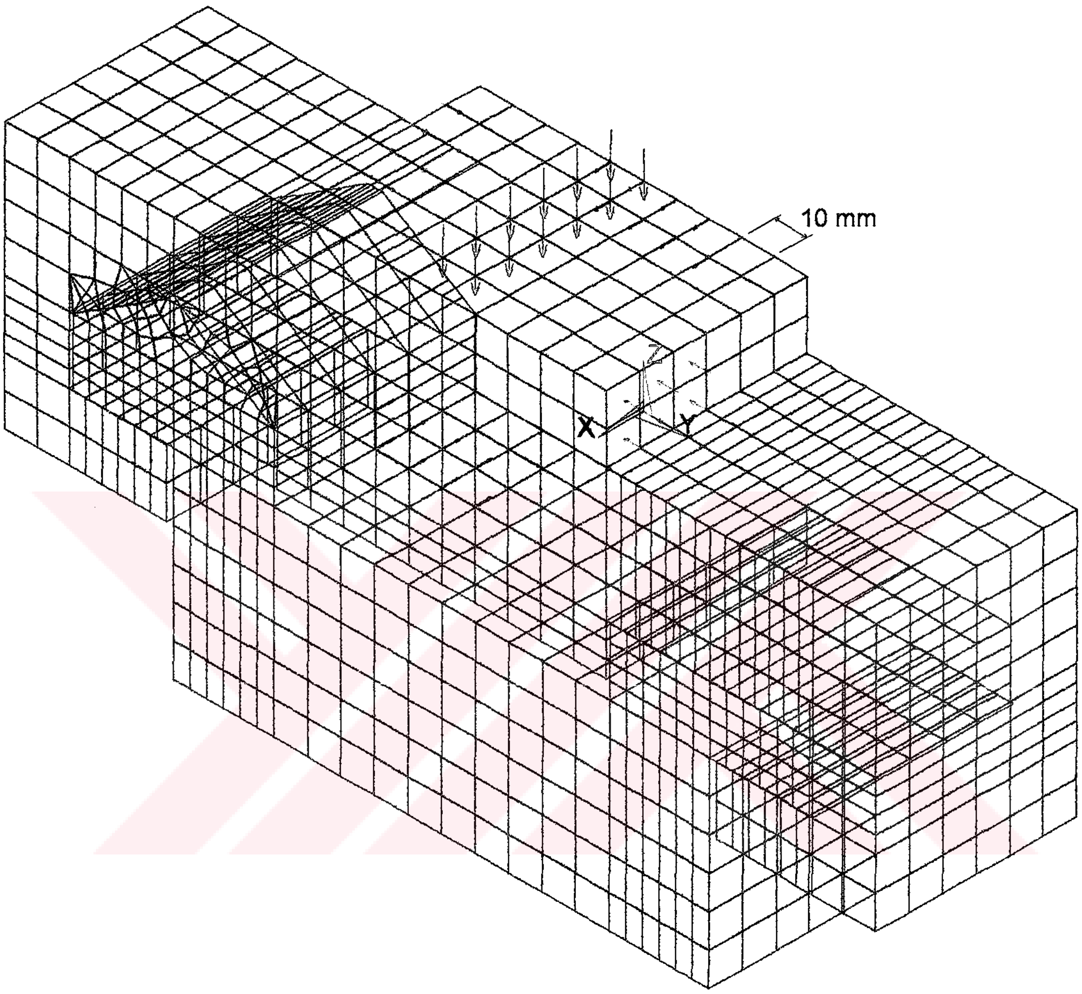

Figure 7.16 Finite Element Division of Combined Slideway Model and Load Application Points

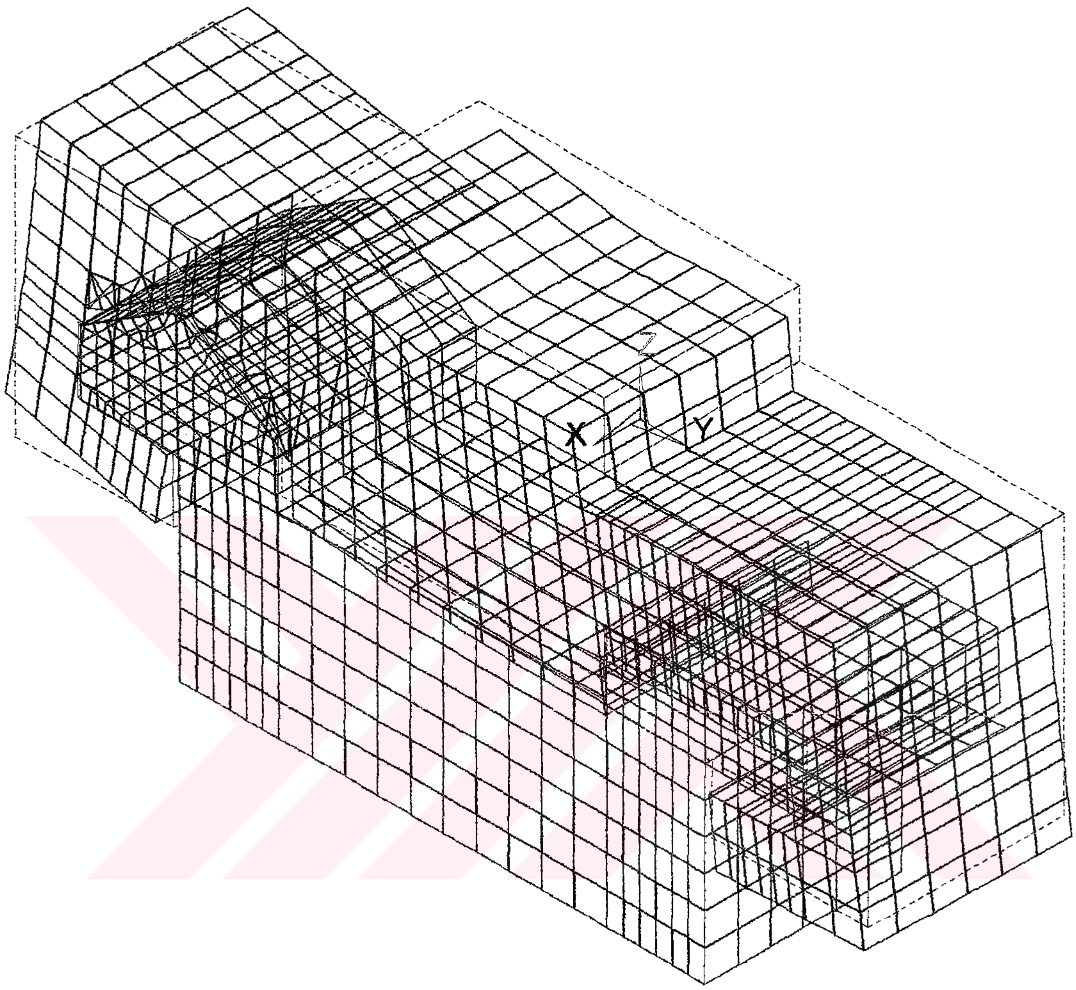

Figure 7.17 Deformed Shape of Combined Slideway Model for 1.6 MPa Mean Interface Pressure.

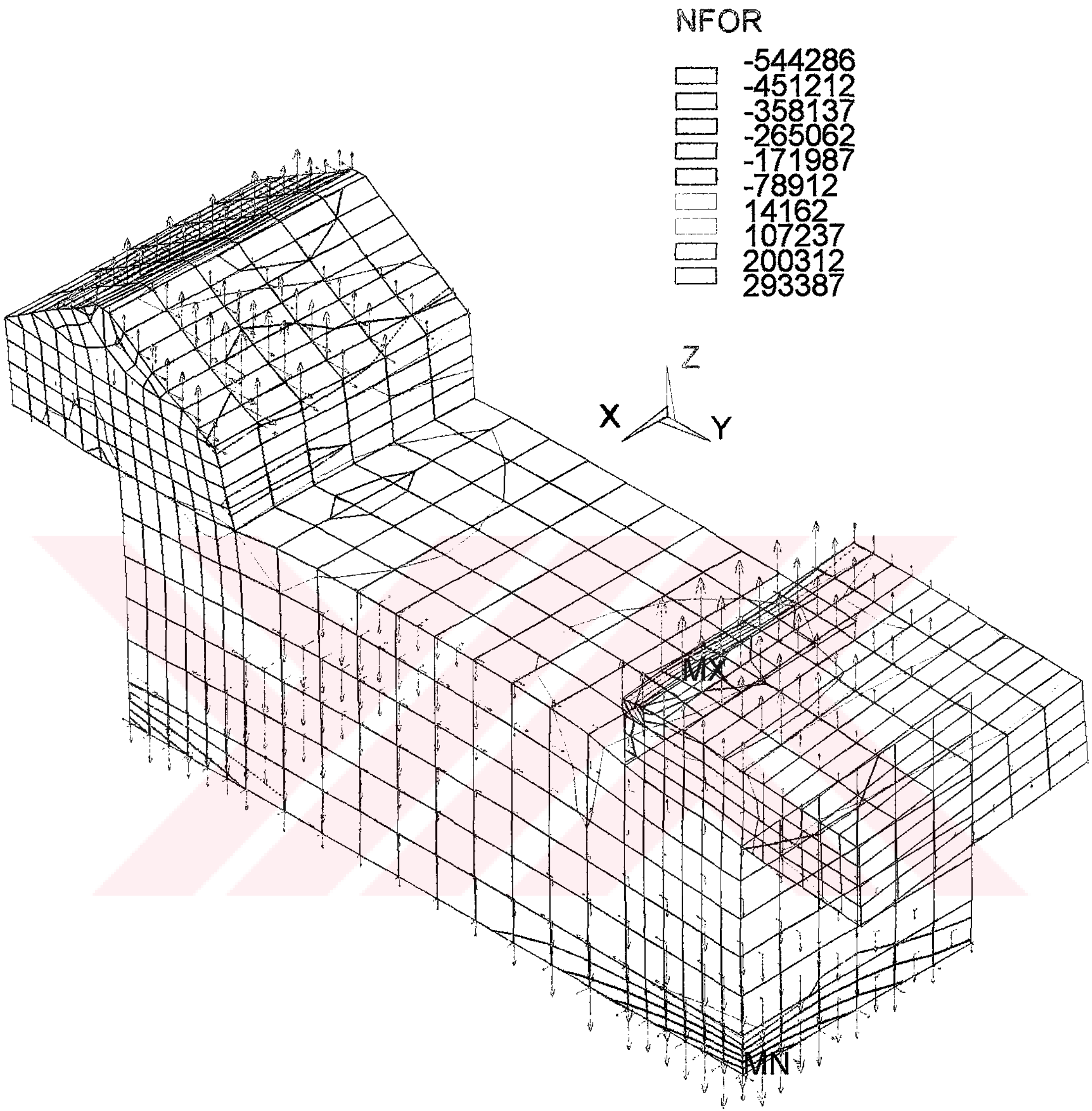

Figure 7.18 Pressure Distribution at the Contacting Surfaces and Stress Distribution in x-axis for 0.4 MPa Mean Interface Pressure (for Example 4)

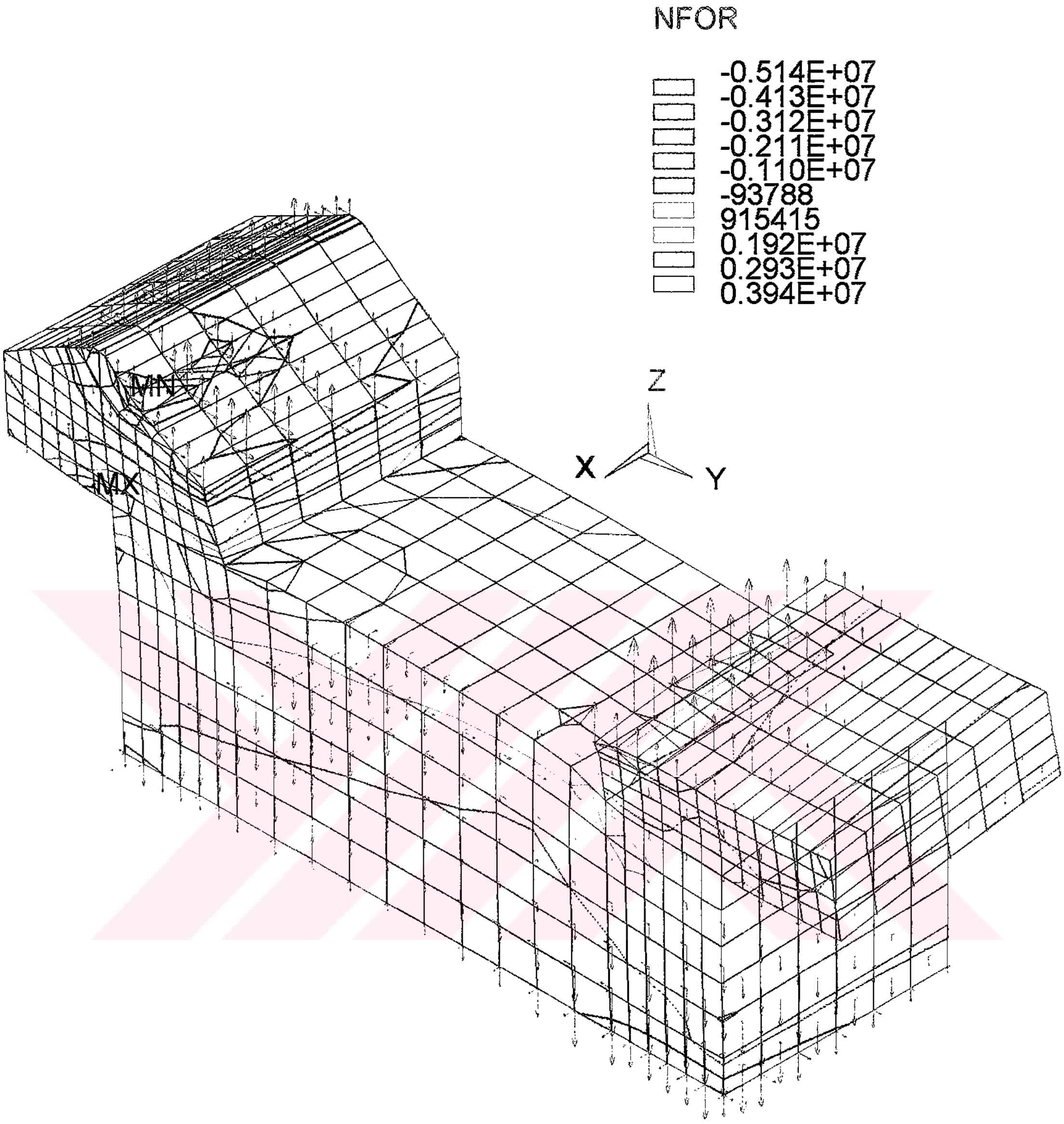

Figure 7.19 Pressure Distribution at the Contacting Surfaces and Stress Distribution in y-axis for 1.6 MPa Mean Interface Pressure (for Example 4)

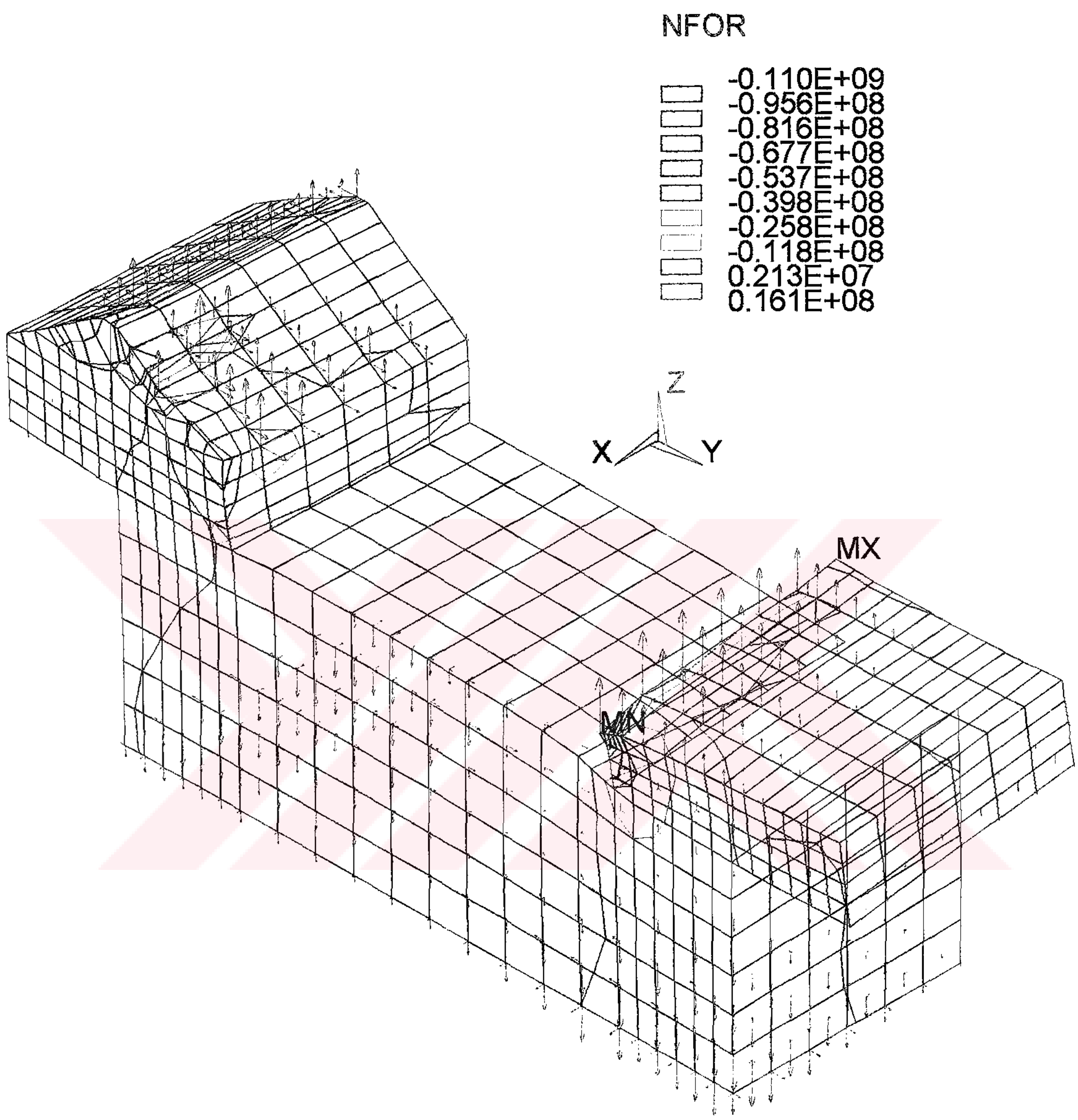

Figure 7.20 Pressure Distribution at the Contacting Surfaces and Stress Distribution in z-axis for 6.4 MPa Mean Interface Pressure (for Example 4)

7.3.5 Example 5: Small Student Lathe

Dimensions and finite element model of the small student lathe is shown in Figure 7.21. Contact elements are defined between contacting surfaces of which edge views are seen as red lines in Figure 7.21. In this example, to represent a real case of the analysed lathe, concentrated forces were applied on x, y and z axis. The tangential component of cutting force is calculated for the maximum loading conditions of the lathe and its was found as 4240 N. For axial and radial directions, they were assumed as 0.5 and 0.3 times of the tangential component of cutting force as suggested by Koenigsberger[57]. The surface compliance parameters and material properties are the same with the Example 1 in chapter 6. The deformed shape of the fifth example is shown in Figure 7.22.

Figures 7.23, 7.24 and 7.25 show the normal force distribution (pressure distribution) on the contacting guideway surfaces and stress distribution on x, y and z axis respectively. The mean interface pressure is 1.2 MPa. The value of maximum interface pressure, for this example, is 3.04 MPa and it is about 1.9 times of the mean interface pressure. Maximum deflection at the tip of tool holder is 0.272 mm in x direction.

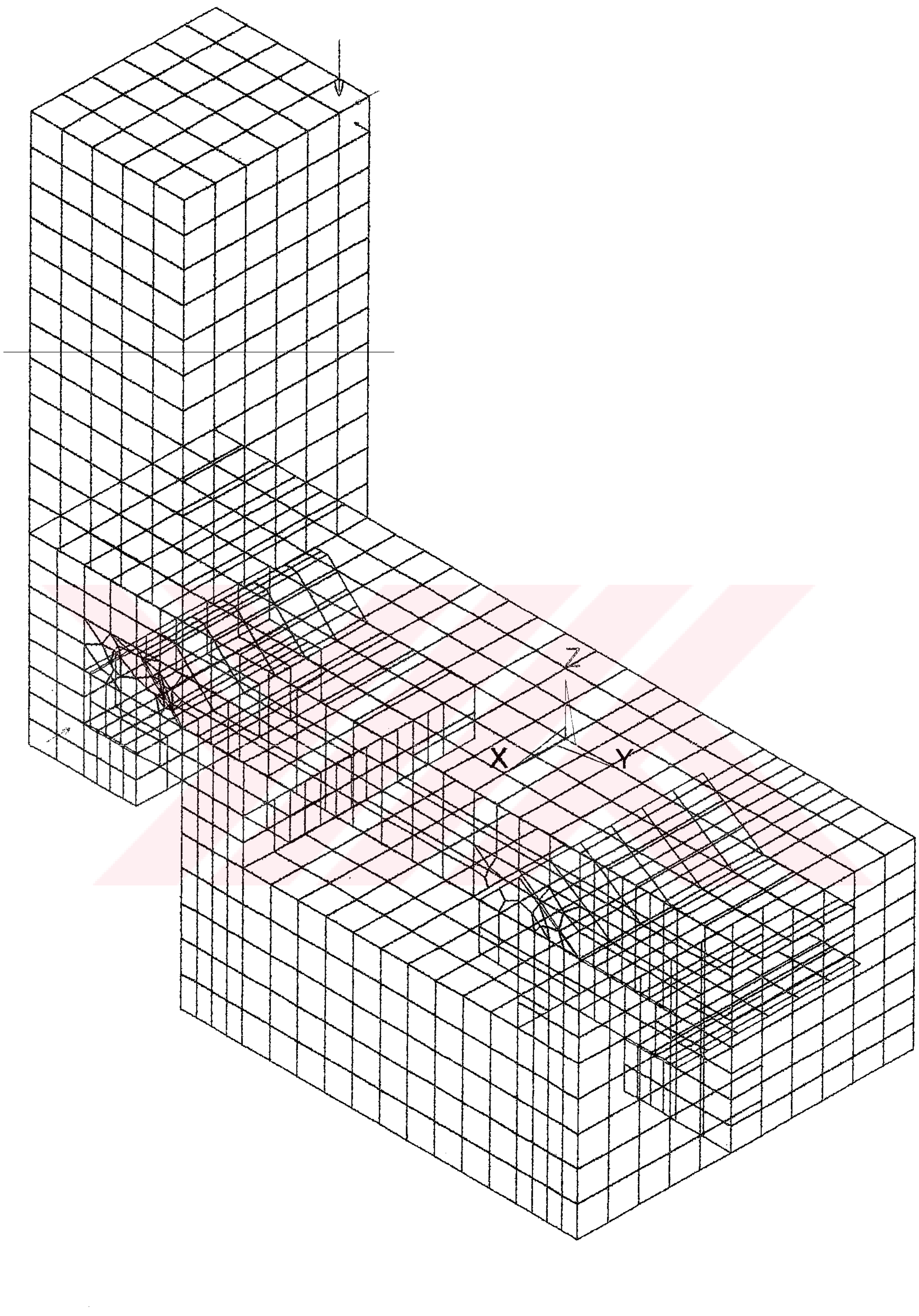

Figure 7.21 Finite Element Division of Small Student Lathe and Force Application Points

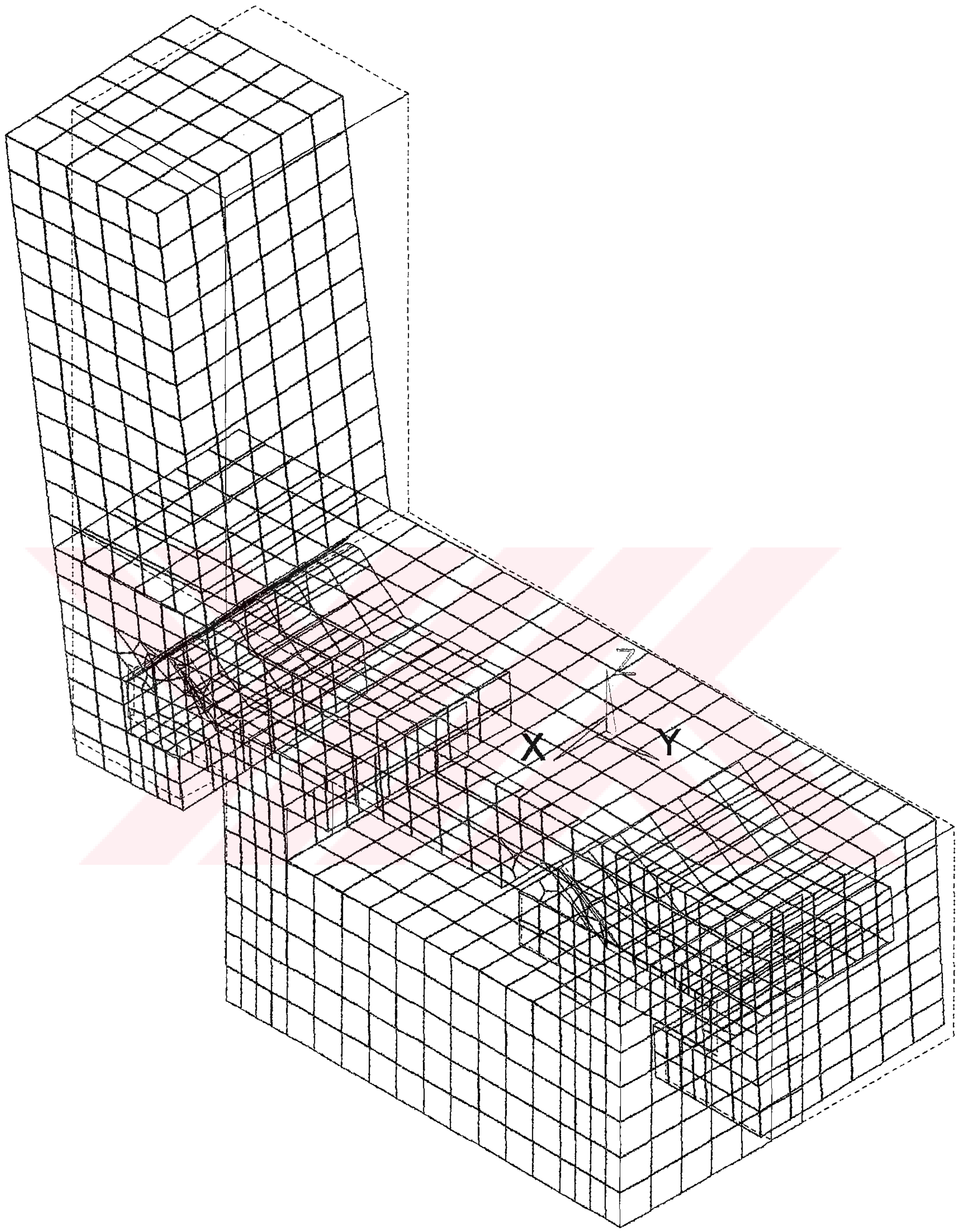

Figure 7.22 Deformed Shape of the Small Student Lathe

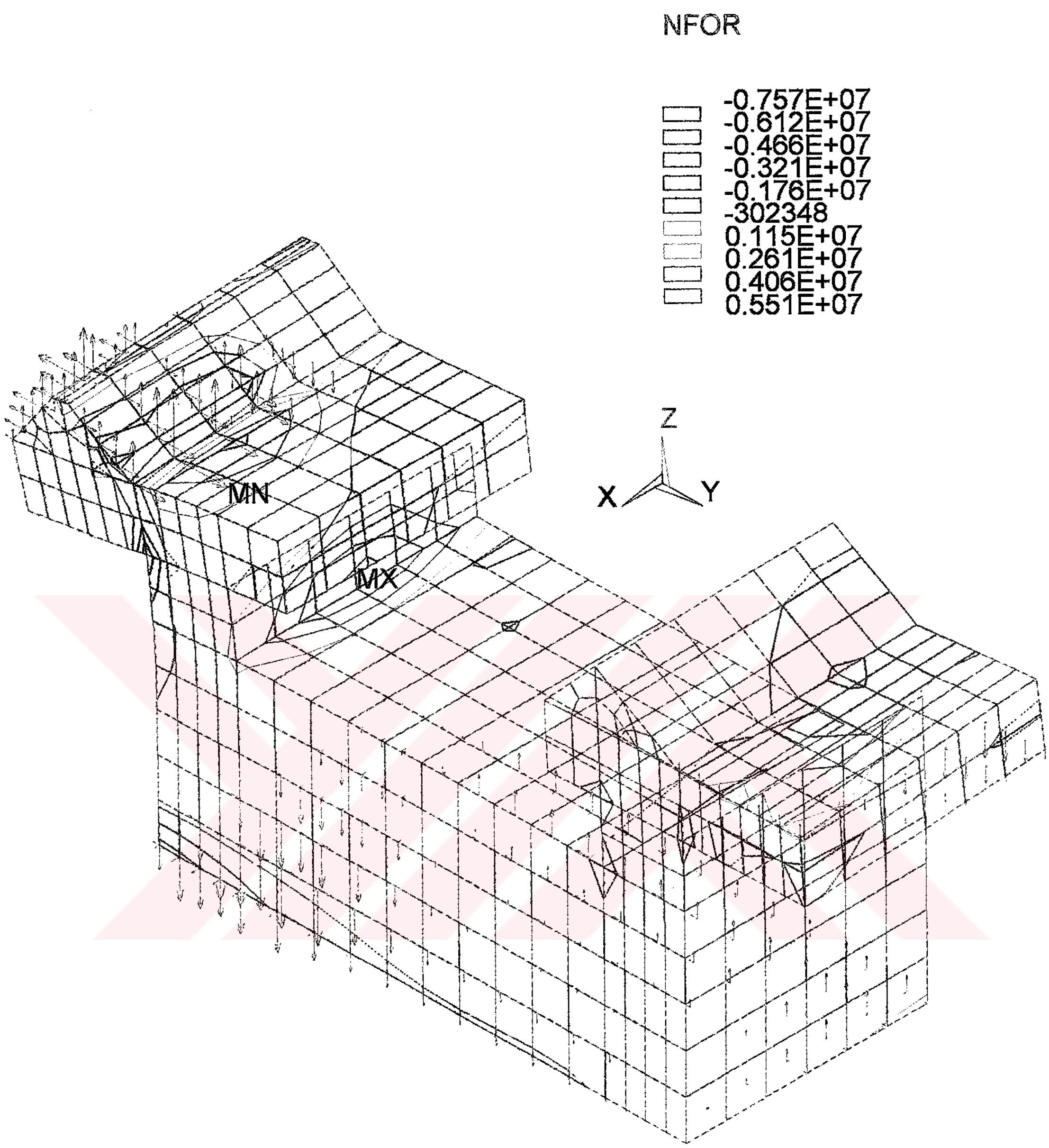

Figure 7.23 Pressure Distribution at the Contacting Surfaces and Stress Distribution in x direction (for Example 5)

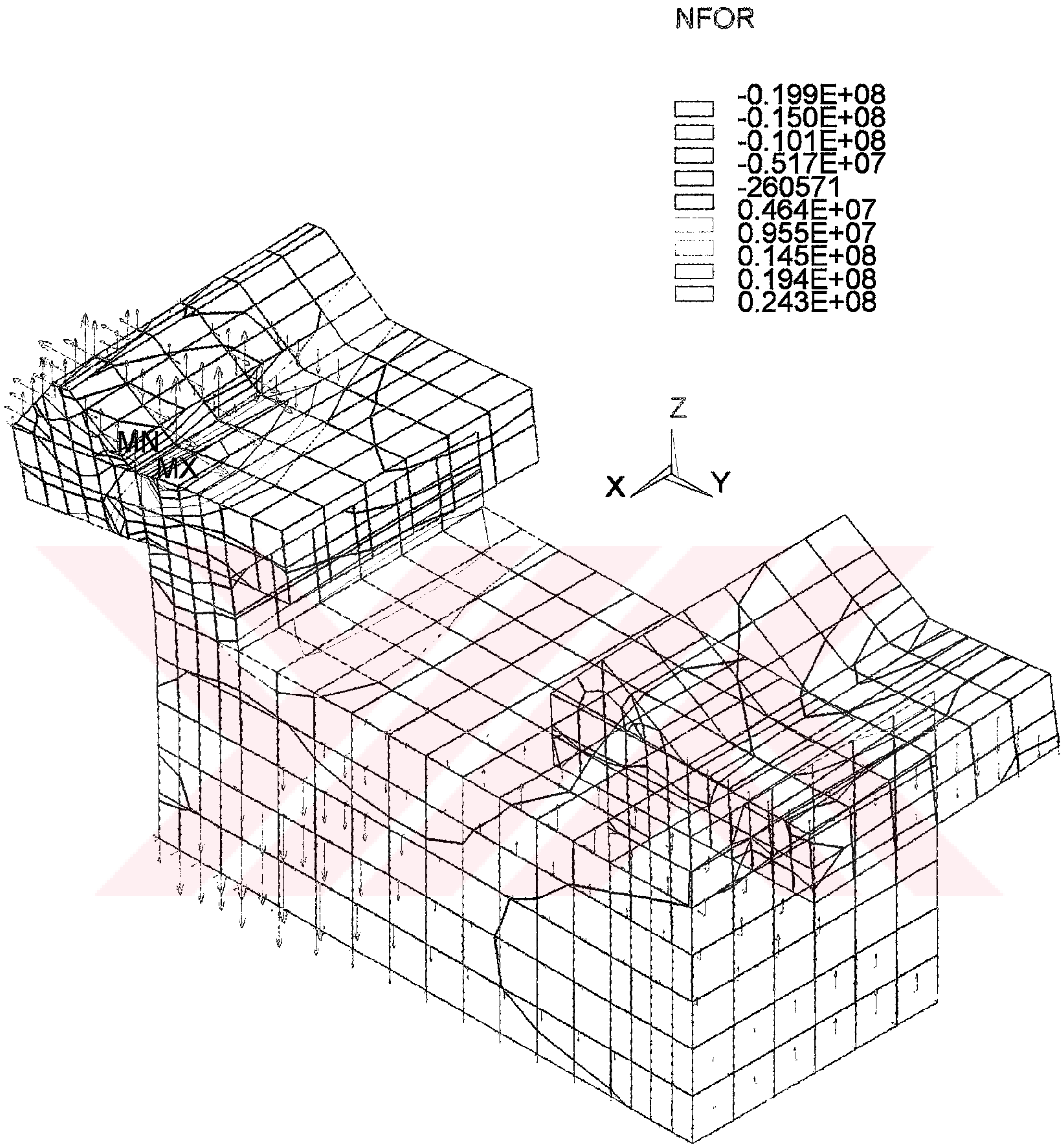

Figure 7.24 Pressure Distribution at the Contacting Surfaces and Stress Distribution in y direction (for Example 5)

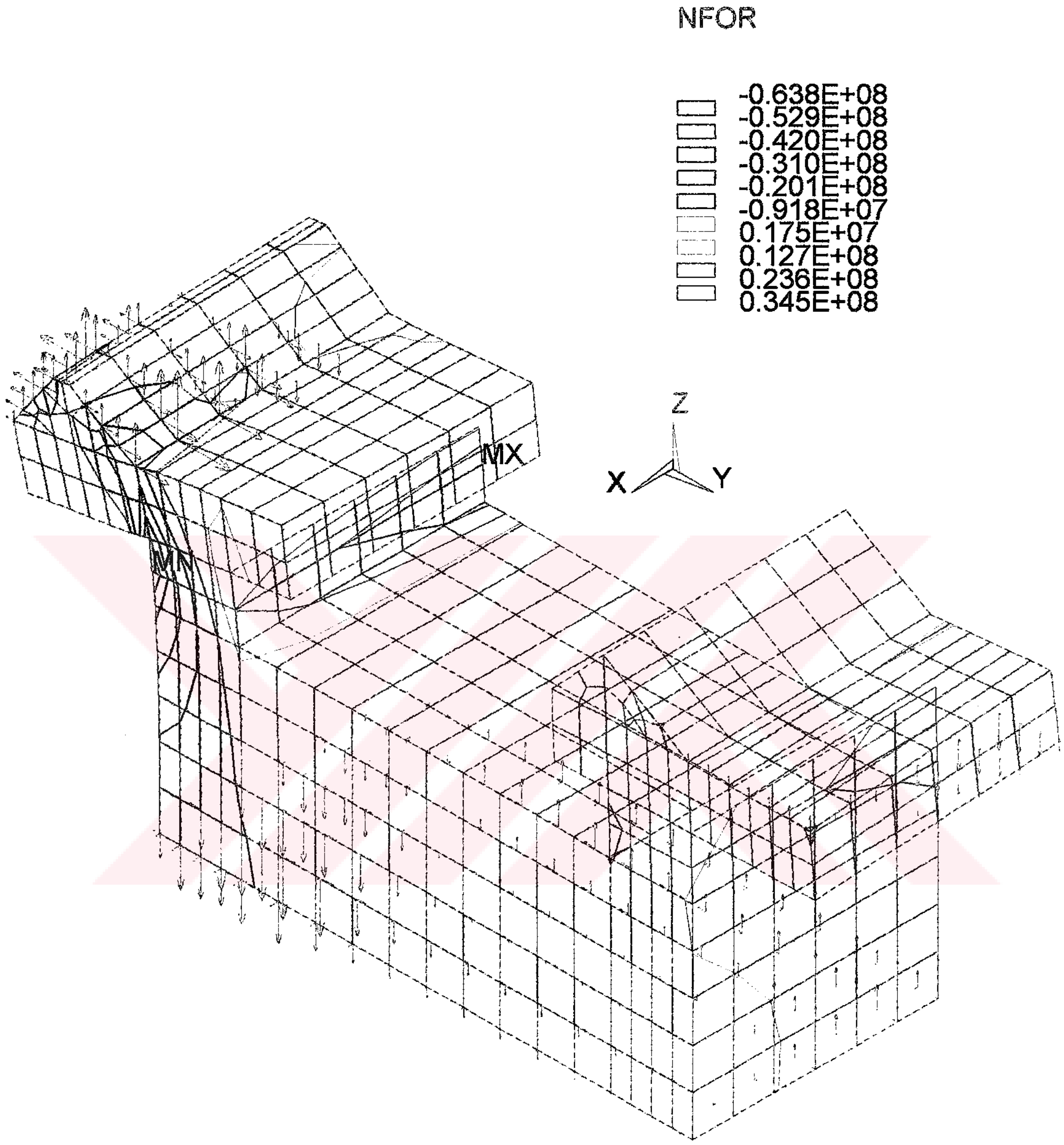

Figure 7.25 Pressure Distribution at the Contacting Surfaces and Stress Distribution in z direction (for Example 5)

CHAPTER VIII

DISCUSSIONS

AND

CONCLUSIONS

8.1 DISCUSSIONS AND CONCLUSIONS

The work presented in this thesis is mainly concerned with design of slideway systems in machine tools. Slideways may be integral part of main body of machine tools or they may be joined to the main body by using welds or bolts. Design study of these joints (slideways, bolted joints, or welded joints) is mainly dependent on their deflection characteristics. In other words, stiffness is the governing criteria in the design of these joints. Additionally, pressure or stress distribution on the slideway surfaces is another important criterion in finalising the design study. FEM is a very useful tool in this respect.

In the analysis of bolted joints,the finite element results obtained in this study agreed with the finite element results of Wileman et al.[34] and

and with the experimental results of Yıldırım[32] and Maruyama et al.[51] which validate the method of solution followed and the code developed.

A formula is obtained by modifying Wilaman's equation to include the effects of thickness ratio and different materials. Correction factor for d/L is also introduced. The results obtained from this formula (Equation 4.3) are compared with the results of previous studies (Figures.4.7, 4.8 and 4.9). The result had verified that this formula could be used safely in the design of bolted joint.

In the design of welded joints the important parameters to be considered are the manner of loading on the joint, the types of materials in the weld and in the members to be joined, and the geometry of joint itself. In this study two types of joints were analysed to show effects of loading and joint geometry.

In practice, in the design of fillet welds, the average stress in throat area is taken as 1.414 of nominal stress. The maximum shear stresses occur at the throat area about 1.69 and 2.66 times of nominal stresses for the first and second examples respectively. The maximum shear stress values obtained at point A are 2.3 and 3.43 times of nominal stresses. There is a ratio of about, (2.3/1.414) 1.63 and (3.43/1.414) 2.43 between the calculated and theoretically suggested values of the maximum shear stresses in two examples. To be able to design a safe weldement for the fillet welded joints like above models, the design stress values must be increased from the values given in literature ($1.414\sigma_0$).

Machine tools have complicated structures and their analyses are extremely difficult by analytical methods. Both two dimensional and three dimensional slideway models presented in this study cover some common types used in machine tools. As seen in Figure 6.3. (a), there is almost 100 % correlation between the results given by Back[21] and the pressure distribution of our two dimensional slideway model.

When solution times are compared; two dimensional slideway models are advantageous, because the solution times of three dimensional models are about ten to fifteen times of two dimensional models. But in two dimensional models it is not possible to apply all forces and moments on a machine tool.

Stiffness and pressure distribution in machine tool slideways can be calculated easily and precisely by using ANSYS with the modified finite element non-linear contact analysis. Depending upon the deflection requirements, modifications such as; changing the length of main sliding surfaces or auxiliary sliding surfaces, changing the length and locations of narrow guideways and changing the geometry of the slideway systems could be done in a very short time. Ease of the construction of the models and faster solution times are the advantages of this method.

Careful consideration must be given to increase mean interface pressure, because maximum pressure may reach to a value greater than permissible value for the selected slideway material. With the available tools and methods presented in this thesis, it is always possible to see pressure (or stress) distribution on each face and its maximum value to compare with the permissible value for the slideway material under different loading conditions.

It is also possible to see how the slideway system will deform. This will provide an opportunity to the designer to modify the design (changing the slideway dimensions, location of main sliding surfaces, location of driving system etc.).

8.2 RECOMMENDATIONS FOR FUTURE WORKS

With the method developed in the present work, it is possible to extend the analysis of machine tools to provide many option to the machine tool designers:

1. The analysis of anti-friction slideways can be performed by using ANSYS non-linear contact elements.

2. The effects of preloading on design of bolted and sliding joint can be evaluated in detail.

3. A detailed evaluation of clearances on the design of slideways can be performed.

4. The dynamic stiffness of machine tool slideways can be evaluated in detail with the aid of developed method for static stiffness.

5. The method can be integrated into CAD package for a complete CAD package for the design of machine tools.

LIST OF REFERENCES

1. Taylor, S., 1973, "Computer Aided Design of a Planning Machine Structure", Proc. 13th Int. Machine Tool Design and Research Conference, Manchester, Macmillan, pp. 737-758.

2. Levina, Z. M., 1965, "Calculation of Contact Deformations in Slideways", Machines and Tooling, Vol. 36, pp. 8-17.

3. Levina, Z. M., 1967, "Research on the Static Stiffness of Joints in Machine Tools", Proc. 8th Int. Machine Tool Design and Research Conference, Manchester, Macmillan, pp. 737-758.

4. Kragelskii, I, V.,1965, "Friction and Wear", Butterworths, London.

5. Ostrovskii, V. I., 1965, "The Influence of Machining Methods on Slideway Contact Stiffness", Machines and Tooling, Vol. 36, pp. 17-19.

6. Greenwood, J., A., 1967, "The Area of Contact Between Rough Surfaces and Flats", Journal of Lubrication Technology.

7. Buc, J., and Nowicki, B., 1967, "The Measurement of the Real Area of Contact Between Two Metal Surfaces", Proc. 8th Int. Machine Tool Design and Research Conference, Manchester, Macmillan.

8. Schofield, R. E., and Thornley, R. H., 1971, "Calculating the Elastic and Plastic Component of Deflection of Plane Joints Formed From Machined Surfaces", Proc. 12th Int. Machine Tool Design and Research Conference, Manchester, Macmillan, pp. 89-95.

9. Schofield, R. E., 1967, "An Investigation Into the Fundamental Problems of the Static Stiffness of Bolted Joint", PhD Thesis, U.M.I.S.T.

10. Dolbey, M. P., and Bell, R., 1971, "The Contact Stiffness of Joints at Low Apparent Interface Pressures. Annals of the C. I. R. P. Vol. 19, pp. 67-79.

11. Levina, Z. M. and Reshetov, D. N.,1965, "Machine Design for Contact Stiffness", Machines and Tooling, Vol. 36, No. 12.

12.Tenner, D. G., 1968, "Contact Stiffness of Friction Slideways", Machines and Tooling, Vol. 39, No. 3., pp. 3-6

13.Connolly, R., and Thornley, R. H., 1967, "Determining the Normal Stiffness of Joint Faces", ASME Paper No. 67, Prod. 6.

14.Connolly, R., Schofield, R. E., and Thornley, R. H., 1967, "The Approach of Machined surfaces with Particular Reference to Their Hardness", Proc. 8th Int. Machine Tool Design and Research Conference, Manchester, Macmillan, pp. 759-775.

15.Schofield, R. E. and Thornley, R. H., 1968, "Mathematical Expressions of Surface Finish Characteristics", Conf. on Properties and Metrology of Surfaces, Oxford.

16.Thornley, R. H., Connolly, R., and Koenigsberger, F., 1967, "The Effect of Flatness of Joint Faces Upon the Static Stiffnes of Machine Tools Joints", Proc. of the Inst. of Mech. Eng.

17.Thornley, R. H., Connolly, R., Barash, M. M., and Koenigsberger, F., 1965, "The Effect of Surface Topography Upon the Static Stiffness of Machine Tools Joints", Proc. 5th Int. J. Machine Tool Design and Research Conference, Manchester, Macmillan, pp. 57-74.

18.Filiz, İ. H., Akpolat, A., Güzelbey, İ. H., 1996, "Stiffness of Bolted Member," Turkish. J. of Engineering and Environmental Sciences, Vol. 20, No. 5., pp. 273-279.

19.Filiz, İ. H., Akpolat, A., Güzelbey, İ. H., 1997, "Deformations and Pressure Distribution on Machine Tool Slideways," Int. J. of Machine Tools and Manufacture, Vol. 37, No. 3., pp. 309-318.

20.Hinduja, S., 1971, "Analysis of Machine Tool Structures by Finite Element Method", PhD Thesis, U.M.I.S.T.

21.Back, N., 1972, "Deformations in Machine Tool Joints", PhD Thesis, U.M.I.S.T.

22.Back, N., Burdekin, M. and Cowley, A., 1973, "Review of the Research on Fixed and Sliding Joints", Proc. 13th Int. Machine Tool Design and Research Conference, Manchester, Macmillan, pp. 87-97.

23.Back, N., Burdekin, M. and Cowley, A., 1975, "Analysis of Machine Tool Joints by the Finite Element Method", Proc. 15th Int. Machine Tool Design and Research Conference, Manchester, Macmillan, pp. 529-537.

24.Fritsche, G., 1962, "Grundlagen einer genaueren Berechnung statisch and dynamisch beanspruchter Schraubenverbindungen," Dissertation, Technischen Universtat Berlin.

25.Stuck, K., 1968, "Untersuchungen Ueber Die Federeigen schaften der Verpantenn Teile von Schraubenverbindungen," Dissertation, Aachen Th.

26.Dann, R. T., 1975, "How Much Preload for Fasteners," Journal of Machine Design, August 21, pp. 66-99.

27.Ito, Y., Toyada, J., and Nagata, S., 1979, "Interface Pressure Distribution In a Bolted-Flange Assembly," ASME Journal of Mechanical Design, Vol. 101, No. 2, pp. 330-337.

28.Shigley, J. E., and Mischke, C. R., 1989 Mechanical Engineering Design, Fifth Edition, New York, McGraw Hill, Inc.

29.Motosh, N., 1976, "Determination of Joint Stiffness in Bolted Connections," ASME Journal of Engineering for Industry, Vol. 98, No. 3, pp. 858-861.

30.Osman, M. O. M., Mansour, W. M. and Dukkipati, R. V., 1976, "On the Design of Bolted Connections with Gaskets Subjected to Fatigue Loading," ASME paper No.76-DET-57.

31.Akkurt M., 1982, "Makina Elemanları," Vol.1, İstanbul, İstanbul Technical University Press, pp. 316-318.

32.Yıldırım, N., 1988, "Experimental Determination of the Stiffness of Connected Parts in Preloaded Bolted Joints," Master's Thesis, METU, Gaziantep, Turkey.

33.Filiz, İ. H., Yıldırım, N., 1990, "Experimental Determination of Member Stiffness in Preloaded Bolted Joints", Proceeding of 4th National Congress on Machine Design and Manufacturing, 19-21 September, METU, Ankara, Turkey, pp. 479-487.

34.Wileman, J., Choudhury, M., Green, I., 1991 "Computation of Member Stiffness in Bolted Connections," Journal of Machine Design, Vol. 113, pp. 432-437.

35.Masuko, M. and Ito, Y., 1969, "Distribution of Contact Pressure on Machine Tool Slideways", Proc. 10th Int. Machine Tool Design and Research Conference, Manchester, Macmillan, pp.641-650.

36.Furukawa, Y., and Moronuki, N., 1987, "Contact Deformation of a Machine Tool Slideway and Its Effect on Machining Accuracy", Int. J. Japanese Society of Mechanical Engineers, Vol. 30. No. 263, pp. 868-874.

37. Hashimoto, M., Marui, E., and Kato, S., 1994, "Estimation of Contact Stiffness at Interfaces in Machine Structures by a Beam Model on an Elastic Foundation", Tribology International., Vol. 27, No. 6., pp. 423-431.

38. Zienkiewicz, O. C., 1977, "The Finite Element Method", Third. Edition., McGraw-Hill, Inc.

39. Kardeştuncer, H., and Norrie, D. H., 1987, "Finite Element Handbook", McGraw-Hill, Inc.

40. Iron, B., and Ahmed, S., 1986, "Techniques of Finite Elements", Ellis Horwood Ltd., England.

41. Reddy, J. N., 1993, "An Introduction to the Finite Element Method", McGraw-Hill, Inc., Second Ed., Singapore.

42. Güzelbey, İ.H., 1992, "Finite and Boundary Element Analysis of Elasto-plastic Finite Strain Contact Problems", Ph.D Thesis, Cranfield Institue of Technology.

43. ANSYS User's Manual for Revision 5.0A, 1992, Volume I Procedures, Swanson Analysis Systems, Inc., Houston, USA.

44. ANSYS User's Manual for Revision 5.0A, 1992, Volume II Commands, Swanson Analysis Systems, Inc., Houston, USA.

45. ANSYS User's Manual for Revision 5.0A, 1992, Volume III Elements, Swanson Analysis Systems, Inc., Houston, USA.

46. ANSYS User's Manual for Revision 5.0A, 1992, Volume IV Theory, Swanson Analysis Systems, Inc., Houston, USA

47. ANSYS Structural Nonlinearities, 1993, User Guide for Revision 5.0, Swanson Analysis Systems, Inc., Houston, USA.

48. Selyukov, Yu. Z. and Niberg, A. N.,1979, "The Effect of the Characteristics of Cast Iron and Certain Plastics on Sliding Stability", Machines and Tooling, Vol.50, No. 5., pp.12-14

49. Levina, Z. M.,1978, "Ways of Improving Slideways in Modern NC Machines", Machines and Tooling, Vol. 49, No. 10., pp. 16-18.

50. Levina, Z. M. and Nazarov, V. L., 1969, "Determining Stiffness Factors of Single Column Jig Borer", Machines and Tooling, Vol. 40, No. 6.

51. Maruyama, K., Yoshimoto, I., and Nakano, Y., 1975, "On Spring Constant of Connected Parts in Bolted Joints, "Bulletin of the Japanese Society of Mechanical Engineers, JSME, Vol. 18, No. 126, pp. 1472-1480.

52. Choudhury, M., 1988, "Member Stiffness of Bolted Joints," Master's Thesis, Georgia Institute of Technology.

53. Shigley, J. E., 1993, "Mechanical Engineering Design", Third Ed., McGraw-Hill, Inc., Tokyo.

54. Acherkan, N.,1973, "Machine Tool Design", Vol. 3, MIR Publishers, Moscow.

55. Filiz, İ. H., 1981, "Computer Aided Design of Feed Drives for N. C. Machine Tools", PhD Thesis, U.M.I.S.T.

56. Sundararajan, V., 1977, "Contributions to the Study of the Dynamic Behaviour of a Machine Tool Slideway", PhD Thesis, U.M.I.S.T.

57. Koenigsberger, F., 1964, "Design Principle of Metal Cutting Machine Tools", Pergamon Press, Oxford.

VITA

Abdullah AKPOLAT was born in Tatlarin, Nevşehir, in 1959. He received B. Sc. and M. Sc. degrees in Mechanical Engineering from the Middle East Technical University, Extension Campus, Gaziantep in 1983 and 1988, respectively.

He has studied as a Research Assistant in the Mechanical Engineering Department at University of Gaziantep in between the years of 1986-1994. He has been studying at the same university as an instructor since 1994.

His research interests include Computer Aided Design and Analysis with FE Packages (stiffness of machine tool joints, contact stiffness of slideways) and mechanical properties of steels.